Double-Band Hysteresis Current Control Method for Three-Phase Shunt Active Power Filters

Farshid Allahakbari

Submitted to the
Institute of Graduate Studies and Research
in partial fulfillment of the requirements for the Degree of

Master of Science
in
Electrical and Electronic Engineering

Eastern Mediterranean University
August 2013
Gazimağusa, North Cyprus

Approval of the Institute of Graduate Studies and Research

Prof. Dr. Elvan Yılmaz
Director

I certify that this thesis satisfies the requirements as a thesis for the degree of Master of Science in Electrical and Electronic Engineering.

Prof. Dr. Aykut Hocanın
Chair, Department of Electrical and Electronic Engineering

We certify that we have read this thesis and that in our opinion it is fully adequate in scope and quality as a thesis for the degree of Master of Science in Electrical and Electronic Engineering.

Prof. Dr. Osman Kükrer
Co-Supervisor

Prof. Dr. Hasan Kömürcügil
Supervisor

Examining Committee

1. Prof. Dr. Hasan Kömürcügil

2. Prof. Dr. Osman Kükrer

3. Prof. Dr. Runyi Yu

4. Assoc. Prof. Dr. Hasan Demirel

5. Asst. Prof. Dr. Alper Doğanalp

ABSTRACT

The widespread use of nonlinear loads in all branches of industry and in the power electronic equipment has increased the harmonic current distortion on the power system which leads to poor power factor, increased heating losses, and harmful disturbance to other loads connected at the same point of common coupling (PCC). For harmonic elimination and improving the power factor, passive LC filters have conventionally been used although, they have many drawbacks. Alternatively, shunt active power filters (APFs) have been considered as a potential candidate. In recent publications, diverse control strategies have been introduced for three-phase APFs. Among the current-control strategies, the conventional single-band hysteresis current-control (SBHCC) has received much attention due to its major advantages such as higher accuracy, fast dynamic response, robustness and simplicity in implementation. Despite these advantages, the SBHCC has a major disadvantage that the switching frequency is very high which increases the switching losses. These losses can be decreased by increasing the hysteresis band, at the expense of decreasing the switching frequency. In this thesis, a double-band hysteresis current-control (DBHCC) scheme is introduced for three-phase shunt active filters. First, the mathematical modeling of the three-phase APF is developed. Then, it is implemented by using SIMULINK/MATLAB. Finally, the results are compared with that of obtained by the SBHCC method.

Keywords: Active Power Filter, Power Electronics, Hysteresis Current Control Method

ÖZ

Doğrusal olmayan yüklerin endüstrinin tüm dallarında ve güç elektroniği cihazlarında yaygın olarak kullanımı güç sistemlerindeki harmonik akım bozunumunu artırmıştır. Akımdaki bu bozunum ise güç faktörünün istenen değerden küçük olmasına, ısı kayıplarının artmasına ve ortak noktaya bağlı olan diğer yüklerin de olumsuz etkilenmesine neden olmaktadır. Geleneksel olarak, akımdaki istenmeyen harmoniklerin yok edilmesi ve güç faktörünün de iyileştirilmesi için pasif LC süzgeçler kullanılmıştır. Ancak, bu süzgeçlerin birçok dezavantajları bulunmaktadır. Bunlara çare olarak, paralel aktif güç süzgeçleri potansiyel bir aday olarak dikkate alınmıştır.

Yakında yapılan çalışmalarda, üç fazlı aktif süzgeçler için çeşitli kontrol yöntemleri önerilmiştir. Bu akım kontrol yöntemlerinin içinde geleneksel tek bandlı histeresiz akım kontrolü, yüksek doğruluk, hızlı dinamik cevabı, parametrelere olan dayanıklılığı ve uygulamada olan kolaylığı gibi önemli avantajlarından dolayı çok dikkat çekmiştir. Bu avantajlara rağmen, tek bandlı histeresiz akım kontrolunun önemli bir dezavantajı ise anahtarlama frekansının çok yüksek olmasıdır. Yüksek anahtarlama frekansı anahtarlama kayıplarının artmasına neden olmaktadır. Bu kayıplar, histeresiz bandını artırmak suretiyle azaltılabilir. Histeresiz bandının artırılması anahtarlama frekansının azalmasına sebebiyet verir.

Bu tezde, üç fazlı paralel aktif güç süzgeçleri için iki bandlı histeresiz akım kontrol yöntemi tanıtılmıştır. İlk olarak, üç fazlı paralel güç süzgecinin matematiksel modellenmesi yapılmıştır. Daha sonra ise, önerilen kontrol yönteminin MATLAB

ortamında benzetimi yapılmıştır. Son olarak, elde edilen sonuçlar, tek bandlı histeresiz akım kontrol yönteminden elde edilen sonuçlarla karşılaştırılmıştır.

Anahtar Kelimeler: Aktif Güç Süzgeci, Güç Elektroniği, Histeresiz Akım Kontrol Yntemi

I would like to dedicate my thesis to my beloved parents who were very supportive and always encouraged me.

ACKNOWLEDGMENTS

I would like to express my deepest gratitude to my both supervisor and co-supervisor Prof. Dr. Hasan Kömürcügil and Prof. Dr. Osman Kükrer for their excellent guidance, caring, patience and providing me with an excellent atmosphere for doing research. I would never have been able to finish my dissertation without their guidelines and supervision.

I wish to thank my committee members who were more than generous with their expertise and precious time. A special thanks to Prof. Dr. Aykut Hocanın, the department chairman for his countless hours of reflecting, reading and encouraging throughout the entire process.

I would also like to acknowledge and thank Prof. Dr. Runyi Yu for guiding my research for the past two years and helping me to develop my background in signal processing and linear systems gradually.

Special thank goes to Assoc. Prof. Dr. Hasan Demirel and Asst. Prof. Dr. Alper Doğanalp who were always willing to help and give their best suggestions.

Finally, I would like to thank my parents and my older sister. They were always supporting and encouraging me with their best wishes.

TABLE OF CONTENTS

LIST OF TABLES

LIST OF FIGURES

LIST OF SYMBOLS / ABBREVIATIONS

e	Error
i_c	Filter Current
i_l	Load Current
i_s	Source Current
i_{sm}	Source Current Amplitude
i_c^*	Reference for the Filter Current
v_c^*	Reference for the Capacitor Voltage
AHCC	Adaptive Hysteresis Current-control
APFs	Active Power Filters
BJT	Bipolar Junction Transistor
DBHCC	Double-band Hysteresis Current-control
DSP	Digital Signal Processor
GTO	Gate Turn-off Thyristor
IGBT	Insulted Gate Bipolar Transistor
IGCT	Integrated Gate-Commutated Thyristor
MCT	MOS Controlled Thyristor
PCC	Point of Common Coupling
PF	Power Factor
PID	Proportional–Integral–Derivative
PLC	Programmable Logic Controller
PV	Photovoltaic
RMS	Root Mean Square
SBHCC	Single-band Hysteresis Current Control

SCR	Silicon-Controlled Rectifier
SIT	Static Induction Transistor
SVM	Space Vector Modulation
THD	Total Harmonic Distortion
VSI	Voltage-source Inverter

Chapter 1

INTRODUCTION

1.1 Introduction

In an ideal power system, electrical energy should be transferred from the source to the load with the sinusoidal voltage and current in fixed-frequency. But in practice, existence of nonlinear elements, especially power electronic devices, in the different parts of the system render this impossible, because they always produce harmonic distortion in the system.

As an instance, in an industrial application we may need to convert the DC voltage to AC voltage. It means that the usage of inverter is inevitable, but inverters and any other equipment such as converters, rectifiers etc. which consist of power electronic devices, inject harmonics into the system.

According to the nature of power electronic devices, which is often nonlinear and based on switching operation, lead to the generation of harmonics distortion. So, it causes to have poor power quality. Hence the requirement to have systems with minimum harmonic distortion (minimum THD) compelled scientists and engineers to introduce passive and active power filters (APFs) as a solution of this problem and they are still optimizing both passive and active power filters (APFs) as much as possible [1].

In the following, we will discuss passive filters, then the types of APFs and their applications would be dealt with. Next, in chapter 2 and 3 we focus on only two control methods including single- and double-band hysteresis control methods which are well-known in industrial applications. But, power semiconductor devices, harmonics and interharmonics, are required to be shortly introduced for better understanding the concept of passive and active power filters.

1.2 Power Semiconductor Devices

There is no doubt that power semiconductor devices can be considered as the heart of modern apparatus and power electronic devices became more sophisticated as semiconductor devices developed [2]. In industrial applications, they are well-known as switches (ON or OFF) and they also help to convert power from AC to DC (rectifiers), DC to DC (choppers), DC to AC (inverters) and AC to AC in constant frequencies (AC controllers) or AC to AC in different frequencies (cycloconverters).

The systems can be reformed by using power semiconductor devices as highly efficient tools, but unfortunately there is a huge drawback coming from non-linear characteristics of switching. Bear in mind that there are no switches with ideal characteristics. This means that switching losses occur when they are switched ON and OFF. Nowadays, semiconductor devices are widely used in very modern applications such as: lighting, heating, motor drivers, AC/DC power supplies and motors, and active power filters (APF). Technically, we can classify semiconductor devices based on materials out of which they are manufactured, as follows:

Diodes, Thyristors or Silicon-Controlled Rectifiers (SCR), Gate Turn-off Thyristors (GTO), Triacs, Bipolar Junction Transistors (BJT or BPT), Power MOSFET, Static

Induction Transistors (SIT), Insulted Gate Bipolar Transistors (IGBT), MOS-Controlled Thyristors (MCT), Integrated Gate-Commutated Thyristors (IGCT).

1.3 Interharmonics

Interharmonics are voltages and currents having frequencies which are not equal to integer multiples of the fundamental frequency. These kinds of harmonics can be found in all power systems and they are often produced by cycloconverters, induction motors and inverters [2] , [3]. It should be noted that inverters are the main factors to create interharmonics in photovoltaic systems or PV systems (it is a kind of system that can generate electricity by converting sunlight energy into electricity by using solar panels) [4].

1.4 Harmonics and Power Quality

Harmonics are sinusoidal voltages and currents which have frequencies equal to integer multiples of fundamental frequency. Harmonics co-exist with the fundamental voltages or currents, and then they generate distortion in the system. It is clearly obvious that harmonic distortions are generated, because of the non-linear characteristics of power electronic instruments and loads. We can also measure these harmonics by using total harmonic distortion (THD). The current THD is defined as:

$$\text{THD} = \frac{The\ root\ mean\ square\ (RMS)\ value}{The\ RMS\ value\ of\ its\ fundamental} = \frac{\sqrt{I_2^2 + I_3^2 + I_4^2 + I_5^2 + \cdots + I_n^2}}{I_1} \qquad (1.1)$$

where I_n represents the RMS value of n^{th} harmonic.

THD can also be applied on voltage as:

$$\frac{The\ root\ mean\ square\ (RMS)\ value}{The\ RMS\ value\ of\ its\ fundamental} = \frac{\sqrt{V_2^2 + V_3^2 + V_4^2 + V_5^2 + \cdots + V_n^2}}{V_1} \quad (1.2)$$

where V_n represents the RMS value of nth harmonic.

As mentioned before, most of generated distortions that appear in voltage and current waveforms arise from non-linear loads. Rapid progress of power semiconductor devices brought the revolution in controlling industrial processes and converting energy. In fact, semiconductor devices are used in all driver circuits, controllers for DC or AC motors, domestic appliances, and photovoltaic systems which produce harmonics.

When we are considering the effect of system's inductances and capacitors, the importance of harmonic distortion would extremely increase. Indeed, there is a huge possibility for creating resonance among capacitors and inductances at one of the frequencies in the distorted signal. Likewise the amplitude of harmonics related to the resonance frequency would also increase consequently [2]. The sources of harmonics can be classified into two basic groups as below:

- Harmonic producers which are independent of power semiconductor devices.
- Harmonic producers which depend on power semiconductor devices.

Note that independent harmonic producers are not studied in this thesis. Wide presence of power semiconductor devices in industrial applications leads to the production of more harmonics and without any doubt this would increase in the near future. Here we can mention some significant harmonic effects on industrial systems as follows [4]:

- Devastation of capacitor banks.
- Interfering with programmable logic controller (PLC) systems and other controller devices
- Producing heat and extra losses in motors
- Dielectric breakdown in cables
- Interfering in communication systems
- Producing tolerance in measuring devices
- Producing fluctuation into motors

Such non-sinusoidal signals can be expressed as the summation of sinusoidal waves by using Fourier series that are known as system's harmonics. For better understanding the requisite of THD definition, we need to be more familiar with Fourier series in power electronics applications, so we are proposing an example here.

As indicated in Figure 1.1, the effect of a non-linear load has been considered in a very simple circuit. In this circuit a purely sinusoidal source voltage is applied to a simple non-linear resistor. On Figure 1.1, the variation of voltage and current is shown as well. Although the applied voltage is purely sinusoidal, distortion exists in the current waveform and by a little increase in the voltage, current might grow even by two times and also its waveform will be altered. That is a sample of distortion in power electronic systems [3].

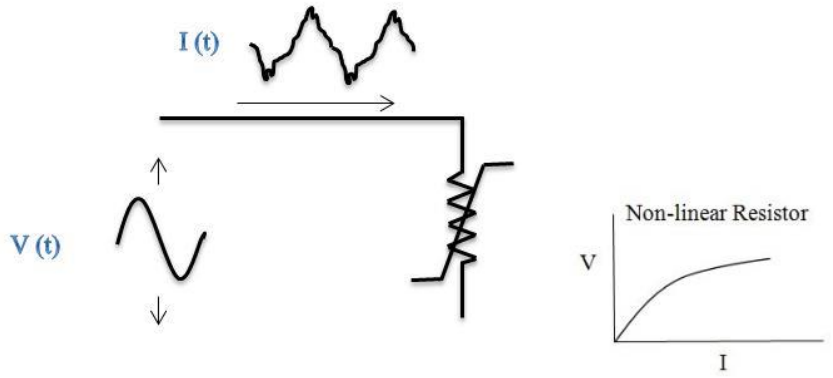

Figure 1.1: Effect of Non-linear Load

Generally, any distorted periodic wave can be analyzed by decomposing it into a summation of a sinusoidal wave, as depicted in Figure 1.2. All frequencies of the decomposed wave are integer multiples of the fundamental frequency. These waves are named as harmonics of the fundamental frequency.

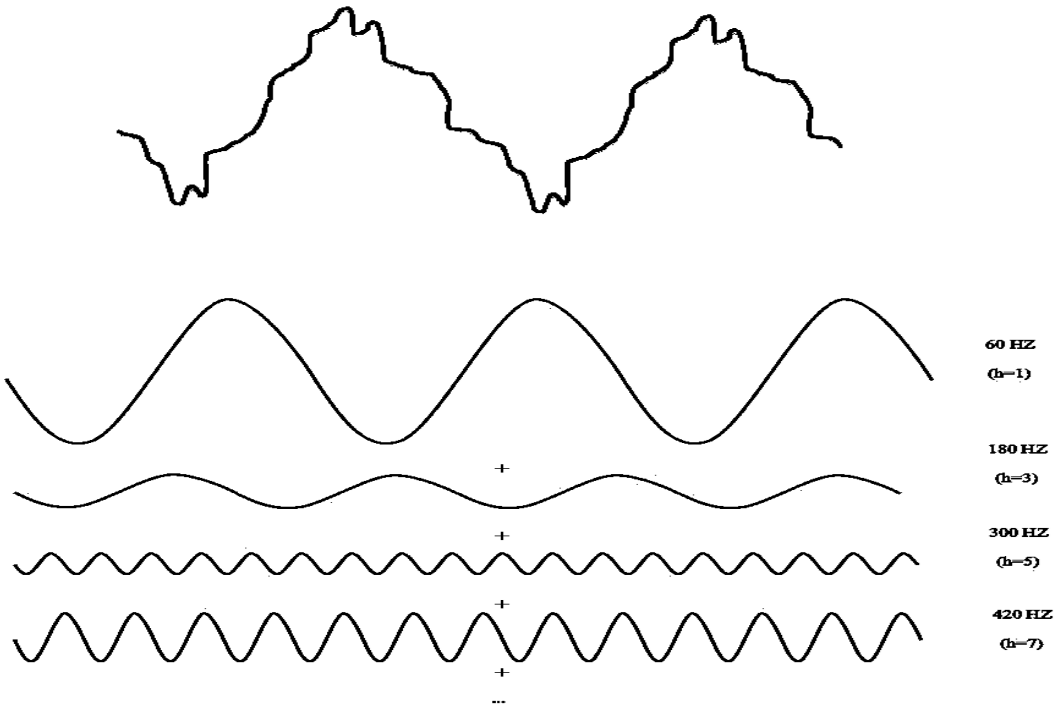

Figure 1.2: Decomposition of Non-linear Current

Note that the above process can be described by a Fourier series defined as:

$$f(t) = \frac{a_0}{2} + \sum_{n=1}^{\infty} a_n \cos\frac{2\pi nt}{T} + \sum_{n=1}^{\infty} b_n \sin\frac{2\pi nt}{T} \tag{1.3}$$

Let $\omega_0 = 2\pi f_0 = \frac{2\pi}{T}$, called the fundamental angular frequency

$$f(t) = \frac{a_0}{2} + \sum_{n=1}^{\infty} a_n \cos(n\omega_0 t) + \sum_{n=1}^{\infty} b_n \sin(n\omega_0 t) \tag{1.4}$$

$$a_0 = \frac{2}{T}\int_{t_0}^{t_0+T} f(t)dt \tag{1.5}$$

$$a_n = \frac{2}{T}\int_{t_0}^{t_0+T} f(t)\cos(n\omega_0 t)\,dt \qquad n = 1,2,\ldots \tag{1.6}$$

$$b_n = \frac{2}{T}\int_{t_0}^{t_0+T} f(t)\sin(n\omega_0 t)\,dt \qquad n = 1,2,\ldots \tag{1.7}$$

$$f(t) = C_0 + \sum_{n=1}^{\infty} C_n \cos(\omega_n t - \theta_n) \tag{1.8}$$

Another issue that recently attracts engineers' attention is the quality of power and this would not be achieved unless by eliminating harmonics. Lately, the majority of electricity companies are focusing on power quality for offering the highest quality to their customers, so having electricity with high quality can be counted as a huge advantage for any company. Also this privilege can convince customers to provide

electricity from their company. As a result, it would lead them to be successful in economic competitiveness. There are so many reasons to emphasize electricity quality but we only bring up four more important reasons [3].

1. Sensitivity of modern electric equipment is increased relative to the past. A great deal of customer's apparatus include control microprocessors and power electronics devices that can be easily destroyed by poor quality electricity and turbulence.
2. The importance of total efficiency of the systems induces us to utilize electricity with high quality.
3. In these days, people's knowledge about electricity services has been improving rapidly and it keeps electricity companies under a massive pressure to have an outlet with high precision and high quality.
4. Constituting of big systems and combining of small systems to generate the enormous systems increases the significance of power quality. Following example can clarify this issue:

Consider an independent small system which is only working with an induction motor and also assume that the poor quality of electricity can have a negative effect on the motor after two years and it can make motor inutile or completely useless. But imagine the same system with a little difference which is no longer independent. Consider that this new system is a small part of a big system which is supporting a big region and it can have direct effect on it. When any small part stops working, this big system would not be able to work anymore. Accordingly, the function of power quality would be more prominent.

1.5 Passive Filters

Passive filters count as the first filters which were mostly used in the past. These filters include several capacitors and inductors which are placed in the harmonic's path in the form of series and parallel connections to play the role as a barrier. Series passive filters must be able to pass the whole line current through itself, which means that their isolation should be considered for the whole phase voltage with respect to the ground (high cost). Parallel passive filters (shunt-passive filters) are connected to the ground from one side. They also pass only the fundamental and the harmonic currents which have been adjusted for them. Therefore, a parallel passive filter can handle a series passive filter's task and it can also be cheaply setup in comparison with a series passive filter. Because of this reason the usage of the parallel is more common rather than series passive filters. Note that, shunt-passive filters can only be used on the AC-side.

Without setting up a passive filter, the AC current waveform would contain harmonics and it cannot be sinusoidal. These current harmonics which are injected into the system cause the generation of distortion in the voltage as well.

On the DC-side, a harmonic current is generated by the harmonic voltage with respect to the impedance of the transmission line and DC-side inductor. Hence, this harmonic current creates an electromagnetic field which gives rise to noise and undesirable effects on the neighboring communication systems. Most of the time, DC-side filters are a kind of high-pass filters and they pass the non-harmonic current into the DC-transmission line.

In industrial applications, when a shunt-passive filter is applied to the system, it can attract the large part of the non-linear load current towards itself, because the

impedance of such shunt-passive filters is usually less than the source impedance. Hence, it prevents the flow towards the source voltage. In spite of the simplicity, low cost and high efficiency, there are big disadvantages of shunt-passive filters:

- Dependency of filtering characteristic to the source impedance; this issue can change the characteristic of shunt-passive filters [5] , [2].
- Large size
- Possibility of creating resonance problems between passive filter and source impedance.
- Eliminating only the specific harmonics order

Accordingly, the adjustable and dynamic solutions have been proposed for overcoming the passive filter's problems, and they are named as active power filters (APFs).

1.6 Active Power Filters (APFs)

As mentioned at the beginning of the section, APFs are designed to eliminate harmonics in power systems. But because of some restrictions and variety of different applications in industry, we separate them into three big categories such as shunt, series and combination of both with passive filters, which is named hybrid active power filters.

1.6.1 Shunt-Active Power Filters (Shunt-APFs)

For the first time in the power electronics history, the concept of shunt active power filters has been introduced by L. Gyugyi and E. C. Strycula in 1976 [5] , [3]. In the past, using shunt-APF could not be practicable in actual power systems because there

were no switching devices with high-speed and high-power. But nowadays, shunt active power filters are counted as one of the most useful types of filters around the world. The controllers of shunt-APF can generate compensator reference current and power converters are enforced to follow it up. Bear in mind that, the forthcoming description of shunt active power filters is based on p-q theory. In fact, extending and generalizing instantaneous reactive power theory provides remarkable compensation in the steady state in all circumstances such as sinusoidal or non-sinusoidal, balanced or unbalanced three phase power systems with or without-sequence currents [3].

For resolving the undesirable problems of shunt-passive filters, they have been replaced by shunt-active filters. Next, we are going to deal with harmonic production in detail and then we are going to consider the compensation process.

Basically, harmonic currents are generated because of two reasons:

- Non-linear loads.
- Harmonic voltages in power electronics systems (due to switching).

In Figure 1.3 the action of APFs is explained in summary:

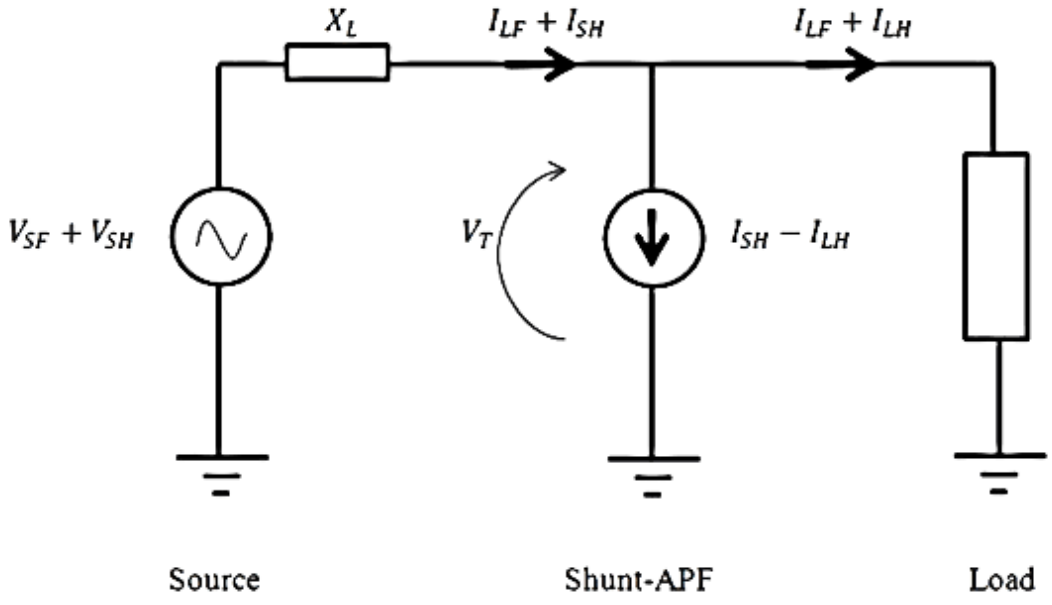

Figure 1.3: Principle of Compensating of Current

There is a non-linear load on the right side of the above circuit drawing current I_{LF} and harmonic current I_{LH} from the power system. Notice that harmonic current I_{SH} is created by harmonic voltage V_{SH}. Actually a shunt active power filter can simultaneously compensate both I_{LH} and I_{SH} currents. Nonetheless, the main role of a shunt-APF is to compensate harmonic load current I_{LH}. In other words, a shunt-APF hampers the penetration of the harmonic load current into the power system by restricting I_{LH}. For simplicity, X_L is indicated as an equivalent of power system impedance. It should be mentioned that if harmonic load current I_{LH} flows into the power system, it generates extra voltage drop equal to $X_L.I_{LH}$ and this causes major reduction of V_T too. Moreover, a shunt-APF should also draw extra harmonic current I_{SH} until voltage becomes sinusoidal and equal to $V_T = V_{SF} - X_L.I_{LF}$ note that if $V_{SH} =$

$X_L.I_{SH}$, harmonic voltage drop across X_L would be equal to the source harmonic voltage. In this situation both harmonic voltages eliminate each other, so that voltage V_T can remain sinusoidal. We can prove it mathematically by using KVL the left loop of the circuit as follows:

$$KVL: \longrightarrow -(V_{SF} + V_{SH}) + X_L(I_{LF} + I_{SH}) + V_T = 0 \tag{1.9}$$

$$\xrightarrow{V_{SH}=X_L.I_{SH}} -V_{SF} - X_L.I_{SH} + X_L.I_{LF} + X_L.I_{SH} + V_T = 0 \tag{1.10}$$

$$\xrightarrow{by\ canceling\ X_L.I_{SH}} -V_{SF} + X_L.I_{LF} + V_T = 0 \tag{1.11}$$

$$V_T = V_{SF} - X_L.I_{LF} \tag{1.12}$$

If the power system has already voltage distortion or if impedance of system X_L has a small value, harmonic current I_{SH} (which should be drawn by shunt-APF) would be very large. Both factors make shunt-APF impractical, so shunt-APF can no longer handle filtering in those situations. As a result, it should be replaced by another type of APF.

The general form of shunt-active power filter is shown in Figure1.4. Note that different control methods and different topologies can be applied instead of active filter block in Figure 1.4, but their aim is to compensate the negative effects of non-linear loads on the power system. On the other hand, shunt-active power filters try to keep voltage in sinusoidal form as much as possible by injecting the current into the point of

common coupling (PCC) to compensate the non-linear load effect and force it to behave like a linear load.

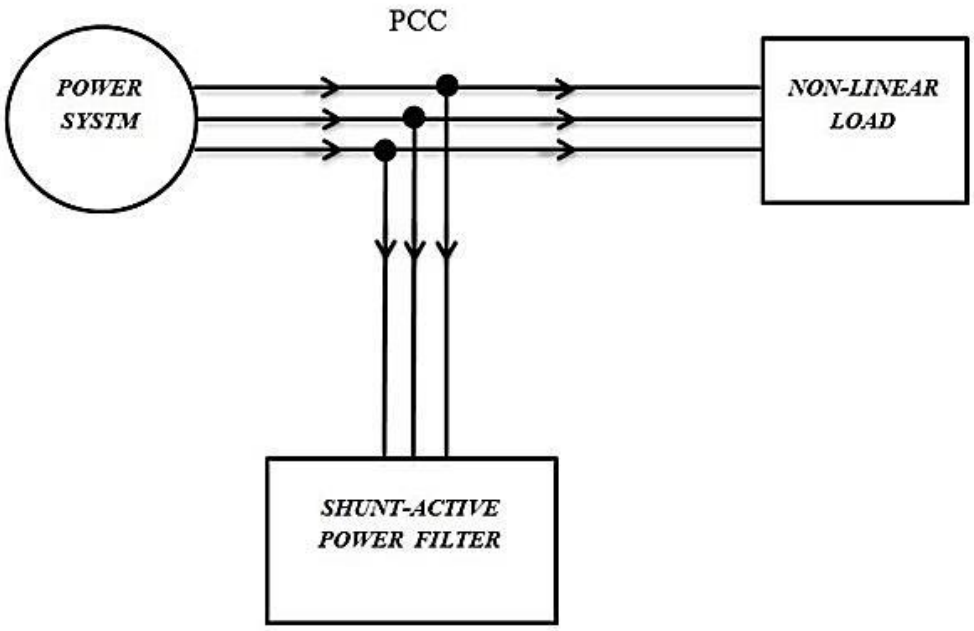

Figure 1.4: The General Form of Shunt-Active Power Filter

Here, we list some advantages of using shunt-APF [5] [1] [6] [7] [3]:

- It can be set up directly into the system without any problem and difficulty.
- No need of expensive tools for protection.
- There is possibility to compensate the active power in addition of eliminating harmonics.
- Harmonic isolation between load and source or customers services.

A series-active filter is a power electronics device which is basically treated as a barrier to prevent appearance of harmonic load voltage in source voltage. In shunt-APFs, the source and load were indicated as a voltage source and a current source respectively, consisting of current harmonics. The shunt-active power filter should generate negative harmonic current for canceling harmonic current effect of the load. But series-active filter should be able to generate negative harmonic voltage for canceling harmonic voltage of the load. It means that while working on series-active filters, the source should be considered as a current source. Note that in some cases, we can consider source and its impedance as a current source. As we mentioned before, general combination of one passive and one active filter to optimize the performance can be assumed as a hybrid-active power filter.

In recent years, the existence of very modern and sensitive apparatus in the industry convinced us to improve power quality to generate electricity without distortion. As a solution of this problem, the active power filter has been introduced by scientists. Therefore the present thesis tries to propose a method for improving active power filter performance.

1.6.2 Series Active Filters

The APFs in this configuration generate a voltage waveform which is added to or subtracted from the source voltage for maintaining its sinusoidal waveform. This configuration of APFs has to handle high load currents which cause to increase their current rating, hence it can be considered as a big drawback. But, series APFs are very appropriate for eliminating voltage harmonics and these are also used for balancing three-phase voltages [5]. It in fact means that, it can provide the load with purely sinusoidal voltage, which is vital for the voltage–sensitive devices such as: superconductive magnetic-energy storage and power system-protection devices.

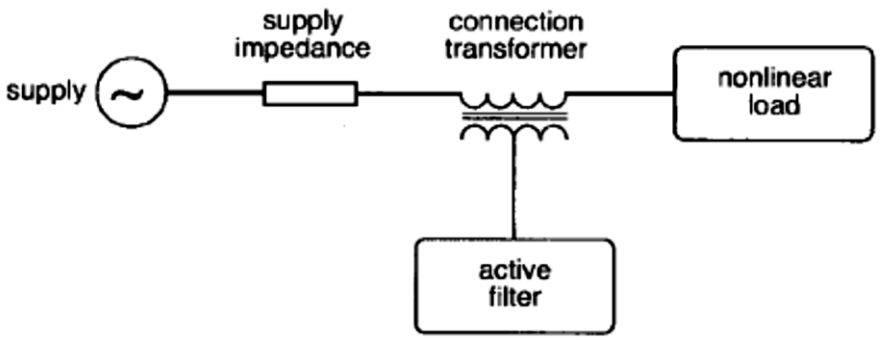

Figure 1.5: Series Active Filters Configuration

1.6.3 Hybrid Active Filters

Actually the origin of hybrid active filters comes from combination of series, shunt and passive filters to achieve greater benefit for some application by using all their advantages simultaneously. It is obvious that control of shunt and series APFs together would be more difficult rather than when we are controlling them separately. It can be counted as a big disadvantage and can also be a reasonable excuse for not using hybrid APFs. Note that hybrid APFs can be used in following configurations [5]:

- Combination of series and shunt-APFs
- Combination of shunt passive-filters and series-APFs
- Combination of passive-filters and shunt-APFs
- APFs in series with shunt passive-filters

Combination of series and shunt-APFs is indicated in Figure 1.6. Shunt and series APFs are combined to gain their advantages together, but it makes us unwilling to use due to the complexity of control and higher cost in implementation. In other words, there is extreme dependency on switching logic of shunt and series which makes control system complicated.

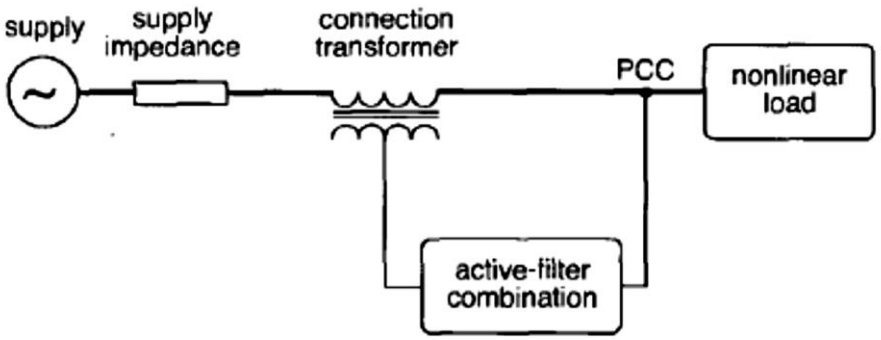

Figure 1.6: Combination of Series and Shunt-APFs

Combination of shunt passive-filters and series-APFs, shown in Figure 1.7, is introduced to reduce this complexity. Technically by providing a path for harmonic currents of the load, it can increase the capability of series APF.

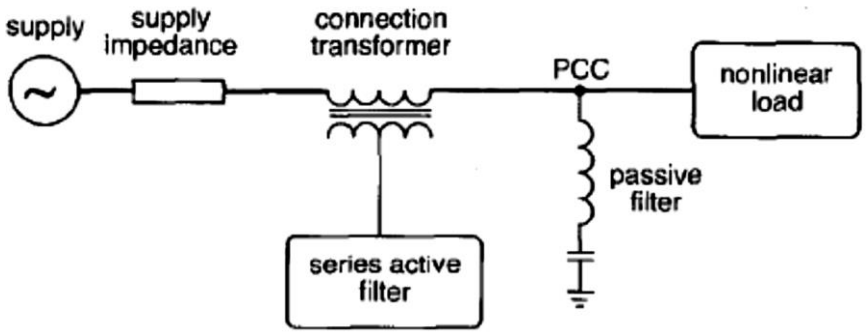

Figure 1.7: Combination of Shunt Passive-filters and Series-APFs

By considering Figure 1.8, combination of passive-filters and shunt-APFs can be counted as one of most important hybrid configurations where the active power filter is devised to get rid of only part of the low-order current harmonics when the passive filter is modeled to eliminate bulk of the high-frequency load-current harmonics. It can be a good idea to benefit from this configuration, because without any excessive cost

we can reach higher power but, it is a suitable approach only for single load with a predefined harmonic source [5].

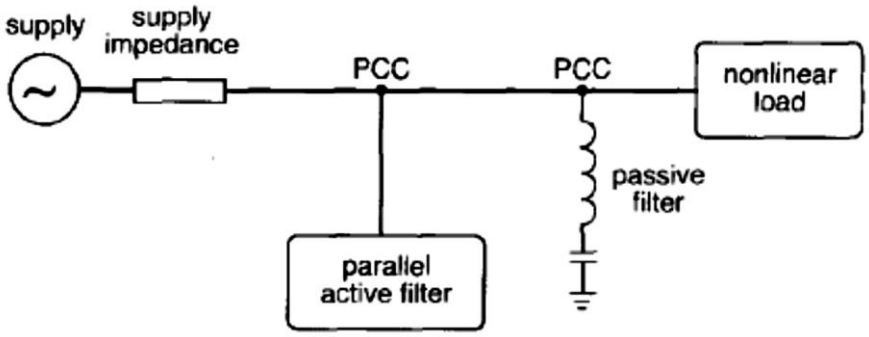

Figure 1.8: Combination of Passive-filters and Shunt-APFs

APFs in series with shunt passive-filters is a special approach that is used only for medium and high-voltage applications. In this topology, the passive filter is utilized for reducing voltage stresses on the active filter switches [5]. Figure 1.9 illustrates this topology:

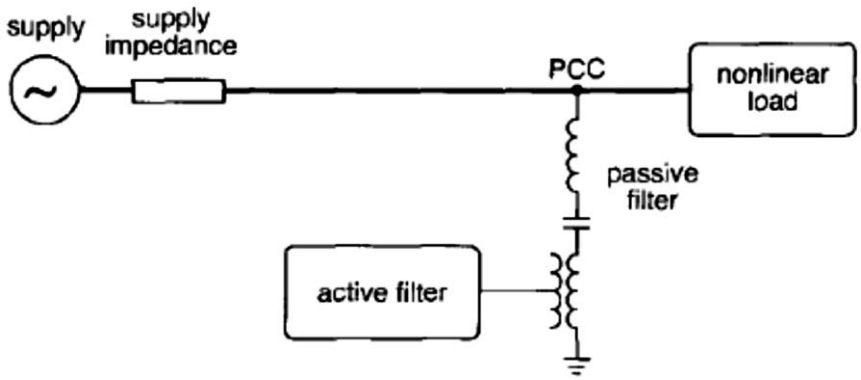

Figure 1.9: APFs in Series with Shunt Passive-filters

Series and shunt active power filters can be considered as rivals in the industry, but series APFs are less common industrially because of the need for handling high load currents especially in the secondary side, which can increase the I^2R losses and the physical size of the filters [5]. Also, hybrid APFs cannot be compared with shunt active filters, because there is complexity in control and high cost in implementation. Lack of interest for studying series APFs causes them to receive less attention than shunt APFs and most of the available hybrid configurations can only be used in special industrial applications. The shunt active power filter is the most widely used active filter because of its superb efficiency and simplicity of implementation, both in single- and three-phase configurations. It also makes us more flexible to work on.

By considering all advantages and disadvantages of APF models, shunt APFs can be introduced as the best candidate that received more attention than the other topologies. As a result, we only focus on the shunt active filter in this thesis. So, in the following, we are going to introduce the instantaneous active and reactive power theory (p-q theory), due to the implemented current control method are based on the p-q theory.

1.7 Instantaneous Active and Reactive Power Theory (p-q Theory)

For the first time the concept of instantaneous active and reactive power was presented by Akagi, Kanazawa and Nabae in 1983 and the large number of scientists and engineers have been developing this theory until today. One of the most significant issues in power systems is to generate a sinusoidal voltage with a fixed-frequency. Actually designing of transformers and transmission lines can be eased when the sinusoidal voltage with fixed-frequency exists, hence there are very few communities that do not have AC power systems with fixed-frequency in these days [3].

With the advent of sinusoidal voltage sources, power systems could be very effective when load current is in phase with source voltage, so the concept of reactive power emerged when the source voltage was not completely in phase with the load current. Note that the average value of the reactive power is zero during a period. On the other hand, reactive power does not function on transmitting energy from source to load or vice-versa [3]. By knowing reactive power definition, concept of apparent power can be introduced as "how much power is distributed or consumed if voltage and current are sinusoidal and completely in phase" [4] and power factor expresses "the relation between real power and apparent power". With respect to equation (1.13) low power factor (having the real power (P) less than the apparent power(S)) causes to generate more current and thereby increases the overall losses in the circuit

$$PF = cos\,\varphi = \frac{P}{S} = \frac{Real\ Power}{Apparent\ Power} \tag{1.13}$$

The traditional definition based on reactive and active power was suitable for analyzing a power system due to the linear load that draws a sinusoidal current from the source in all of circumstances. In the past, non-linear load was negligible and most of the time it had been neglected until power electronic instruments were introduced at the end of the 1960 decade [8], then the usage of non-linear loads which draw non-sinusoidal currents was gradually increased. In some of cases the systems could not act linearly due to all loads being non-linear. For instance, an induction motor can be considered as a completely linear load, but an induction motor needs to have a controller for speed which acts thoroughly non-linear, hence these equipment (induction motors plus their speed controllers) are no longer linear loads. We can

technically assume that the existence of power electronic instruments such as convertors, rectifiers, inverters can only be a reason for acting non-linearly.

As mentioned above, the obstacles which come from using non-linear loads are extremely increased as power electronic instruments improved. Because all modern power electronic equipment are non-linear loads, they would draw harmonic currents from the system. Unfortunately there were so many ambiguities in traditional definition of power, but in some of the cases the power system should be analyzed in non-sinusoidal situation. Afterwards, this issue causes to introduce the several new different theories about power in non-sinusoidal circumstance.

Since there is no limitation for current and voltage in p-q theory, we can easily apply this theory on the three-phase systems with or without neutral wire, therefore it considers the three-phase as a unit at the same time unlike others theories which consider three-phase as three single separated phases P-q theory can be defined by using $\alpha\beta\gamma$ transformation which is called Clarke transformation. In p-q theory, the voltages and currents are firstly transformed from abc coordinate to $\alpha\beta\gamma$, then instantaneous power is defined as a result of the three-phase system considered as a unit [3].

For the next step, suitable control strategy should be selected and it would be discussed in detail in following next chapters.

Chapter 2

SURVEY OF EXISTING CONTROL METHODS

In this section, we briefly review the methods of controlling APFs. Then, the main strategy of single-band hysteresis control method will be introduced. According to [5], APFs can be categorized into two general categories such as open and closed-loop, based on the control techniques. In open-loop systems, the load current and its harmonics are sensed and APFs generate the compensation current and then, inject it into the system. Notice that this kind of systems would not be able to check whether compensation procedure is successful or not. Closed-loop systems can handle this task with more precision by adding a feedback loop into the system and they occasionally employ digital signal processors (DSPs). Because of this reason, the majority of new control methods have been counted as subdivisions of closed-loop systems. Closed-loop systems can be subdivided into five other techniques as follows [5]:

- Constant-capacitor-voltage technique
- Constant-inductor-current technique
- Optimization technique
- Linear-voltage-control technique
- Other techniques

Constant-capacitor-voltage is very popular and can be applied for both single and three-phase. The strategy of this method will be explained in the next section.

Constant-inductor-current technique is very similar to the previous method, but it has been employed for standard converters and having an inductor in DC link is the difference between them. Optimization technique has a main task for minimizing a predetermined load-current harmonic numbers and minimizing THD by using a suitable switching function. The flexibility of current waveform drawn by the filter is another superiority of this method. Linear-voltage-control techniques can only be used for voltage-regulator APFs. Any little change into the mentioned techniques can be placed into the fifth category (other techniques).

According to above classifications, there are many different methods to control the system. For instance: controlling active power filters by using a Lyapunov function [9] controlling active power filters by using fuzzy logic [10], hysteresis band controller [11], controlling active filter by using space vector modulation (SVM), deadbeat control technique, digital control techniques etc.

This thesis tries to apply shunt-APF by considering the voltage-source model which is considered as an efficient filtering solution, and the problem of reactive power compensation as in [12]. A three-phase shunt-APF is depicted in Figure 2.1 (in this thesis different inverter topologies have been applied and they will be shown in Chapters 3 and 4). Note that in this implementation, the thyristor rectifier is modeled as a three-phase non-linear load which draws non-sinusoidal currents from the source.

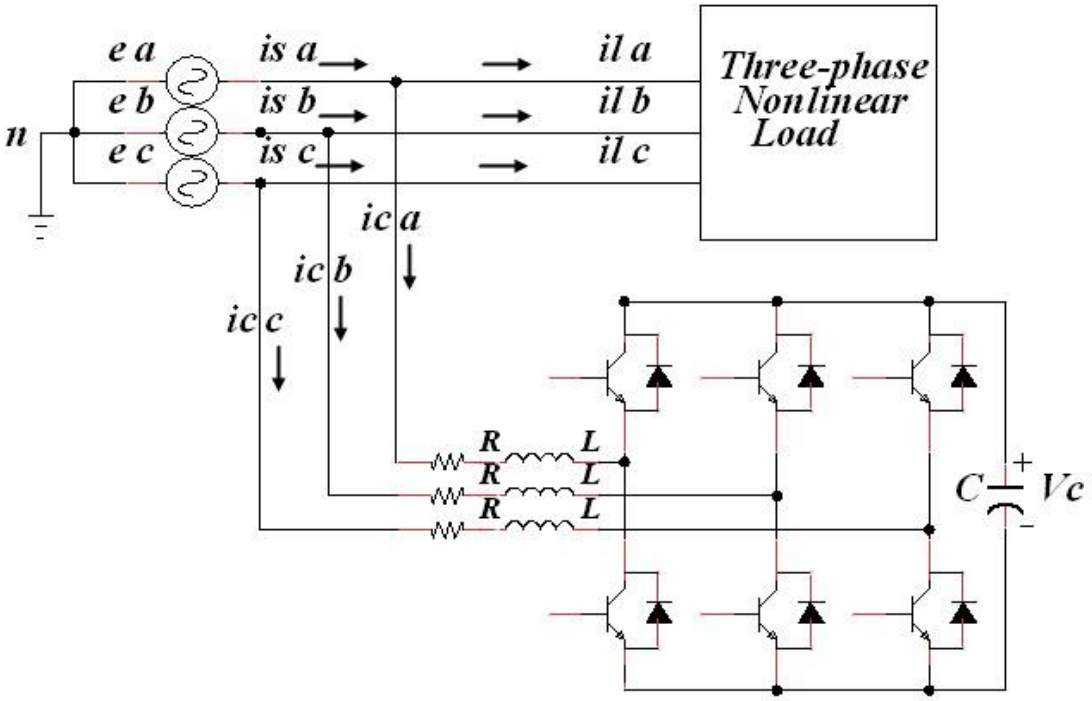

Figure 2.1: Three-phase Shunt Active Filter

2.1 System Modeling

The relation between i_c and v_c is obtained by using KVL:

$$R_l i_c + L\frac{di_c}{dt} = e - \frac{1}{2}dv_c \tag{2.1}$$

where R_l is inductor's resistance and d represents the switching function. Note that the three-phase space vector is defined as:

$$U = \frac{2}{3}\left(\boldsymbol{a^0}U_a + \boldsymbol{a^1}U_b + \boldsymbol{a^2}U_c\right) \tag{2.2}$$

Note that $a = e^{j2\pi/3}$. The three-phase source voltages are:

$$e_a(t) = E_m \cos(\omega t)$$
$$e_b(t) = E_m \cos(\omega t - 2\pi/3) \quad (2.3)$$
$$e_c(t) = E_m \cos(\omega t + 2\pi/3)$$

Applying the Clarke Transformation to the three-phase source currents:

$$I_{\alpha\beta\gamma} = T \times I_{abc} \longrightarrow \begin{bmatrix} I_\alpha \\ I_\beta \\ I_\gamma \end{bmatrix} = \frac{2}{3} \begin{bmatrix} 1 & -\frac{1}{2} & -\frac{1}{2} \\ 0 & \frac{\sqrt{3}}{2} & -\frac{\sqrt{3}}{2} \\ \frac{1}{2} & \frac{1}{2} & \frac{1}{2} \end{bmatrix} \times \begin{bmatrix} I_a \\ I_b \\ I_c \end{bmatrix} \quad (2.4)$$

The inverse transform is:

$$I_{abc} = T^{-1} \times I_{\alpha\beta\gamma} \longrightarrow \begin{bmatrix} I_a \\ I_b \\ I_c \end{bmatrix} = \begin{bmatrix} 1 & 0 & 1 \\ -\frac{1}{2} & \frac{\sqrt{3}}{2} & 1 \\ -\frac{1}{2} & -\frac{\sqrt{3}}{2} & 1 \end{bmatrix} \times \begin{bmatrix} I_\alpha \\ I_\beta \\ I_\gamma \end{bmatrix} \quad (2.5)$$

And also:

$$I_a + I_b + I_c = 0 \longrightarrow I_\gamma = 0 \quad (2.6)$$

For obtaining the filter current reference (i_c^*), the measured load current (i_l) is subtracted from the source current reference (i_s^*) as follows.

$$i_c^* = i_s^* - i_l \quad (2.7)$$

And the three-phase source current reference (i_s^*) is obtained as:

$$i_s^* = i_{sm}(t)e^{j\omega t} \tag{2.8}$$

In this step, a PID controller needs to be introduced after which next steps will be explained.

2.1.1 Proportional–Integral–Derivative (PID) Controller

A proportional–integral–derivative (PID) controller is a kind of generic feedback control. The widespread use of PID-controllers can recently be seen in the industry. A PID-controller computes "error" as the difference between a desired value and an actual value. It helps us to optimize the system and minimize the error by adjusting control gains [13]. PID comes from proportional, integral and derivative respectively which is named as a ‘’three-term controller’’ in some books and it also consists of three independent parameters. The block diagram in Figure 2.2 illustrates a PID-controller topology:

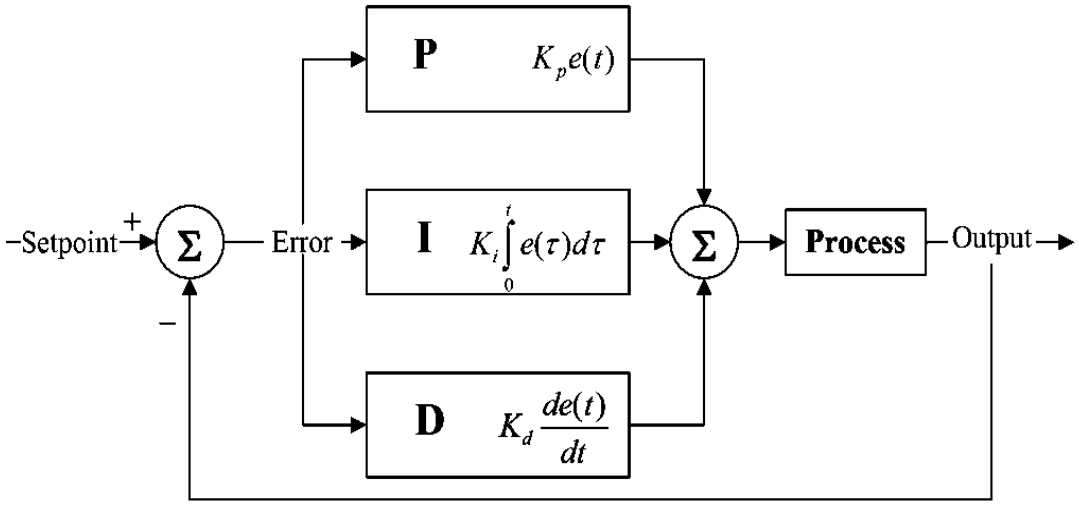

Figure 2.2: PID-Controller

These three values can be expressed based on time; P is affected by present errors, parameter I is affected by all past errors, and D is an anticipation of future errors, with respect to the change rate [14]. It should be mentioned that there is no guarantee, by applying a PID-controller, to achieve the optimal result for any system. On the other hand, it occasionally is better to apply two modes for control. Sometimes, there are some other applications that may require only one mode to provide a control system. Three gains (K_P, K_I, K_D) exist for the PID-controller and we can provide a desired control system such as PI, PD, P and I controllers by setting undesired gain to zero. Among PID, PI, PD, P and I controllers, PI-controllers are frequently used in numerous recent applications due to the derivative action being sensitive to measurement noise, whereas PD-controllers are underutilized, because the absence of the integral term makes the control system unable to reach its target value of zero error.

In fact, a PI-controller generates the source current amplitude reference (i_{sm}) in equation (2.9). Then, the source current space vector reference is computed in equation (2.8). Therefore, (2.8) and (2.9) are the control equations of the proposed shunt-APF [12]:

$$i_{sm}(t) = K_p \Delta v_c + K_i \int \Delta v_c dt \tag{2.9}$$

where $\Delta v_c = (v_c - v_c^*)$ and v_c^* is the capacitor voltage reference.

So far, the current reference is at hand and we need to provide a proper current control strategy that forces the actual current to pursue its reference. So, two-level hysteresis-band control method has been chosen to fulfill this control processing, but high

switching frequency is the major problem of this approach. Therefore, in this thesis it has been tried to replace two-level by three-level hysteresis-band as a remedy of this problem. It is expected that the switching frequency for three-level hysteresis band should be much smaller than two-level hysteresis band by adding a zero sequence and also we expect to have much lower distortion in the output voltage in comparison with two-level hysteresis [15]. The explanations of both methods are available in the next section.

2.2 Single-band Hysteresis Current Control Method

Single-band hysteresis current control method is one of the common current control methods where the actual current is forced to follow its reference current. Technically, this method limits the actual current between two boundaries equally displaced from the reference. It does not let the actual current to leave the band between the boundaries by turning the switches ON and OFF. The current error is obtained by subtracting the actual current from the reference current, shown by '' *e* '' in Figure 2.3. Next, it is sent to the hysteresis block to become restricted between the mentioned boundaries, therefore the error can be controlled between desired values. Then, the output of the hysteresis block is applied for turning the switches ON and OFF. Note that different topologies for the APF can be applied and the control logic will be different for each topology as well. For instance, three-phase APFs are available with six, eight, twelve, twenty four and forty eight switches, but the applied control logic are very different. The basic topology of hysteresis-band control is shown in Figure 2.3.

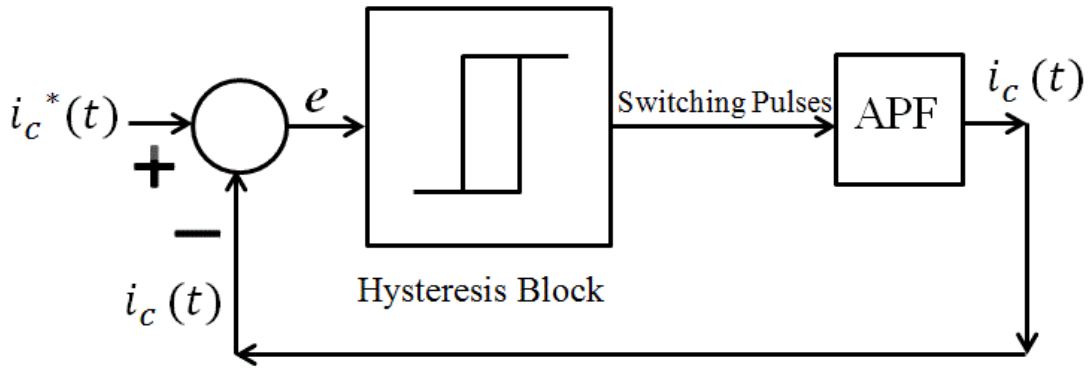

Figure 2.3: Basic Topology of Hysteresis Band

where, the reference current $i_c{}^*$ is compared with the actual current in the hysteresis band. Basically the main principle of operation is as follows:

When the actual current increases and exceeds the prescribed hysteresis boundary, the upper switch would be turned OFF and the lower switch is turned ON. This means that the current is restricted by the upper boundary and it then starts to decay. When the actual current tends to decrease more than below the lower boundary, the upper switch will be ON and the lower switch will be OFF to prevent this descent. Then the current starts to increase again. This process will be constantly repeated to keep the actual ripple in the desired range.

The actual current is increasing and decreasing continually during this period. As a result, the pulse generator should generate $+V_{dc}$ when the slope is positive and $-V_{dc}$ when the slope is negative. Because of this reason this process is named the two-level hysteresis control, and is illustrated in Figure 2.4.

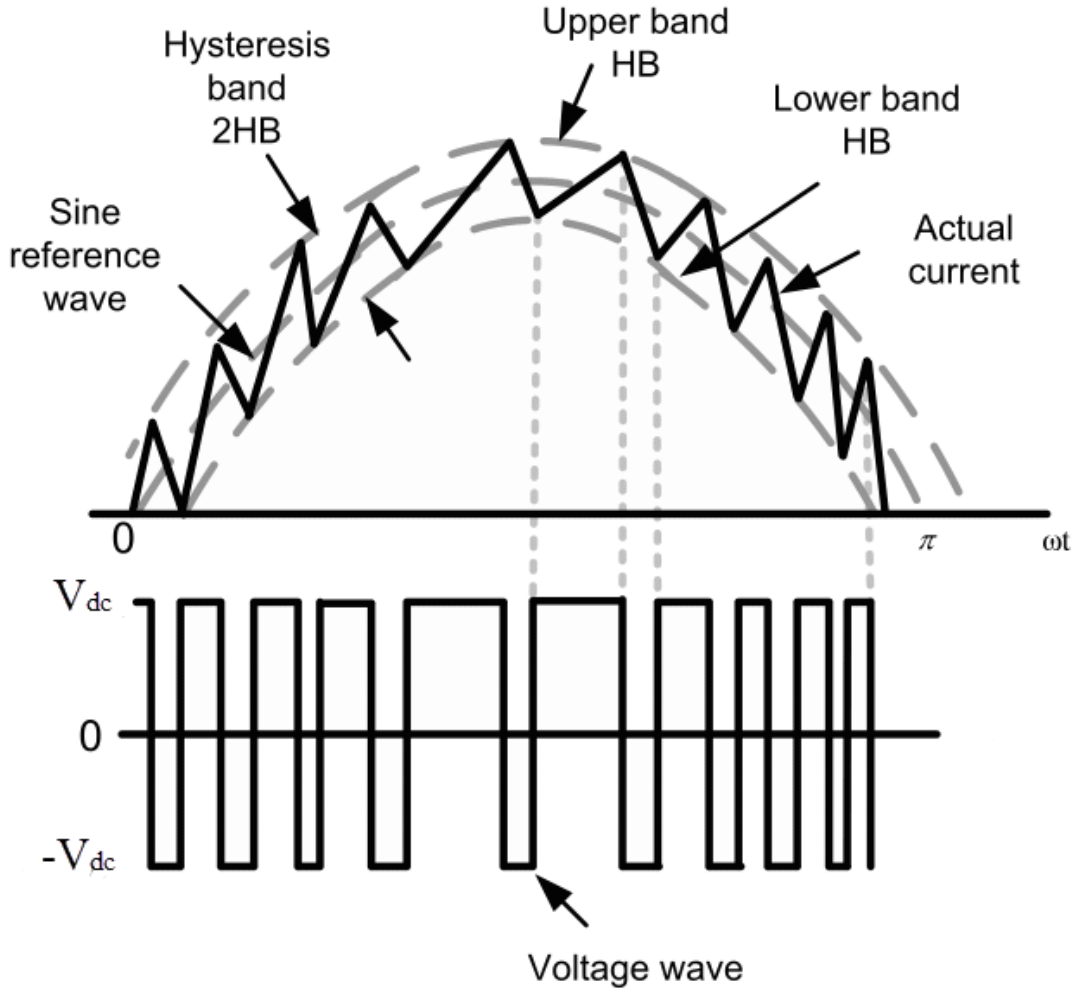

Figure 2.4: Two-level Hysteresis Band Operation [2]

It is very obvious that we can control the ripple and the switching frequency by changing the hysteresis bandwidth. For example, we can have more switching frequency and less ripple by decreasing the bandwidth and vice versa. But, the optimum band should be considered to have desired ripple and switching frequency for the applied system by trial and error.

Hysteresis method can also be applied to three-phase in a similar way to the single-phase system, but all phases should be under hysteresis control separately. The conditions for switching the devices are noted below:

$$\begin{cases} Upper\ switch\ ON \quad or \quad u = 1 \quad for \quad (i^* - i) > HB \\ \\ Lower\ switch\ ON \quad or \quad u = -1 \quad for \quad (i^* - i) < -HB \end{cases} \tag{2.10}$$

where u and HB represent the output of the hysteresis block and the hysteresis bandwidth respectively.

Note that, in spite of the higher accuracy, fast dynamic response, robustness and simplicity in implementation [5], [1], which are counted as major advantages of single-band current control, it has a huge disadvantage such as high switching frequency which gives rise to high switching losses [16]. Therefore, we introduce the optimized hysteresis control method (double-band hysteresis) to overcome this problem.

Chapter 3

DOUBLE-BAND HYSTERESIS CONTROL METHOD

3.1 Double-band Hysteresis Current Control Method

In recent publications, diverse control strategies have been introduced for three-phase APFs. These control strategies have their own advantages and disadvantages related to control complexity, switching frequencies, and dynamic responses. Generally, they consist of three parts, namely: 1) the generation of the reference compensating current from the distorted source current; 2) the current-control of the voltage-source inverter (VSI); and 3) control of DC-capacitor voltage. The reference compensating current generation process usually involves various methods. It is well known that the quality of the current-control strategy greatly influences the overall performance of the APF system. Since the load current harmonics may change rapidly, the APF should have a fast dynamic response for achieving a high accuracy in current tracking. For this reason, the current-control loop, which is always faster than the voltage-control loop, is used to perform the reference current tracking. The voltage-control loop is responsible for regulating the capacitor voltage which is usually achieved by a PI controller. Among the current-control strategies, the conventional single-band hysteresis current control (SBHCC) has received much attention due to its major advantages such as higher accuracy, fast dynamic response, robustness and simplicity in implementation [5] [1]. Despite these advantages, the SBHCC has a major disadvantage that the switching frequency is very high at lower modulation indices which increases switching losses. In principle, high switching frequency leads to a

much better waveform for the compensating current reference. However, high switching frequency also results in high switching losses. These losses can be reduced by increasing the width of the hysteresis band, at the expense of decreasing the switching frequency. Therefore, the hysteresis band is to be chosen to make a compromise between switching frequency and switching losses of the APF. The adaptive hysteresis current control (AHCC) approach overcomes this problem by changing the hysteresis band as a function of reference compensating current variation so as to keep the switching frequency nearly constant [11]. Although this approach gives satisfactory result, a fixed switching frequency is obtained at the expense of additional signal processing and control complexity requirements.

In this thesis, a double-band hysteresis current control (DBHCC) scheme is introduced for three-phase shunt active filters. The double-band hysteresis approach permits the access of the zero level of the active filter's output voltage so that a switching device is only switched during a half-cycle, while it remains either ON or OFF during the other cycle. Such operation not only results in a much lower average switching frequency than that of the SBHCC scheme for the same parameter values, but also offers a smaller source current distortion for small hysteresis band values. First, the mathematical modeling of the three-phase APF will be developed. Then, we will use the proposed DBHCC to simulate the APF using SIMULINK/MATLAB. Finally, the results will be compared with those obtained by the SBHCC method.

In this chapter we investigate double-band hysteresis current control method in detail and SIMULINK/MATLAB results would be compared with single-band in the next chapter.

As seen in Figure 3.1, the reference current i_c is compared with the actual current in the double-band hysteresis similar to single-band, but there is a little difference. It means that the operation of the double-band hysteresis directly depends on the error conditions as follows: When the error value is positive and the actual current exceeds the prescribed 1st upper hysteresis boundary, 1st upper switch would be turned OFF and the 1st lower switch is turned ON at this time and when the actual current passes the 1st lower boundary while it decreases, 1st upper switch would be turned ON and the 1st lower switch is turned OFF. It means that the actual current is restricted by 1st upper and 1st lower boundaries, where the error value is positive. When the error value is negative and the actual current tends to increase beyond the 2nd upper boundary, 2nd upper switch would be turned OFF and 2nd lower switch will be turned ON. When the actual current tends to decrease below the 2nd lower boundary, 2nd lower switch will be OFF to prevent this descent. In this situation the error is changing between 2nd lower and 2nd upper boundaries. On the other hand, single-band operation is applied for both negative and positive error separately. Note that, the zero value cannot be selected for 1st lower and 2nd upper boundary values, because by selecting zero value, the dead-band space (the gap between 1st lower and 2nd upper) will be removed and it may turn the three-level operation to two-level.

So, the actual current is increasing and decreasing continually during this period. As a result, when the error is positive, negative and positive slopes will also appear and the pulse generator should generate $+V_{dc}$ and 0 where the slope is positive and negative respectively. When the error is negative, 0 and $-V_{dc}$ should be generated for the positive and negative slopes respectively. Because of this reason this process is named the three-level hysteresis control, and is illustrated in Figure 3.1.

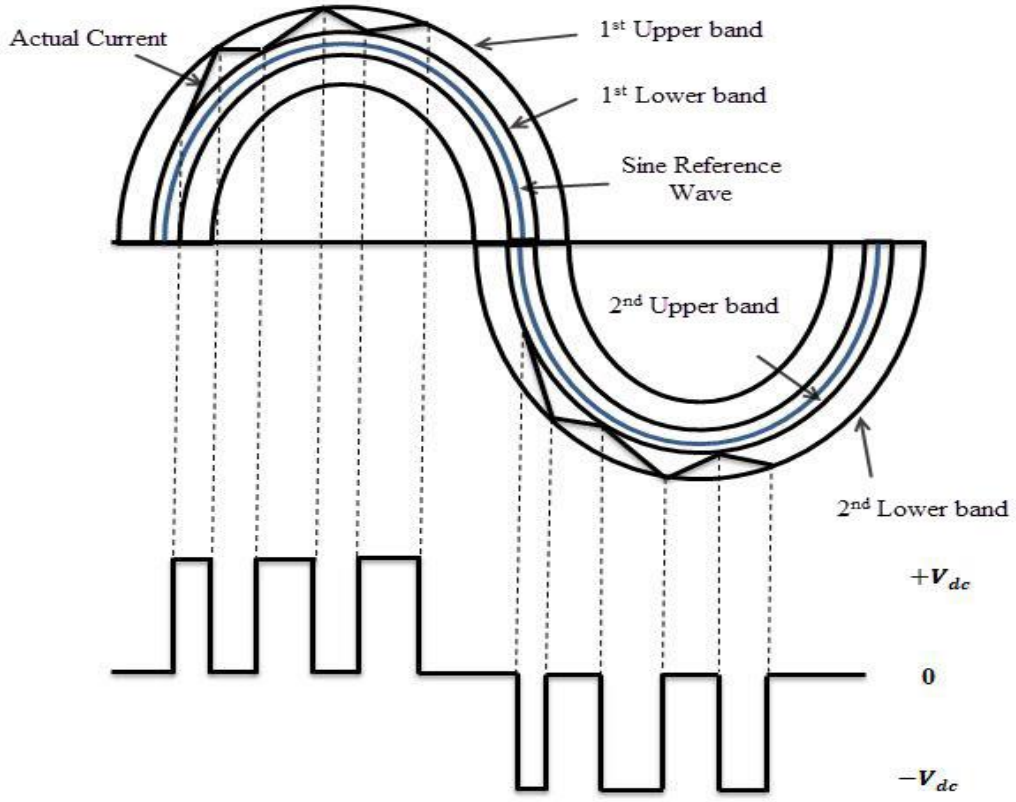

Figure 3.1: Double Hysteresis Band Operation

The hysteresis current control method can also be applied to three-phase similar to the single-phase system. All the phases should be under hysteresis control separately. The conditions for switching the devices are stated below:

$$\begin{aligned} &If \quad Error \geq 0 \quad Then \begin{cases} u = 1 & for\ Error \geq HB \\ u = 0 & for\ Error \leq \delta \end{cases} \\ &If \quad Error < 0 \quad Then \begin{cases} u = -1 & for\ Error \leq -HB \\ u = 0 & for\ Error \geq -\delta \end{cases} \end{aligned} \tag{3.1}$$

where, u, HB and δ represent the output of the hysteresis block, hysteresis bandwidth and dead-band width respectively.

The proposed method has been applied on four different topologies such as:

1. Three-phase two-level four-wire capacitor-midpoint inverter with 6-IGBTs.
2. Three-phase three-level cascaded H-bridge inverter with 12-IGBTs.
3. Three-phase three-level neutral point clamped inverter with 12-IGBTs (NPC-inverter).
4. Three-phase five-level cascaded H-bridge inverter with 24-IGBTs.

Three-phase two-level four-wire capacitor-midpoint inverter in Figure 3.2 is the simplest type of three-phase two-level voltage source converter (VSC) and might be named as a six-pulse bridge where the thyristors have been replaced by IGBTs with inverse-parallel diodes. In most low voltage (LVDC) applications, MOSFETs are used for having a fast switching response. For medium (MDVC) and high voltage (HVDC) applications, which need high conduction current, IGBTs, thyristors or GTOs are employed to have better performance; an IGBT can act like a MOSFET at its input for fast switching response and it can also act like a BJT with less conduction losses at its output. Note that DC capacitors are playing the source voltage role in APF's inverters. On the other hand, there is no power supply on this side of inverters, because active power filter's inverters should act like a compensator, which means that the average of transmitted energy between active power filter and power system must be zero. In addition, APF's controller is designed to keep the DC voltage constant and this action forces the power system to compensate the APF's losses.

For optimizing the harmonic elimination performance, some HVDC systems have been built with three-level. A common type of three-level converter is the neutral-point-clamped (NPC) converter, where each phase contains four IGBT switches. In Figure 3.3 and Figure 3.4 a three-phase three-level cascaded H-bridge and three-phase three-level neutral point clamped inverter are shown as three-level VSC's. Figure 3.5 shows the three-phase five-level cascaded H-bridge inverter which is now becoming the most common type of VSC for HVDC.

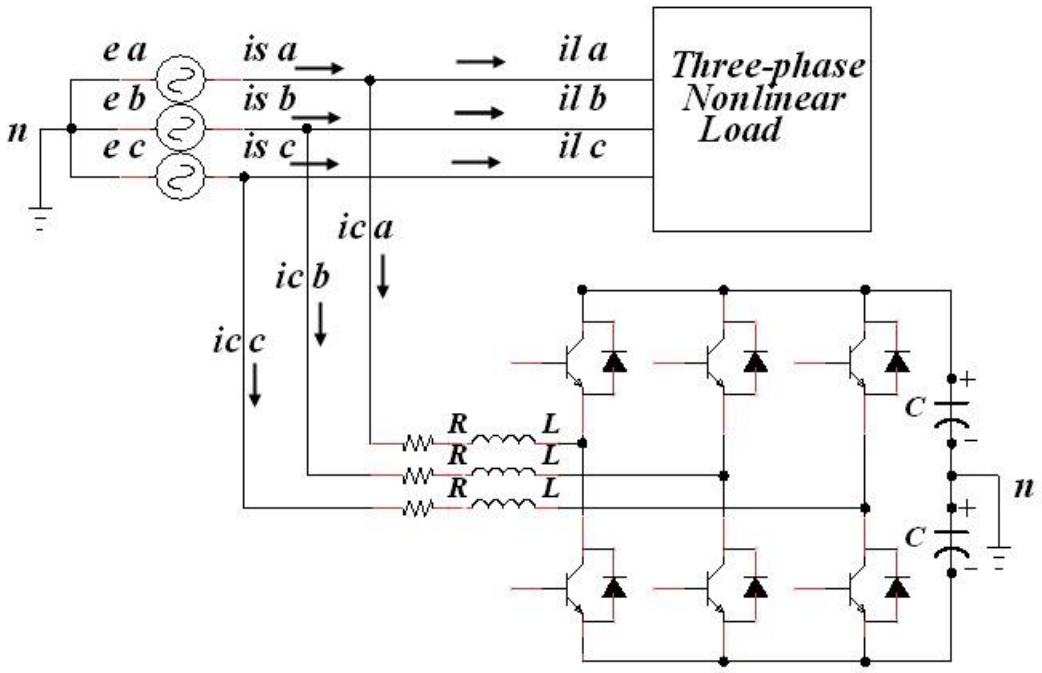

Figure 3.2: Three-phase Two-level Four-wire Capacitor-midpoint Inverter Topology

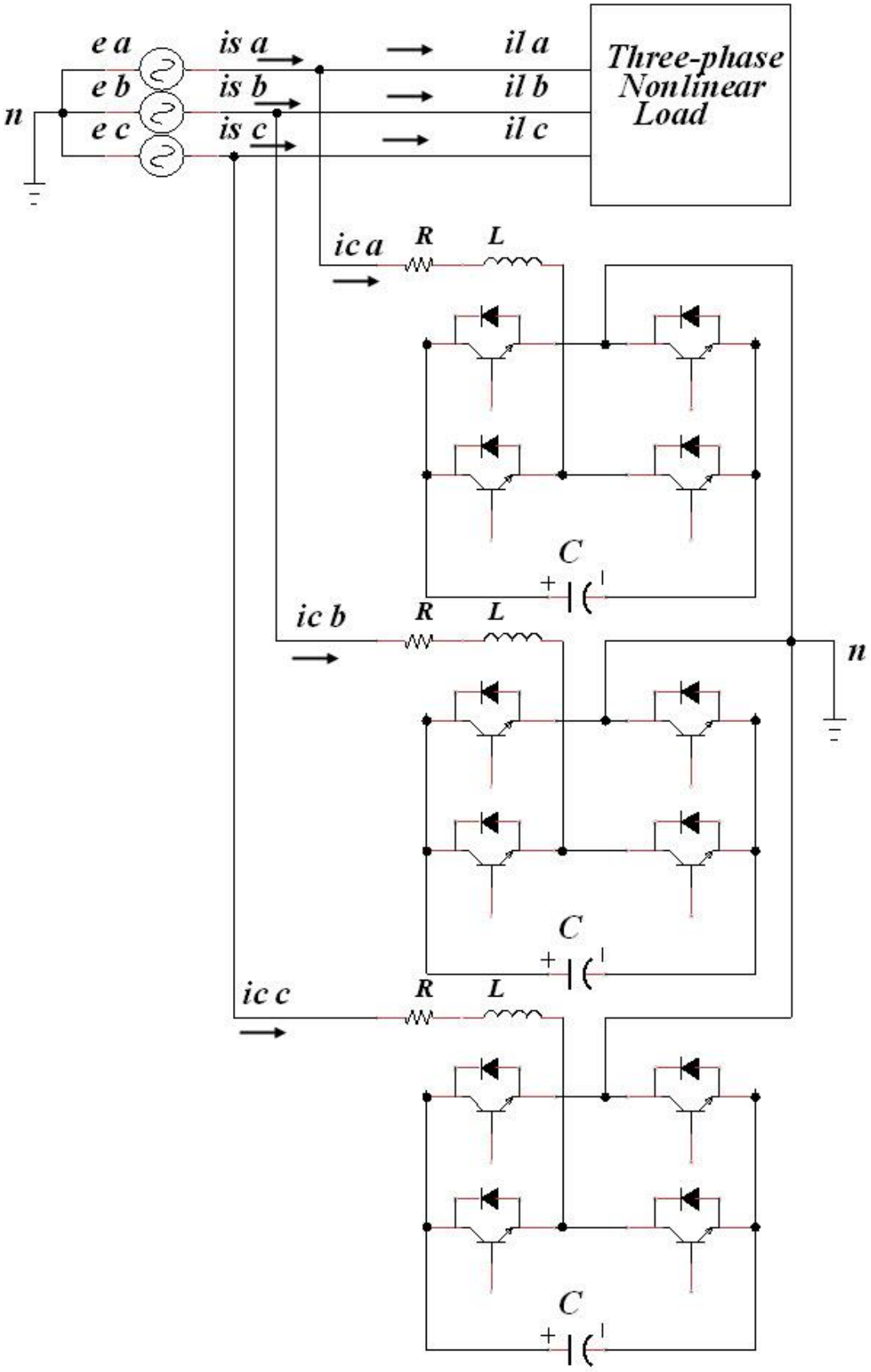

Figure 3.3: Three-phase Three-level Cascaded H-bridge Inverter Topology

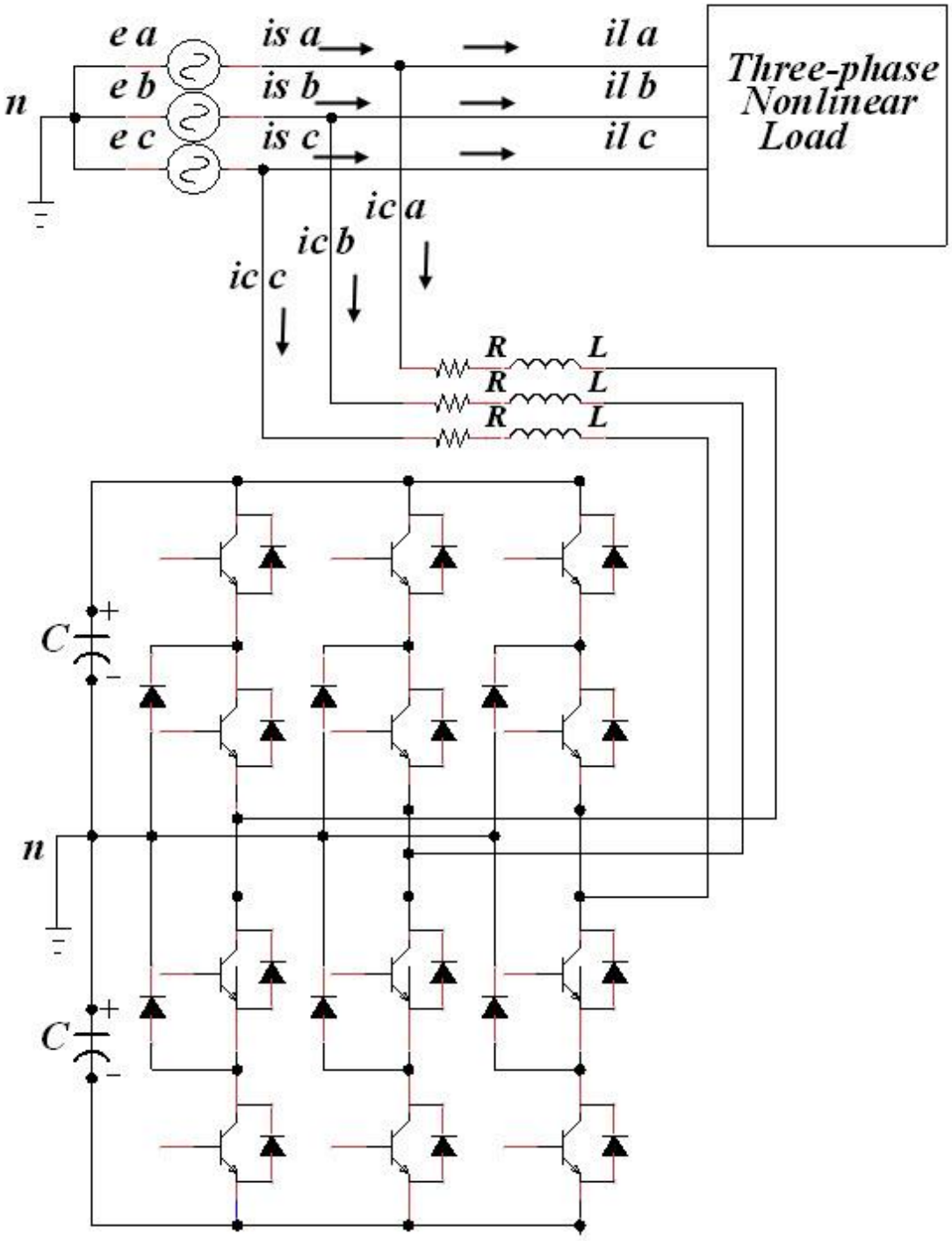

Figure 3.4: Three-phase Three-level Neutral Point Clamped Inverter Topology

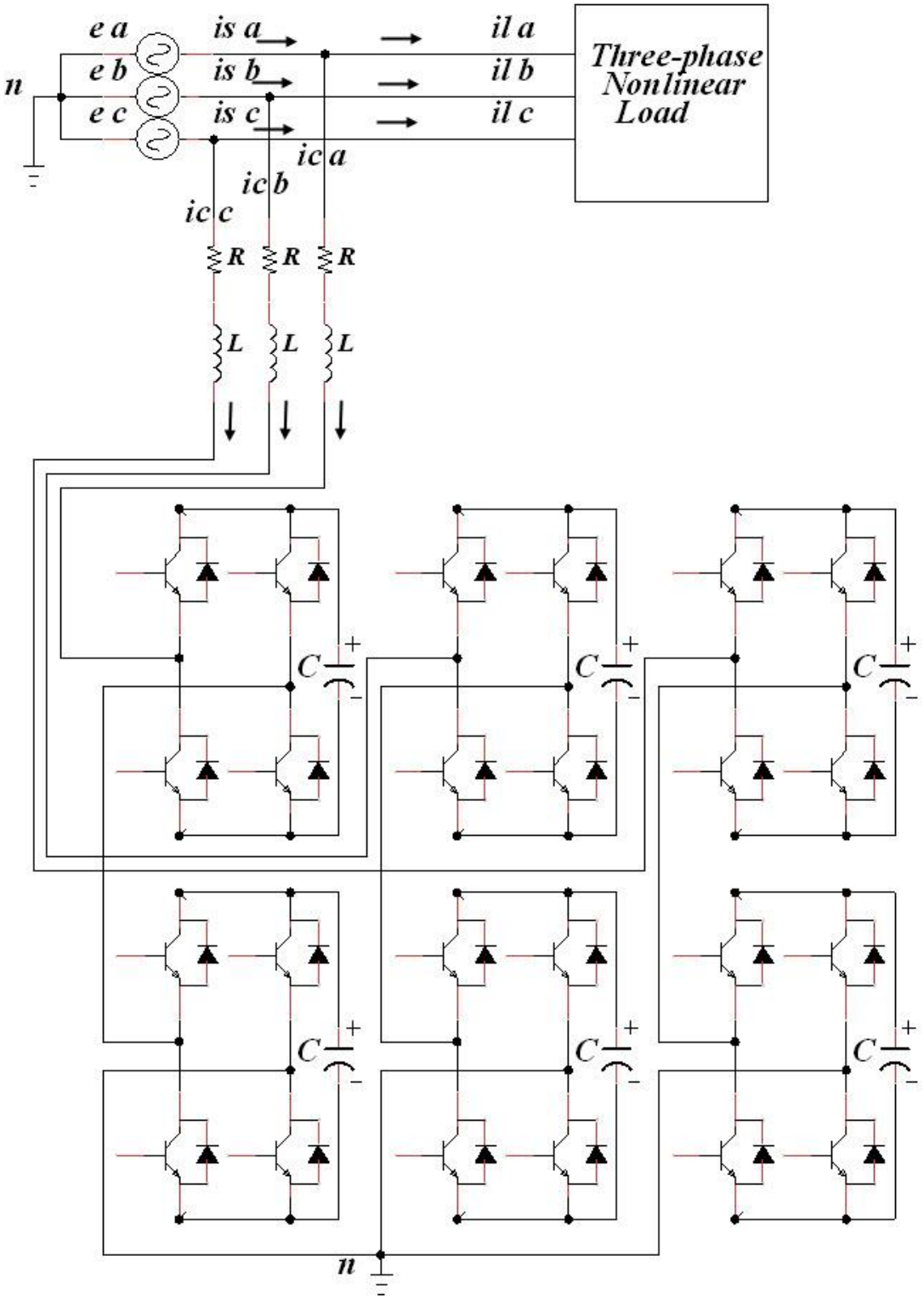

Figure 3.5: Three-phase Five-level Cascaded H-bridge Inverter Topology

3.2 PWM Principle and Controlling the Output Voltage

Pulse Width Modulation (PWM) or Pulse Duration Modulation (PDM) is a common way and technique for representing an analog signal in the digital domain. So, because of the existence of electronic switches in the inverters, there is a possibility to control the inverter output voltage by operating multiple switches. Figure 3.6 clearly explains the output voltage control operation based on the PWM principle [2].

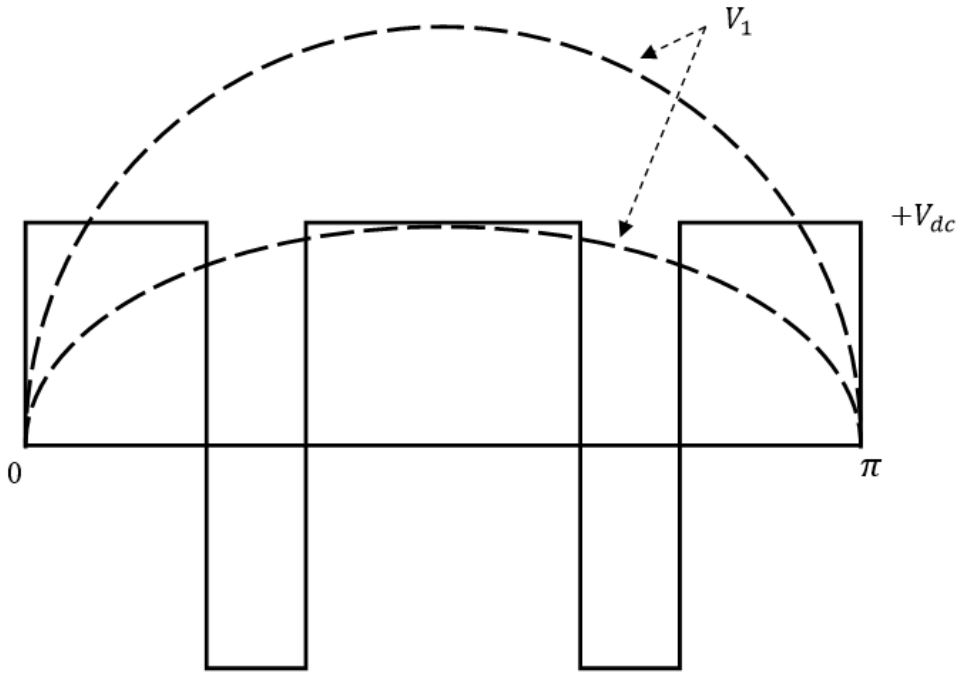

Figure 3.6: Controlling Output Voltage Based on PWM Principle [2]

Assume that V_1 is the fundamental voltage and it has the maximum amplitude for a square wave. As we can see in Figure 3.6, the magnitude has been reduced by creating two notches. Note that, the fundamental voltage would also be reduced if the notch widths are increased.

In this section, we introduce classification of PWM techniques which can be given as follows:

- Sinusoidal PWM (SPWM)
- Selected harmonic elimination (SHE) PWM
- Minimum ripple current PWM
- Space-Vector PWM (SVM)
- Random PWM
- Hysteresis band current control PWM
- Sinusoidal PWM with instantaneous current control
- Sigma-delta modulation

Often, PWM techniques can be categorized based on the current or voltage control, carrier- or non-carrier-based control, feed-forward or feed-back methods, etc. According to the above classification, we only review the sinusoidal PWM technique to show the typical output voltage waveforms for all proposed topologies.

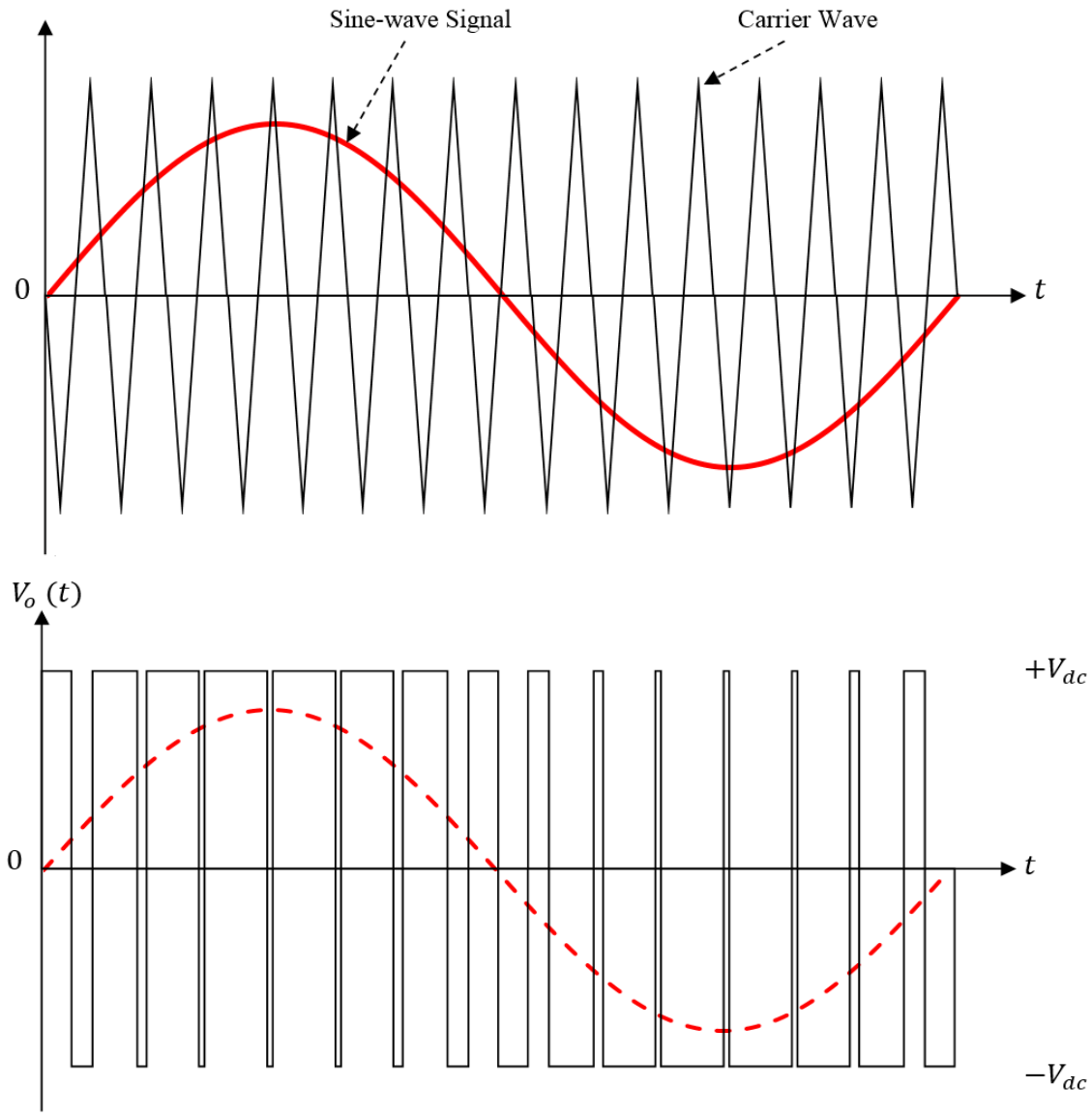

Figure 3.7: Principle of Sinusoidal PWM [2]

Figure 3.7 indicates the principle of sinusoidal PWM, where the triangle carrier wave is compared with sinusoidal wave to produce a PWM wave. Note that the intersection point determines the switching point of power devices [2]. As it is observed, the notches and pulse widths are changed in a sinusoidal manner. In the following figures, all output voltage waveforms are shown for all proposed topologies. Figure 3.8 indicates the output voltage of a two-level inverter. It can be seen that the output

voltage varies between $+V_{dc}$ and $-V_{dc}$ values. Figure 3.9 shows the output voltage of a three-level inverter. The output voltage has three values of $+V_{dc}$, 0 and $-V_{dc}$ and finally, the output voltage of a five-level inverter and the sinusoidal filtered voltage output has been depicted in Figure 3.10.

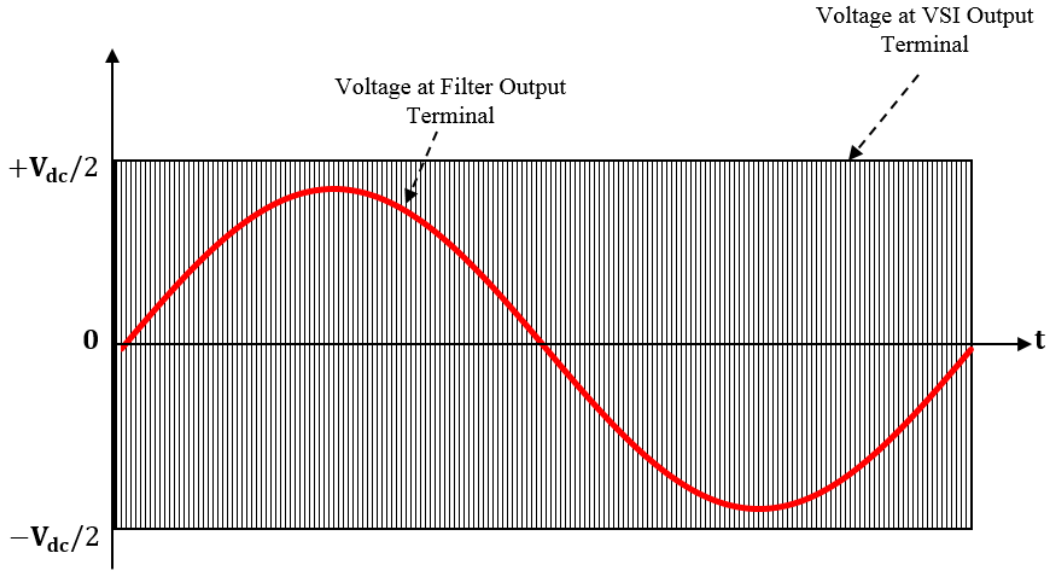

Figure 3.8: The Output Voltages of Two-level Inverter

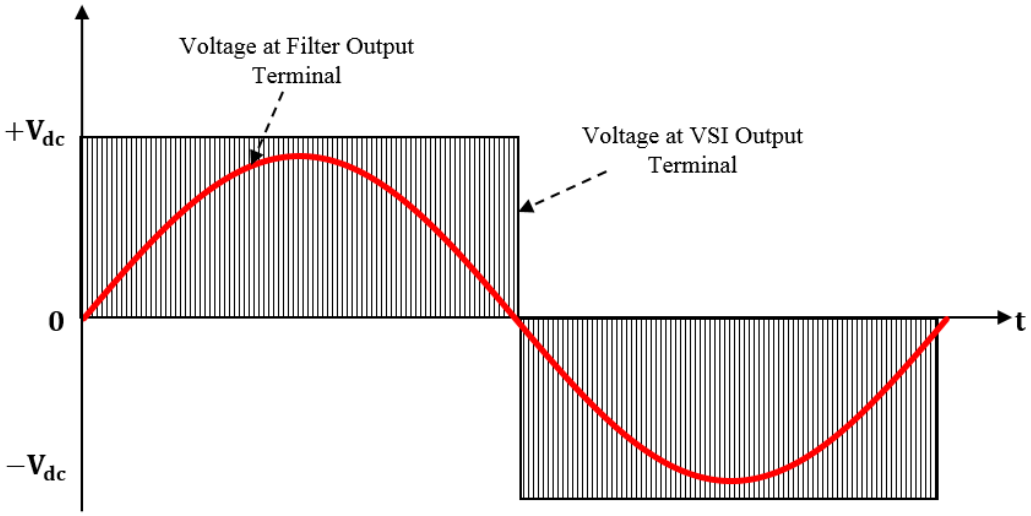

Figure 3.9: The Output Voltages of Three-level Inverter

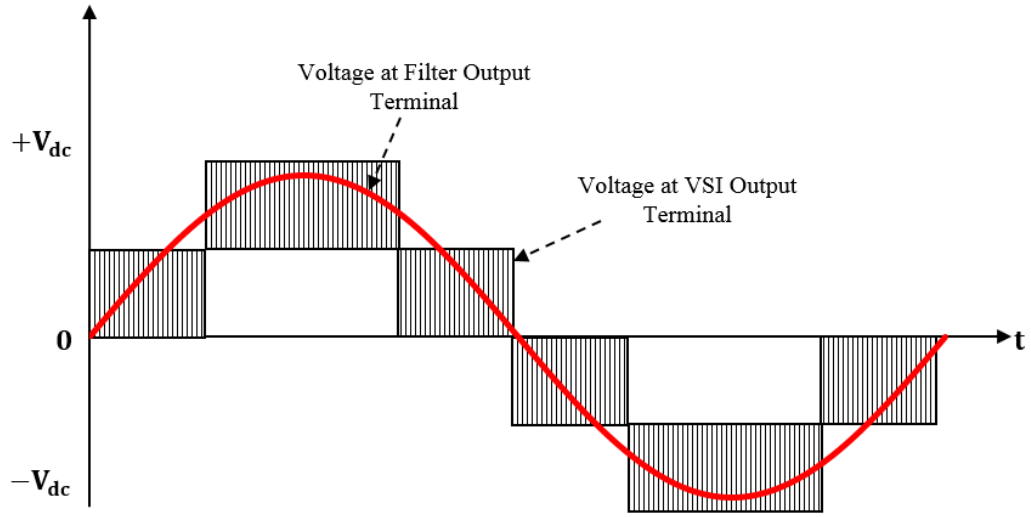

Figure 3.10: The Output Voltages of Five-level Inverter

Chapter 4

SIMULATION RESULTS AND DISCUSSIONS

In this chapter we show the results which have been obtained in SIMULINK /MATLAB/2012a. First, the operation of the system will briefly be explained. Next the results for a three-phase APF system controlled by two-level hysteresis band are shown for the four different topologies.

Then, three-level hysteresis band control method will be applied to the system with similar parameters. Finally, the results of all the simulations will be compared. The schematic involving only one of the four topologies is illustrated in Figure 4.1.

Note that the three-phase load which is located on the top right side of Figure 4.1 is simulated by the thyristor block in MATLAB with given values of $R = 20\ \Omega$ and $L = 1\ mH$. Also the generated waveforms for a three phase load are available in Figure 4.2.

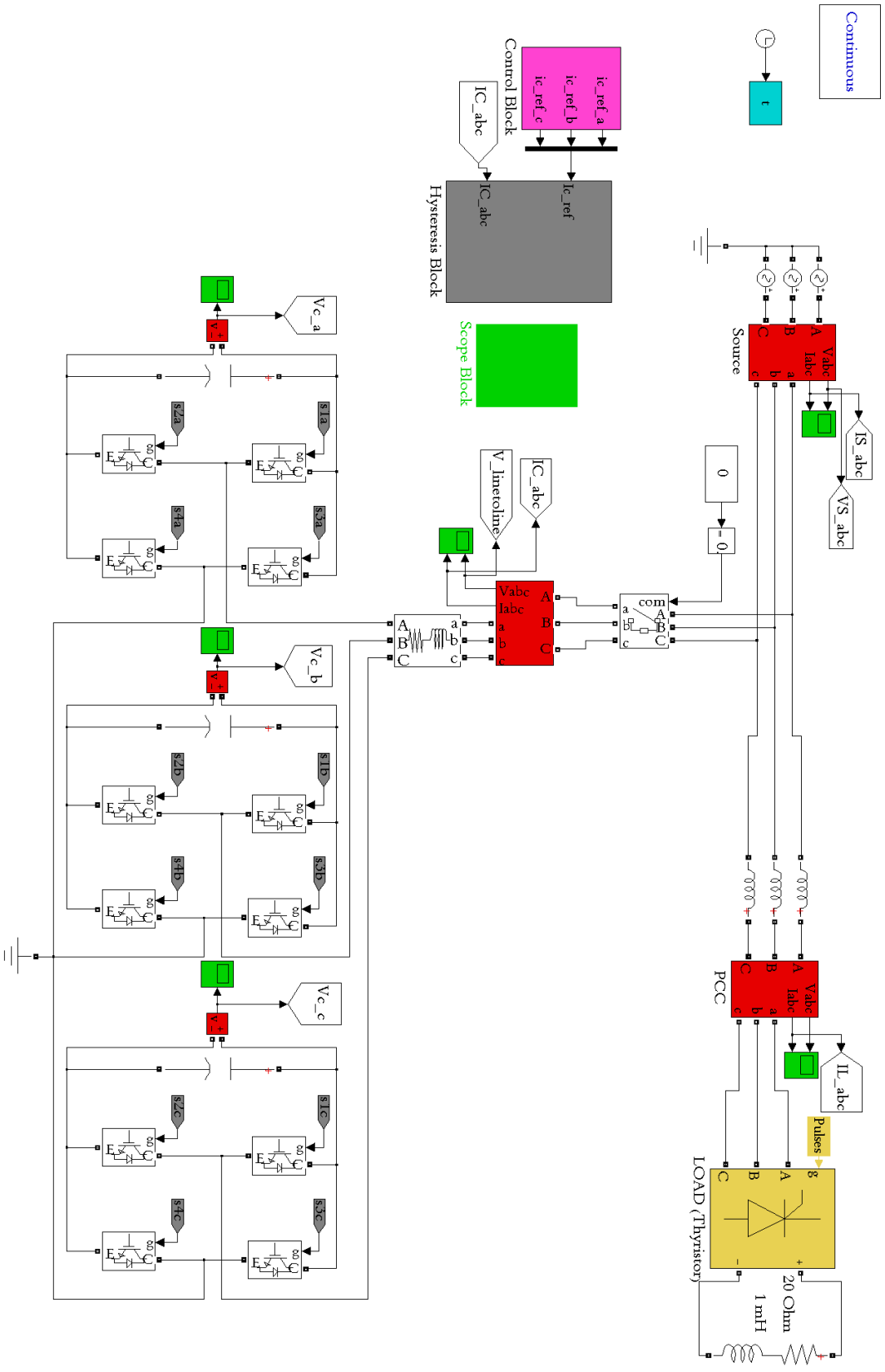

Figure 4.1: Schematic of Implemented System of Three-phase Three-level Cascaded H-bridge Inverter Topology

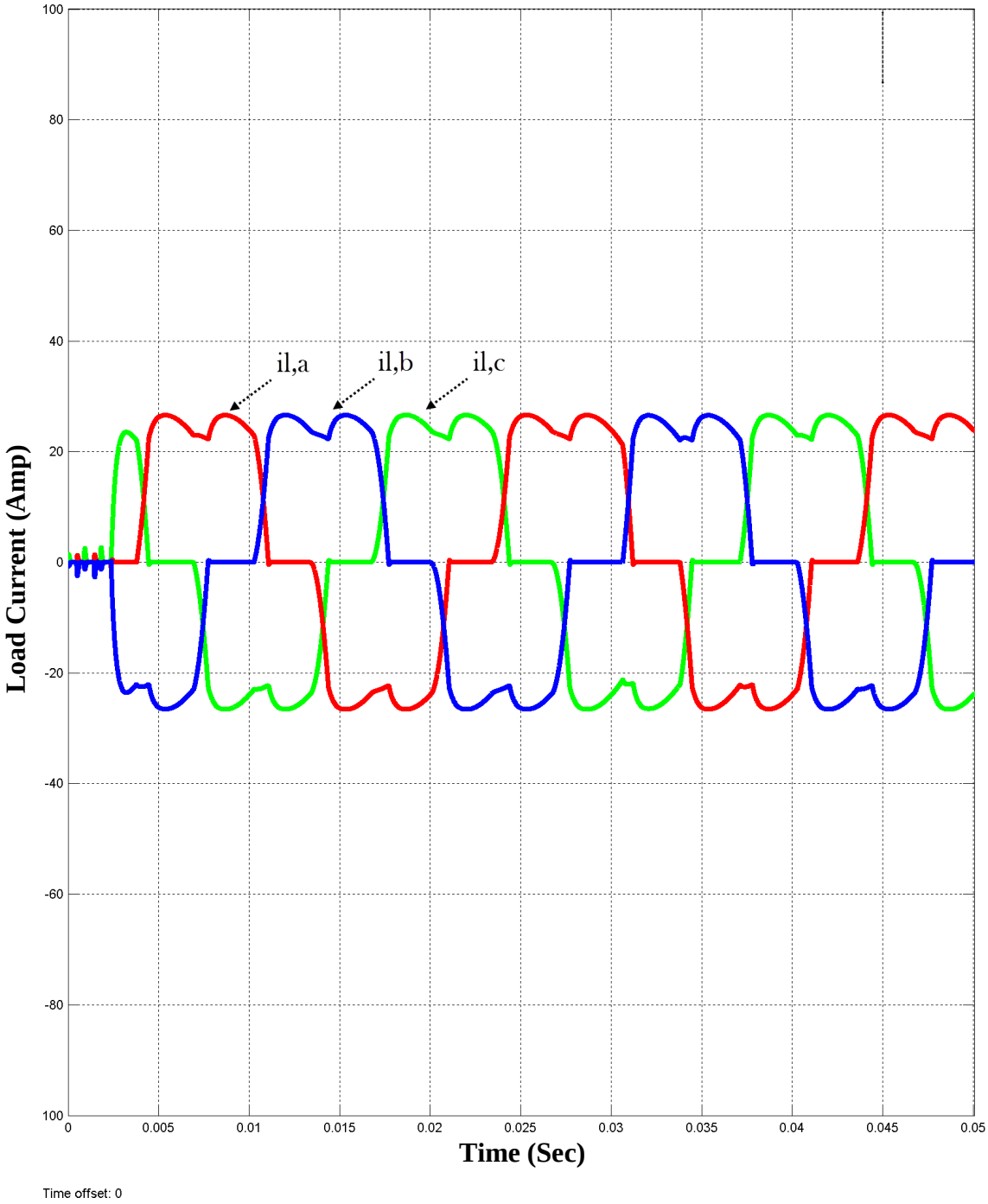

Figure 4.2: Three-phase Load Current Waveforms

As can be seen at the top left side of Figure 4.1, the voltage source is modeled by three separate single phases and the ground is connected to all the three phases. The chosen values for peak amplitude voltage, frequency, and phase angles are $E_m = 310V, f =$

$50Hz$ and $\varphi = -30°, 90°, 210°$ respectively. This kind of supply is named as a balanced voltage supply because all the peak amplitude voltage values for phases a, b, c are the same $E_m = 310V$ and the difference between phase angles is $120°$. On the other hand, applied voltages for phases a, b, c can be expressed as follows:

$$\begin{aligned} e_a(t) &= 310\, sin(\omega t + 90°) \\ e_b(t) &= 310\, sin(\omega t - 30°) \\ e_c(t) &= 310\, sin(\omega t + 210°) \end{aligned} \tag{4.1}$$

Note that, these can also be written as:

$$\begin{aligned} e_a(t) &= 310\, cos(\omega t) \\ e_b(t) &= 310\, cos(\omega t - 2\pi/3) \\ e_c(t) &= 310\, cos(\omega t + 2\pi/3) \end{aligned} \tag{4.2}$$

The APF in Figure 4.1 consists of two control blocks and a three-phase inverter. The values of the boost inductance and resistance are $L = 4\, mH$ and $R = 1.0\, \Omega$. As mentioned in former chapters, the role of the APF is to inject the appropriate compensation current i_c. Using KCL at PCC, equation (4.3) expressing this fact is obtained:

$$i_s - i_l - i_c = 0 \tag{4.3}$$

So, similar to $i_{s_{a,b,c}}$ and $i_{l_{a,b,c}}$, filter current $i_{c_{a,b,c}}$ can be constantly measured by a three-phase measurement block during the process (all red blocks in Figure 4.1

represent the measurements). In this step, we need to generate the reference $i_c{}^*$ for i_c for sending the error to the hysteresis block. Therefore, generating $i_c{}^*$ for all three phases a, b, c can be done after the following steps:

1. PI-controller generates the source current amplitude reference (i_{sm}). Figure 4.3 shows the SIMULINK/MATLAB implementation. Bear in mind that $v_c{}^* = 800V$ is selected due to boost topology.

$$i_{sm}(t) = K_p \Delta v_c + K_i \int \Delta v_c dt \tag{4.4}$$

where $\Delta v_c = (v_c - v_c{}^*)$ and $v_c{}^*$ is the capacitor voltage reference. Note that $K_p$and K_i are the gains for the PI controller and their selected values are -0.3 and -6 respectively.

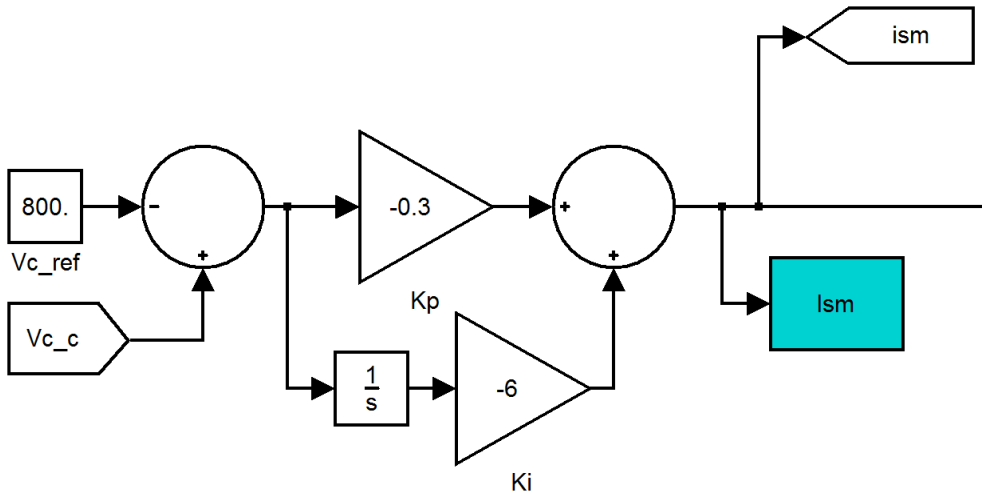

Figure 4.3: Generating Reference Amplitude of Source Current

2. The space vector reference of the source current is then determined by equation (4.5) and Figure 4.4 indicates the implementation.

$$i_s{}^* = i_{sm}(t)e^{j\omega t} \tag{4.5}$$

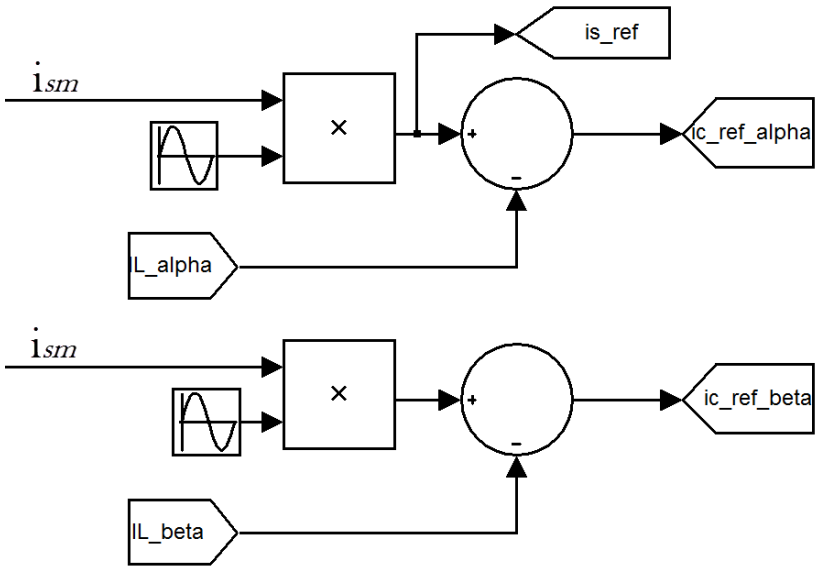

Figure 4.4: Generating Reference for Space Vector of Source Current

Note that $i_s{}^*$ is generated with respect to the two-axis frame but, i_l which has been measured is still in a, b, c frame (three-axis). So, Clarke transformation is applied to obtain the projection of the three-axis representation ($i_{l_{a,b,c}}$) onto the two-axis one ($i_{l_{\alpha,\beta}}$).

3. Then, by using Clarke transformation (see equation (2.4)) $i_{l_{a,b,c}}$ is converted to $i_{l_{\alpha,\beta}}$ and, it is ready to be subtracted from $i_s{}^*$ to generate $i_{c_\alpha}{}^*$ and $i_{c_\beta}{}^*$. (See Figure 4.4 and Figure 4.5).

$$i_c{}^* = i_s{}^* - i_l \tag{4.6}$$

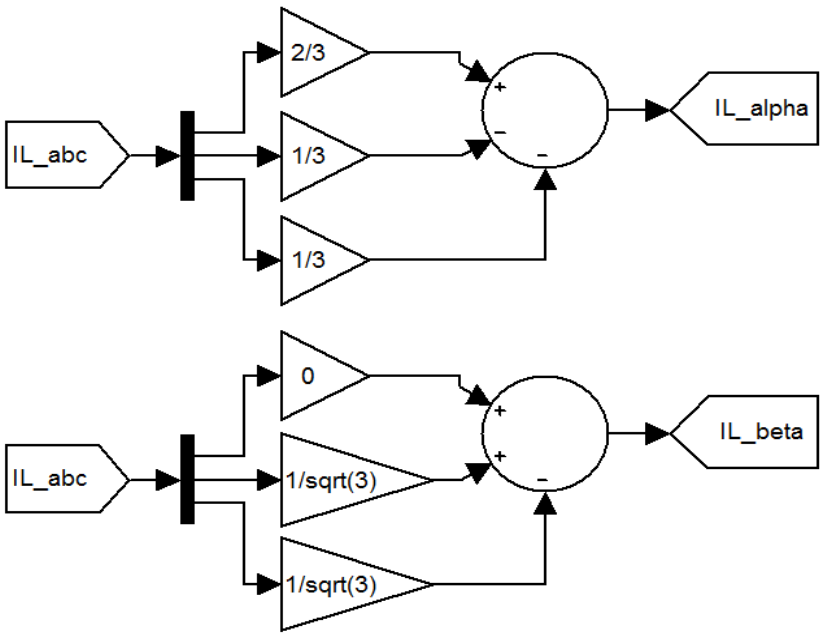

Figure 4.5: Implementation of Clarke Transformation

4. Note that, the resulting i_c^* is not in the $(\mathrm{a}, \mathrm{b}, \mathrm{c})$ frame, so before subtracting $i_{c_{a,b,c}}$ fromi_c^*, an inverse Clarke transformation should be applied to obtain i_c^* in the (a, b, c) frame. The SIMULINK model which implements equation (2.5) is shown in Figure 4.6.

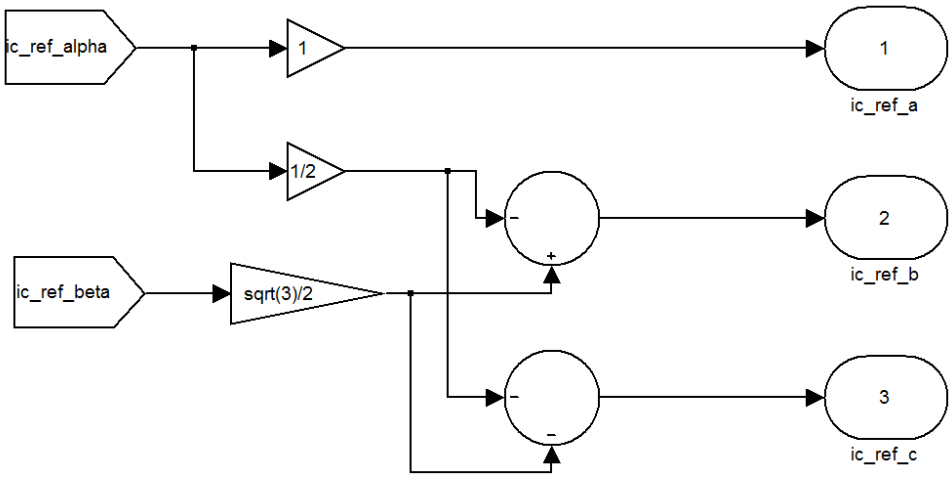

Figure 4.6: Implementation of the Inverse Clarke Transformation

Right now, $i_{c_{a,b,c}}$ and $i_{c_{a,b,c}}{}^{*}$ are available to generate the error values for each phase by subtracting the reference values from the measured ones. The result of this subtraction is denoted ‘’Error’’ (e).

So the resulting error can be applied to the hysteresis block with regard to equations (2.10) and (3.1), which represent the operation of single- and double-band hysteresis controllers respectively. Figures 4.7 and 4.8 show the implementation models of all applied topologies.

Note that in this case, the saturation block is used to convert the hysteresis block output to the logic values of 0 and 1, which should be applied to the switches instead of the hysteresis output levels of 1 and -1.

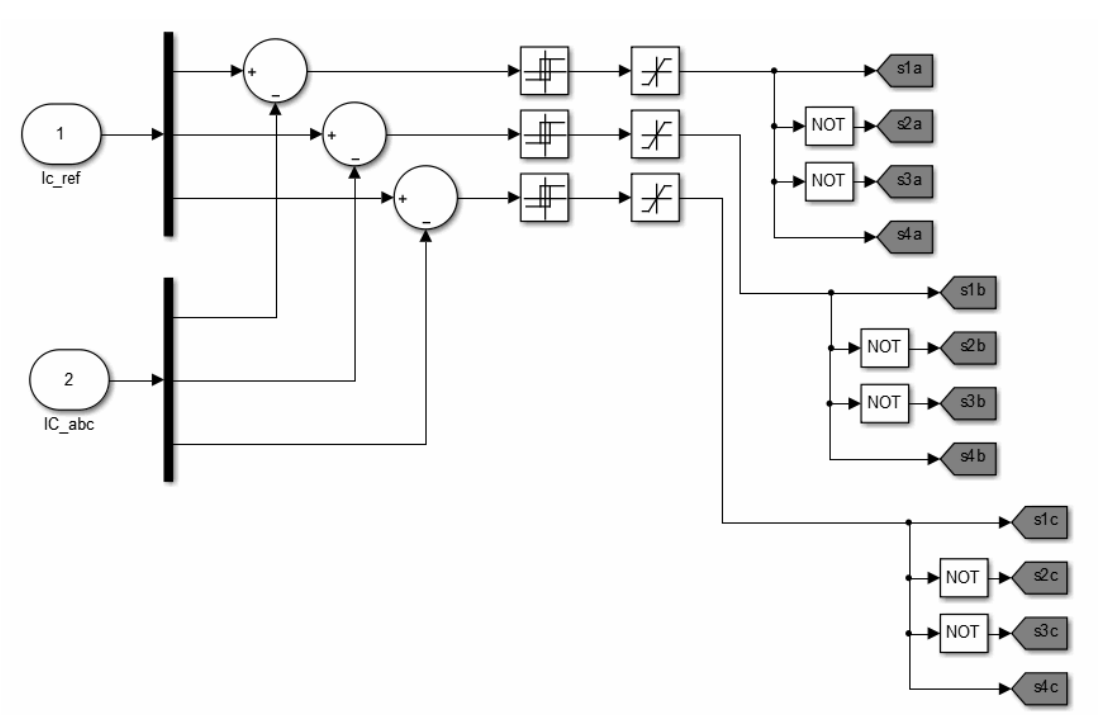

Figure 4.7: Implementation of Single-band Hysteresis Current Control Method

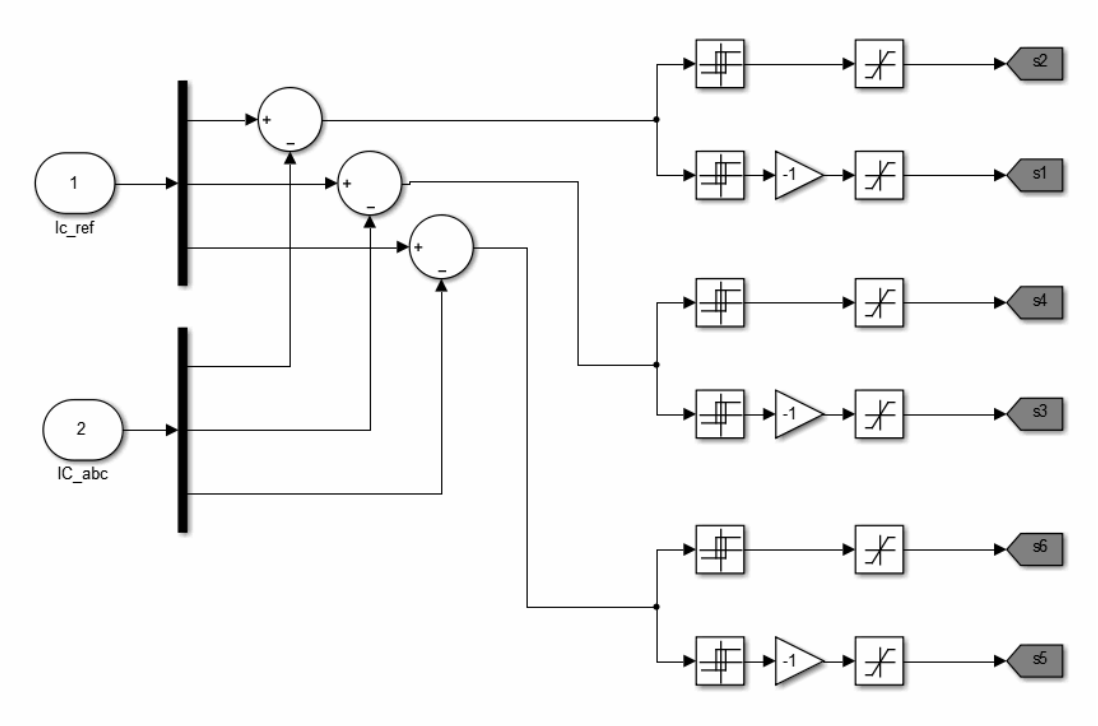

(a) Implementation of Double-band Hysteresis Control of Three-phase Two-level Four-wire Capacitor-midpoint Inverter Topology

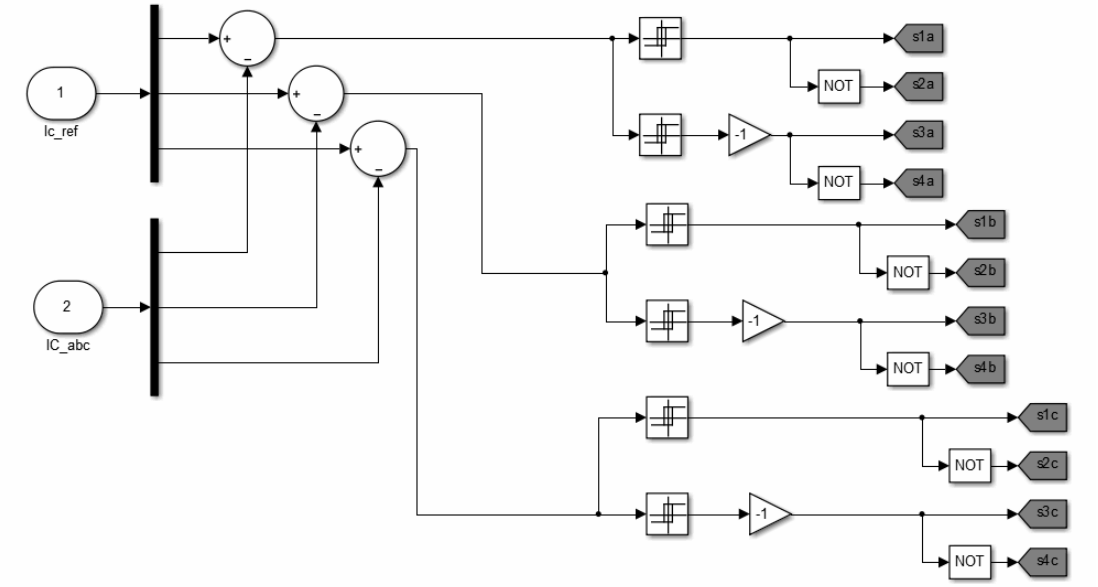

(b) Implementation of Double-band Hysteresis Control of Three-phase Three-level Cascaded H-bridge Inverter Topology

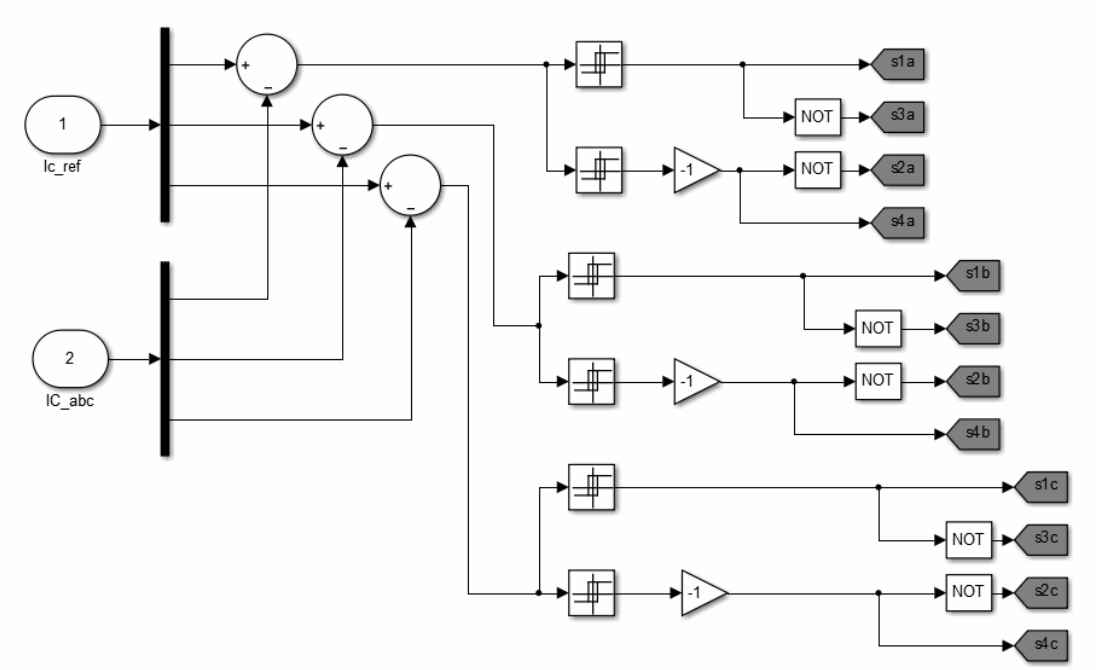

(c) Implementation of Double-band Hysteresis Control of Three-phase Three-level Neutral Point Clamped Inverter Topology

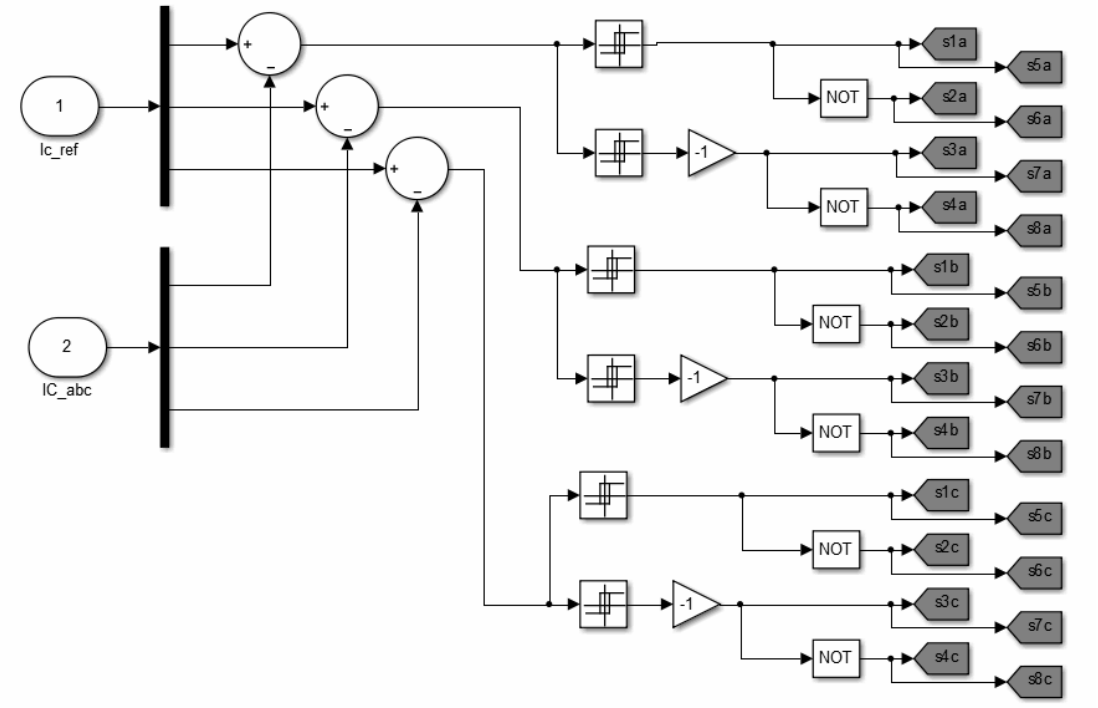

(d) Implementation of Double-band Hysteresis Control of Three-phase Five-level Cascaded H-bridge Inverter Topology

Figure 4.8 Implementation of Double-band Hysteresis Current Control Method on Four Different Topologies

The line current, load current and filter current (only for phase a) are shown in Figures 4.9 and 4.11. But, in Figure 4.9 there are some spikes on the line current which makes it depart from the pure sinusoidal waveform. Note that the generated spikes arise from sudden variations of the load current at certain instants. So, three inductors have been placed in series with the load to overcome this problem.

As it is observed, all existing spikes in Figure 4.9 are completely eliminated in Figure 4.11. Meanwhile, for simplicity all the line, load and filter currents are depicted together in Figures 4.10 and 4.12 with and without spikes respectively. For better understanding the operation of the hysteresis control method, line current i_{s_a} and its reference $i_{s_a}{}^*$ are indicated on the same figure with different colors.

It is obviously clear that line current i_{s_a} follows its reference $i_{s_a}{}^*$ in all circumstances. (See Figures 4.13 and 4.14 for single- and double-band hysteresis control methods). Also the three-phase line currents are shown together in Figure 4.15.

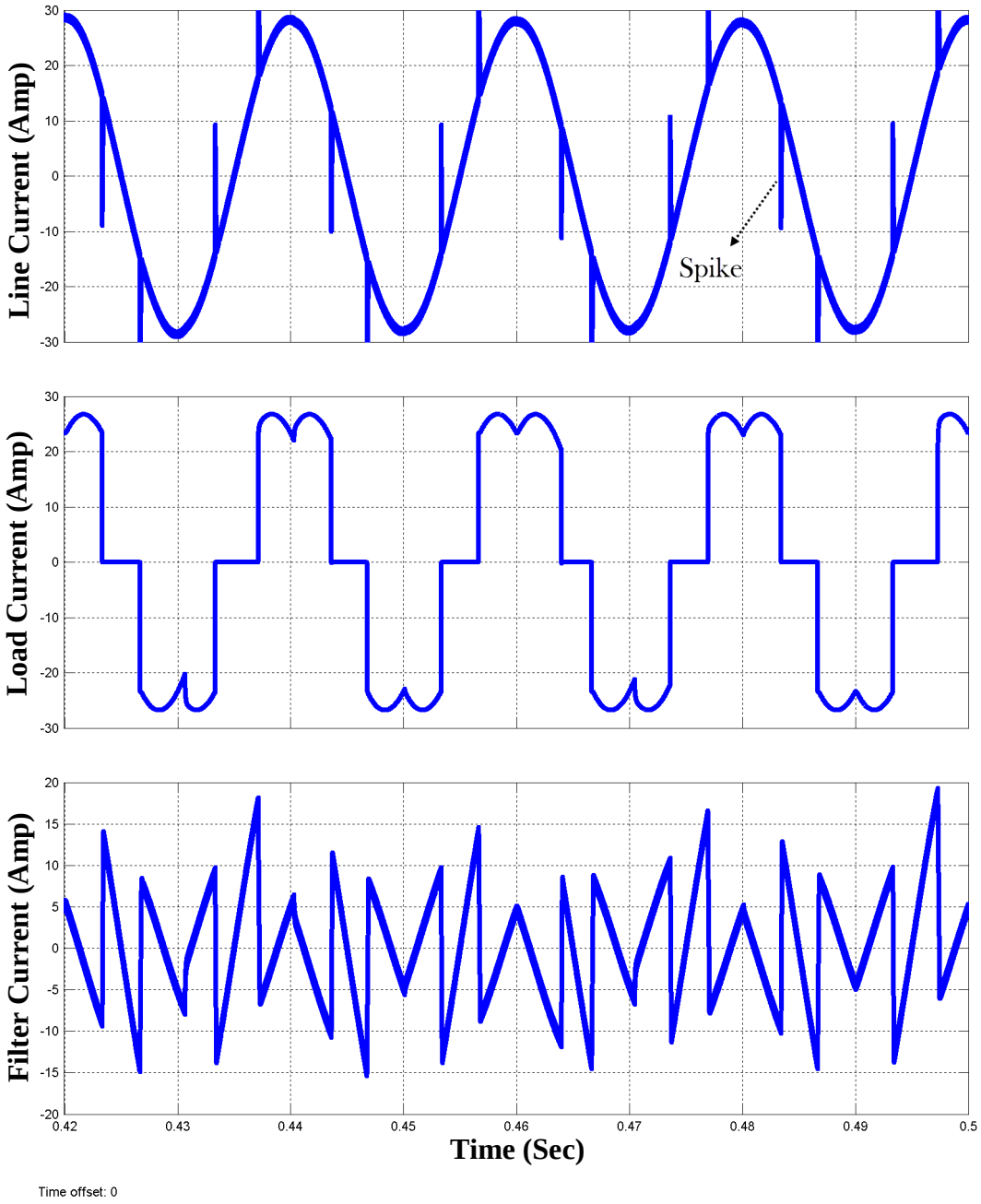

Figure 4.9: Line Current, Load Current and Filter Current with Spikes

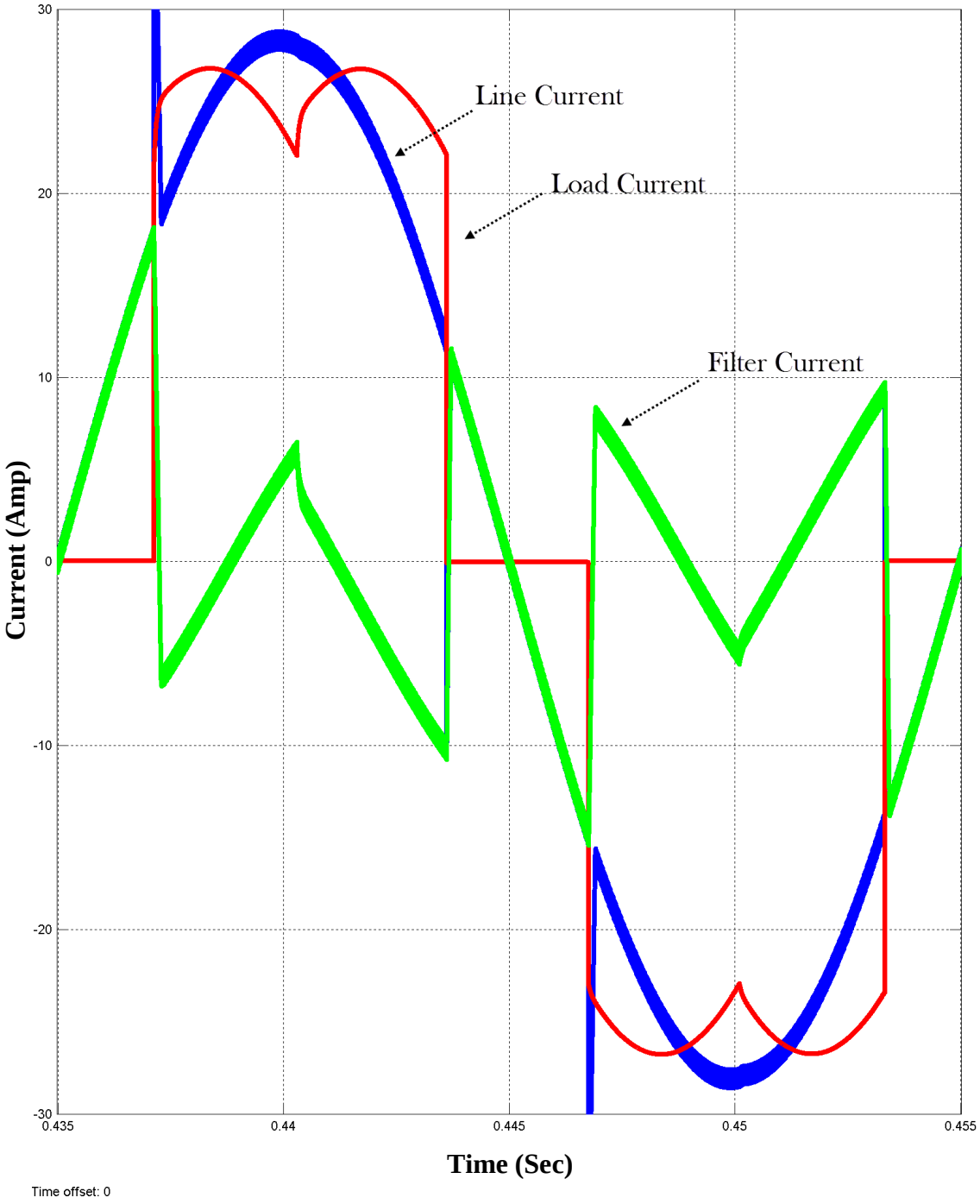

Figure 4.10: Line, Load and Filter Current with Spikes

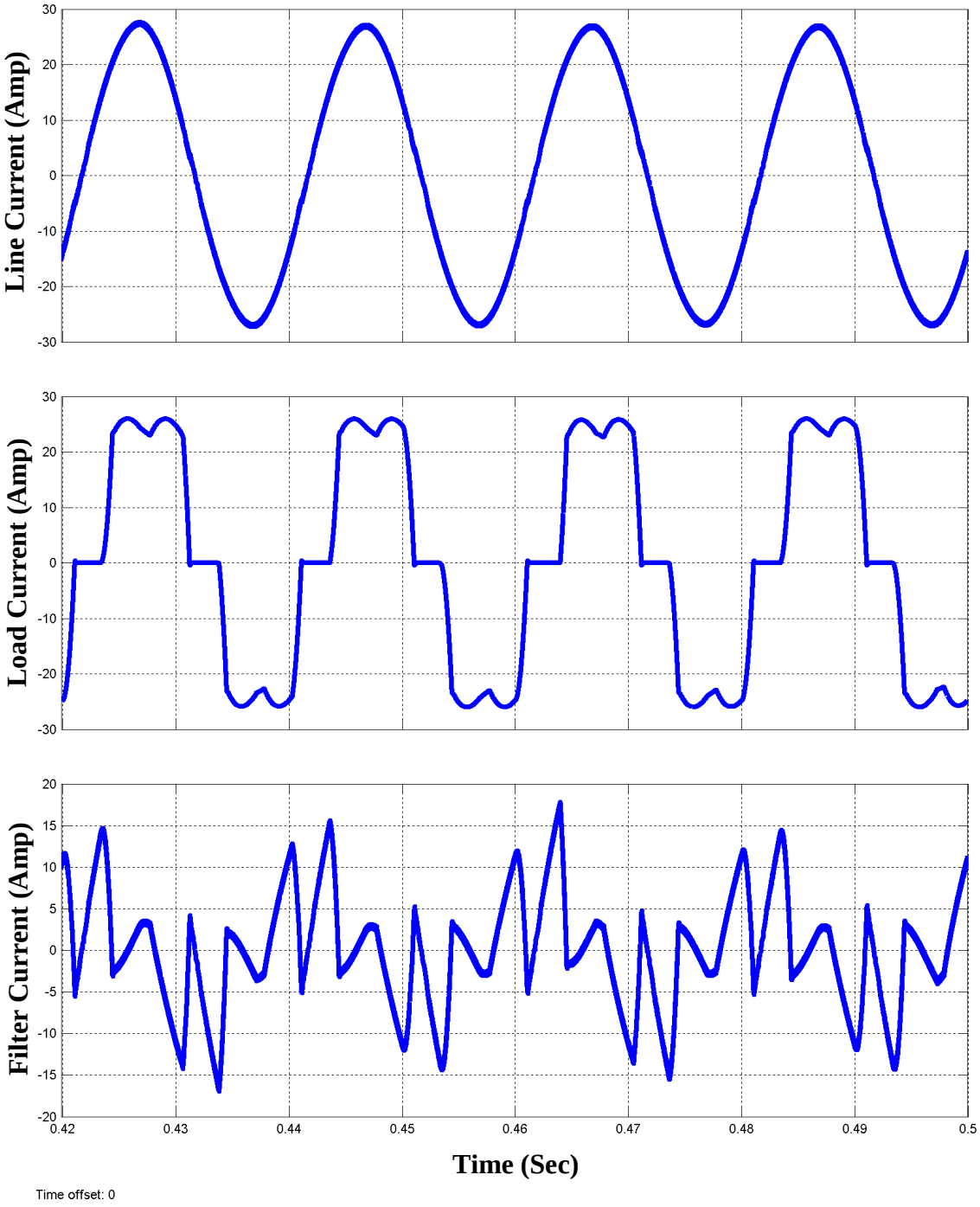

Figure 4.11: Line Current, Load Current and Filter Current without Spike

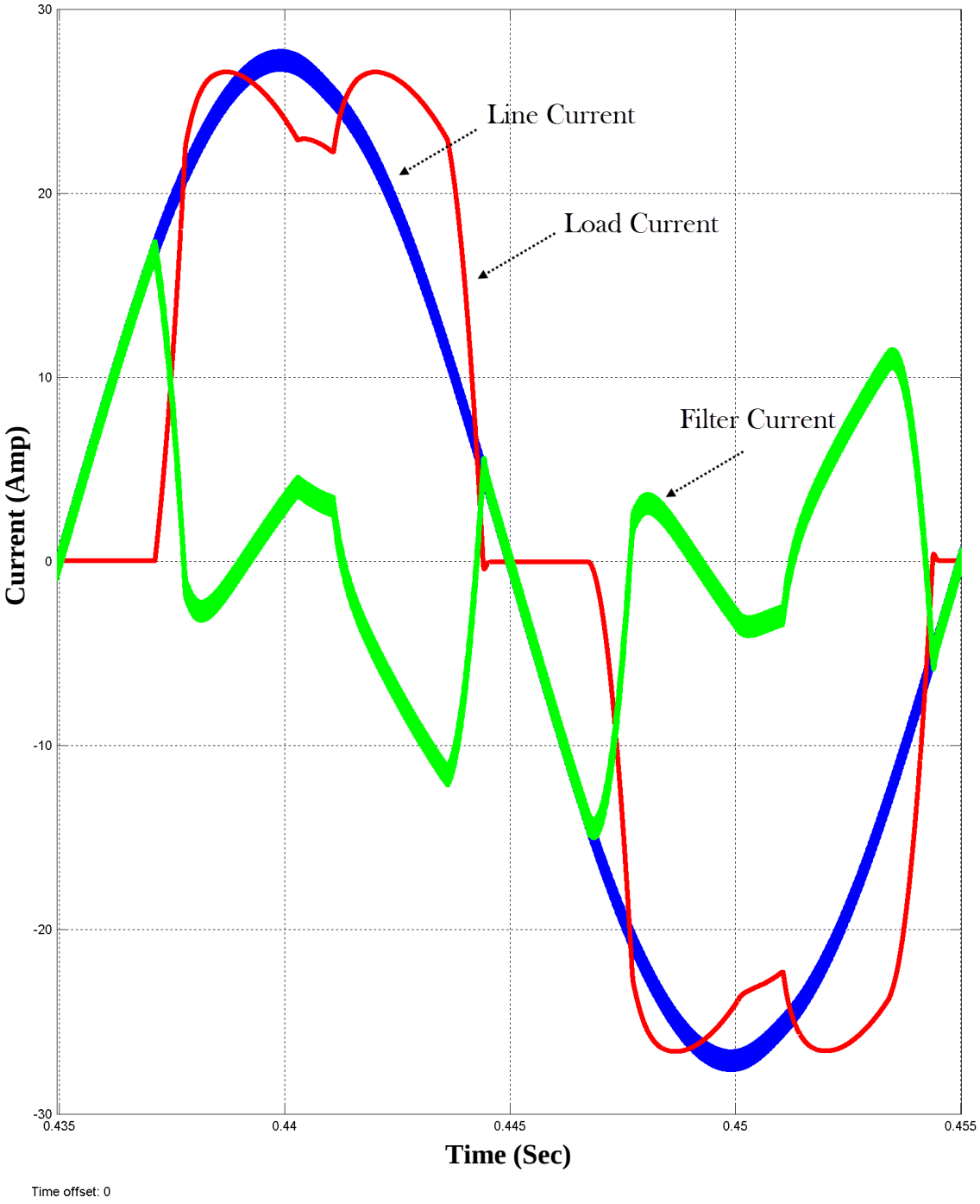

Figure 4.12: Line, Load and Filter Current without Spike

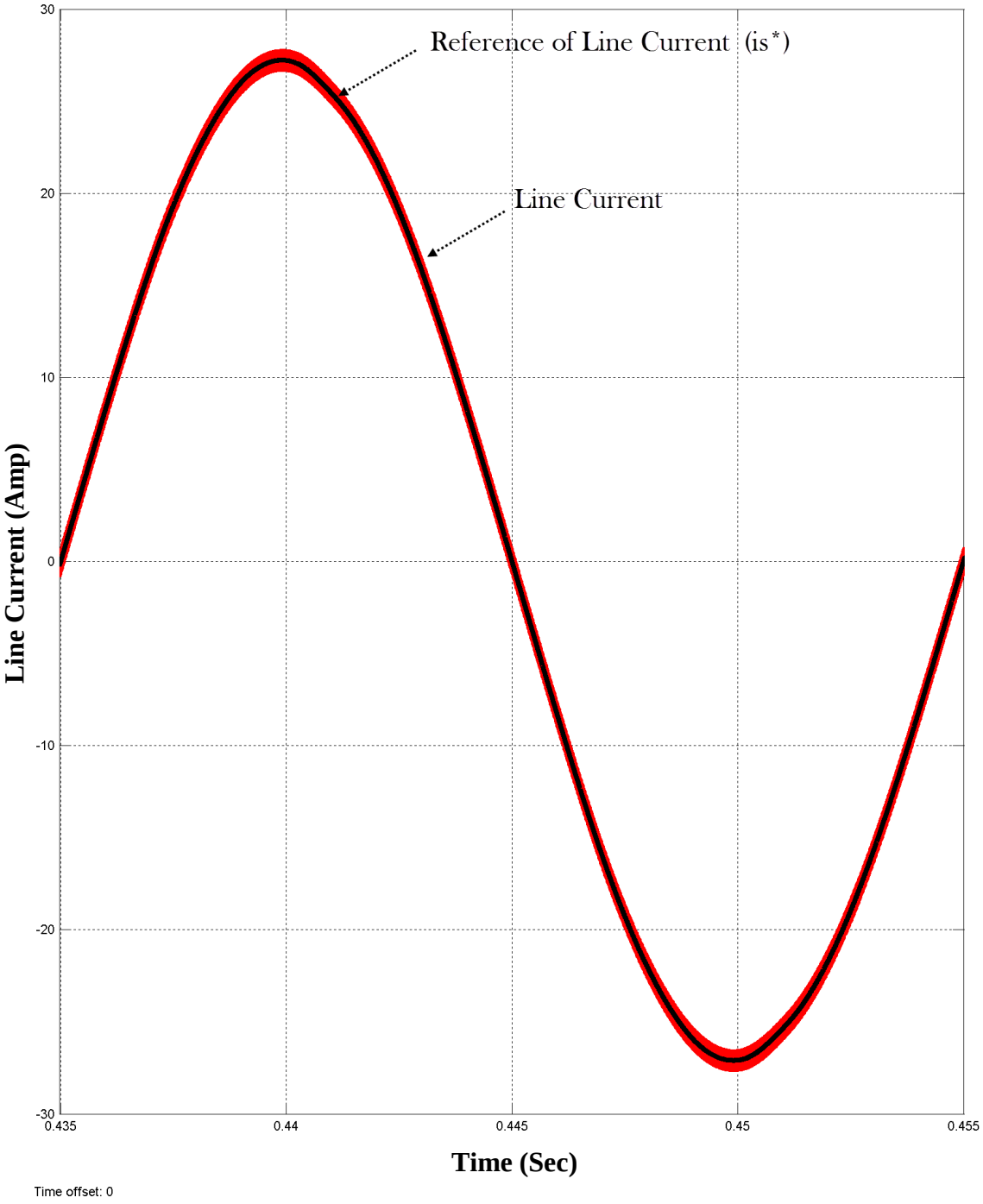

Figure 4.13: Line Current and Its Reference Generated by SBHCC

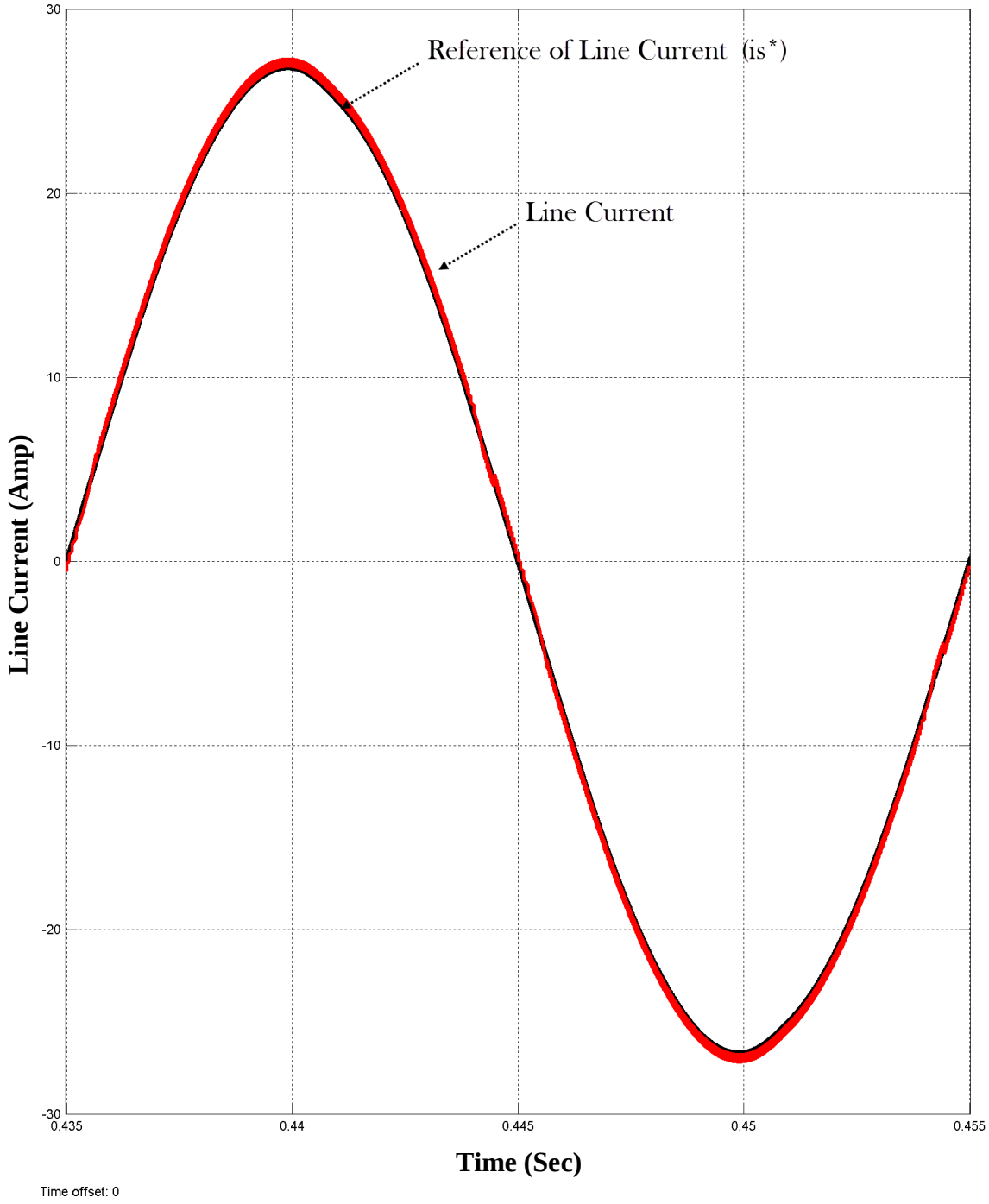

Figure 4.14: Line Current and Its Reference Generated by DBHCC

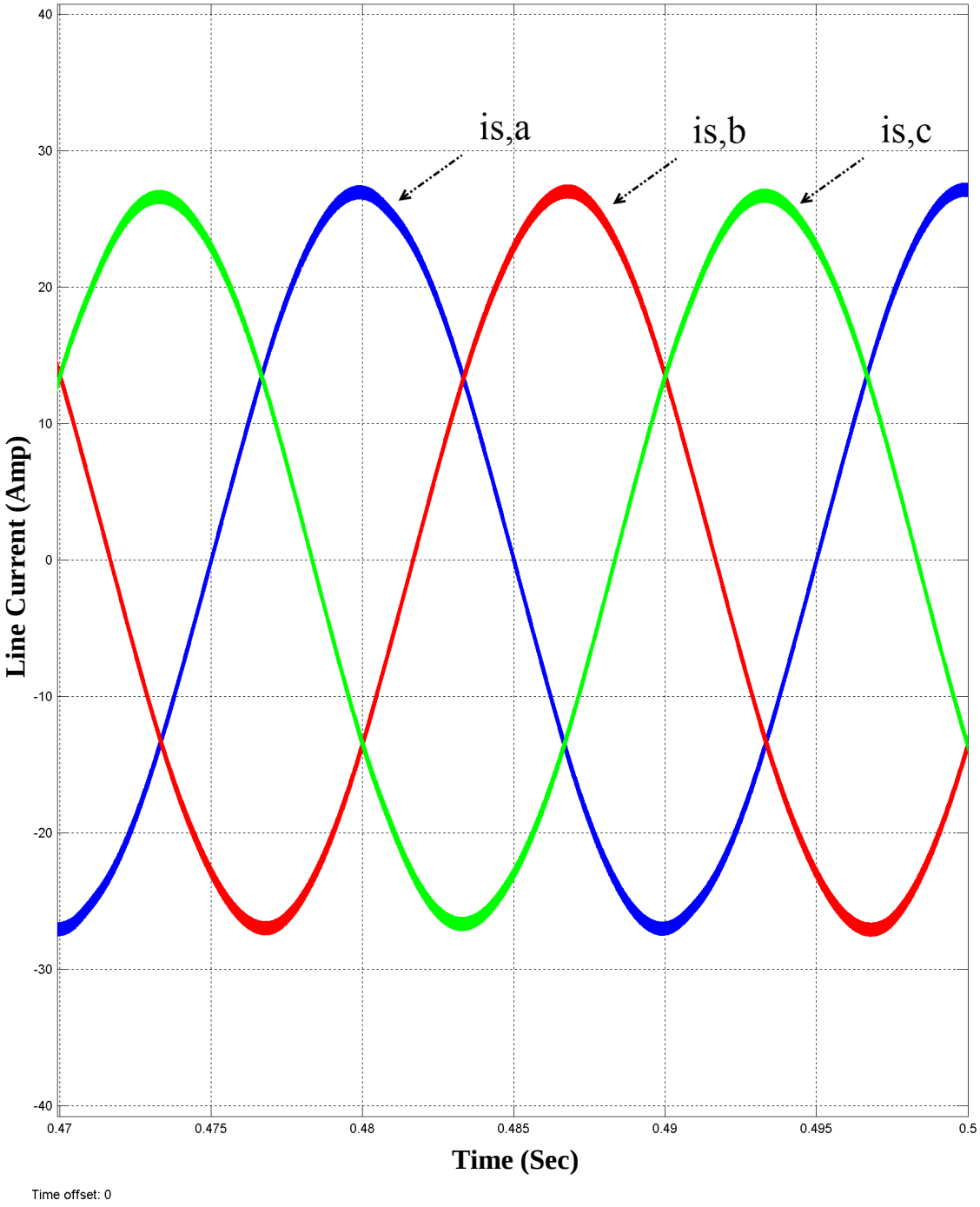

Figure 4.15: Three-phase Line Currents

Line voltage v_{s_a} and line current i_{s_a} are shown in Figure 4.16. It is observed that the current is fluctuating between the maximum and minimum values 30A and -30A

which is purely sinusoidal and also in phase with the voltage in the steady state ($PF = 1$).

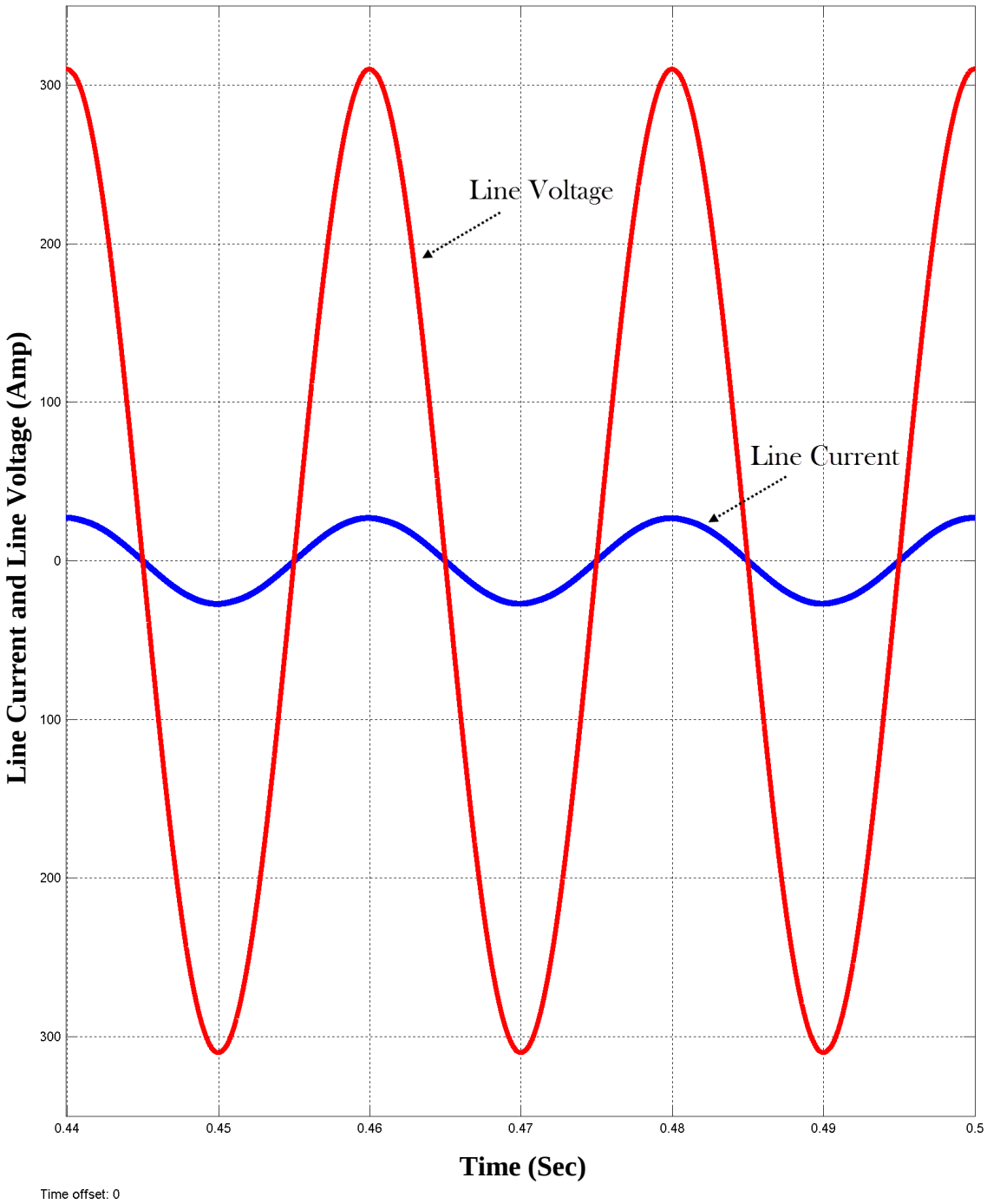

Figure 4.16: Line Voltage and Line Current

Reduction of switching frequency after applying three-level hysteresis band verifies that this implementation is successfully achieved. Figure 4.17 relates to the single and Figure 4.20 represents the double-hysteresis band switching operation.

Measured error values for single and double-band hysteresis methods are indicated in Figures 4.18 and 4.21 respectively. Both error and hysteresis block outputs are shown in large scale in Figures 4.19 and 4.22 to explain the validity of equations (2.10) and (3.1). Computed THD values when the active filter is connected to the system for both single- and double-band are shown in Table 4.1.

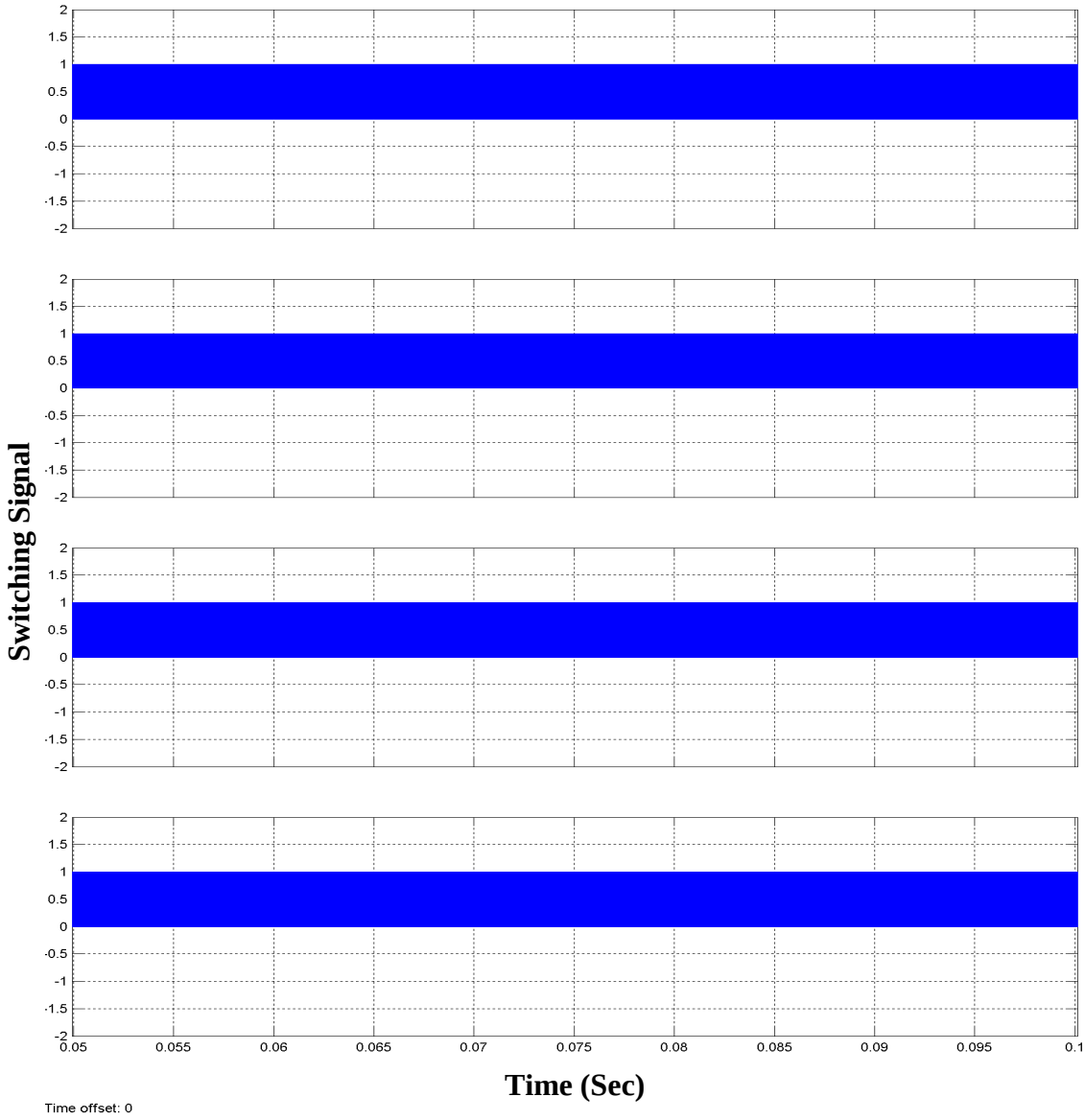

(a) Switching Signals of Four Switches of Phase $\boldsymbol{a}$

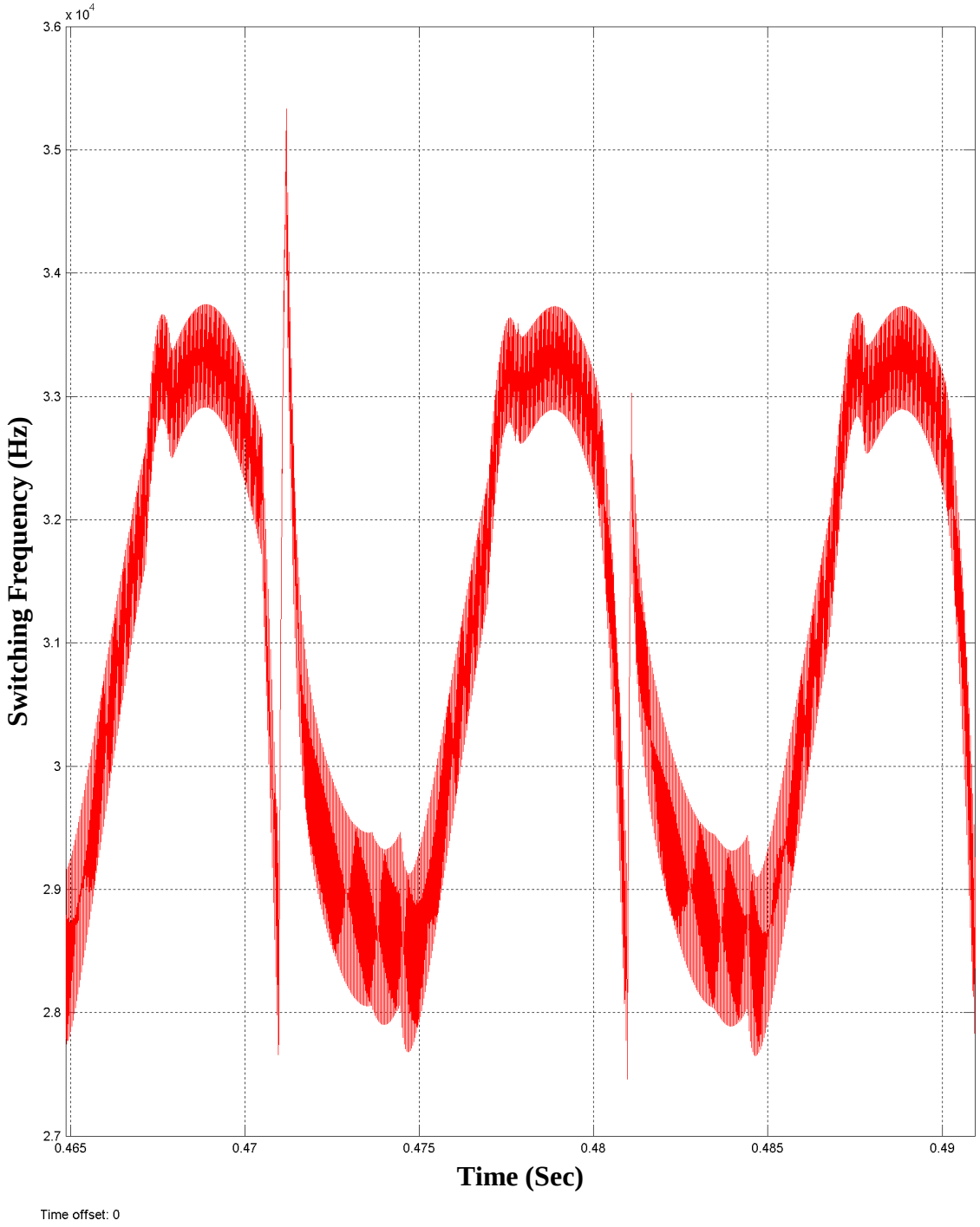

(b) The Variation of Switching Frequency

Figure 4.17 Switching Signals and Variation of Switching Frequency for Single-band Hysteresis of Three-phase Three-level Cascaded H-bridge Inverter Topology

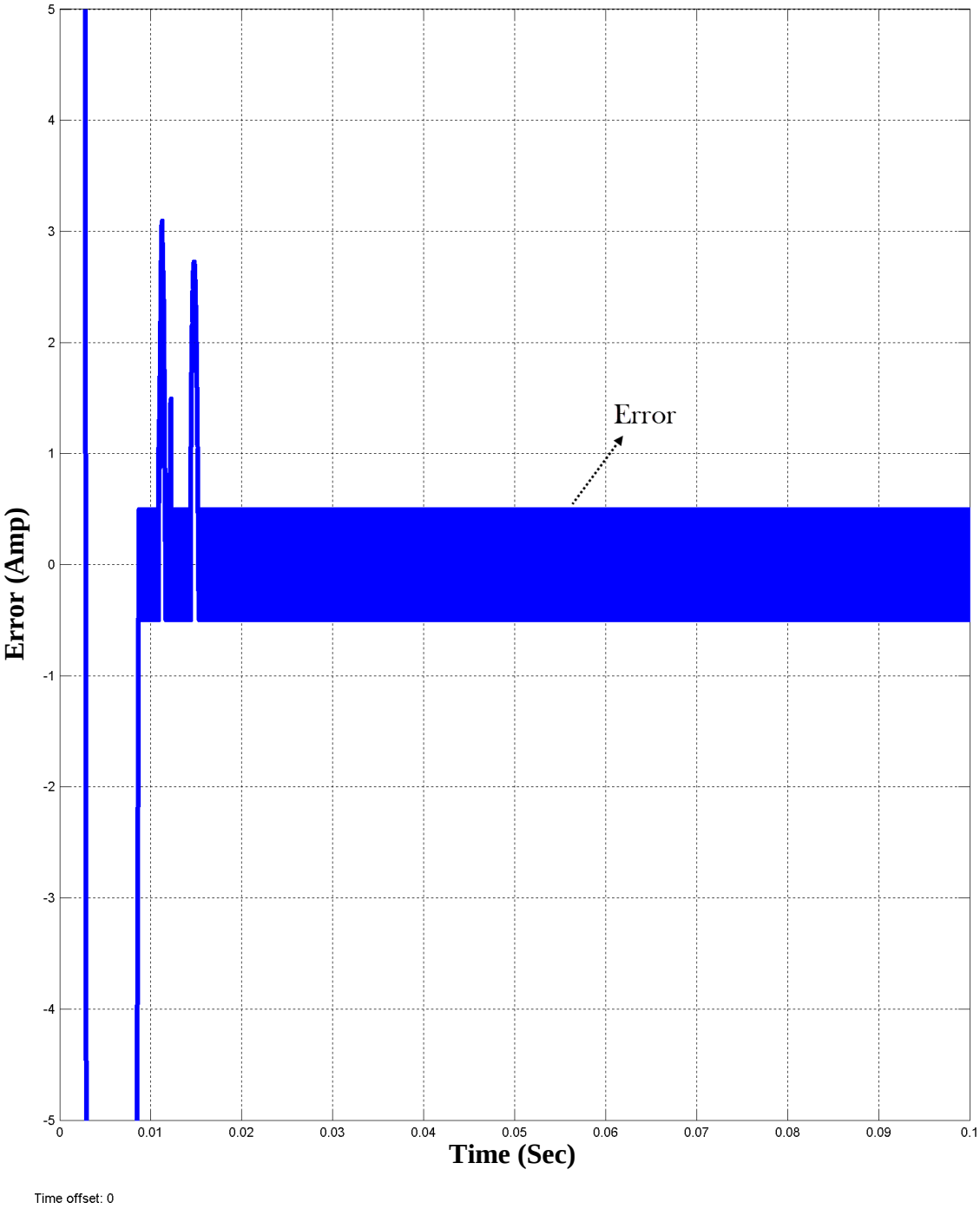

Figure 4.18: Error for Single-band Hysteresis Control

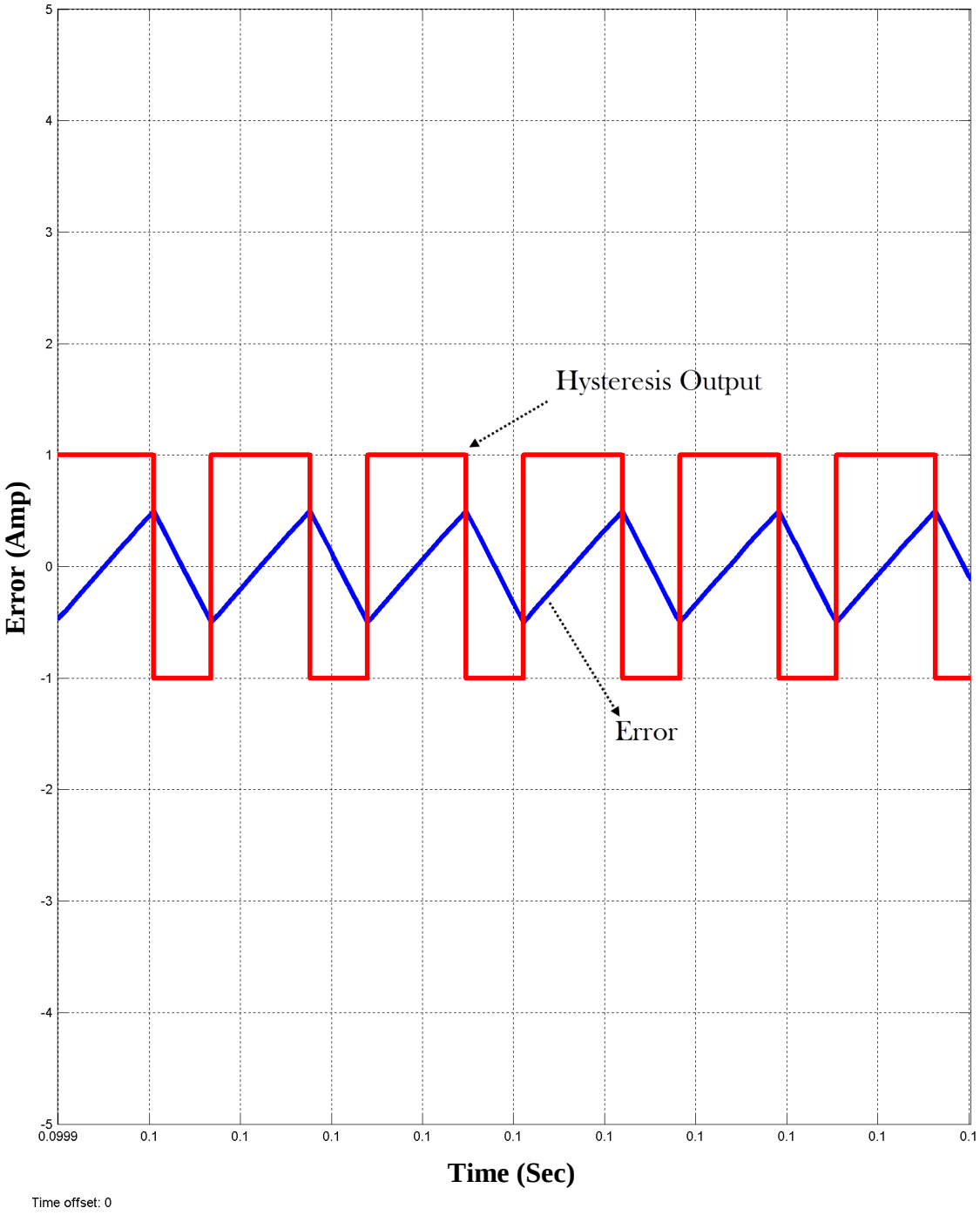

Figure 4.19: Error and Hysteresis Block Output for SBHCC

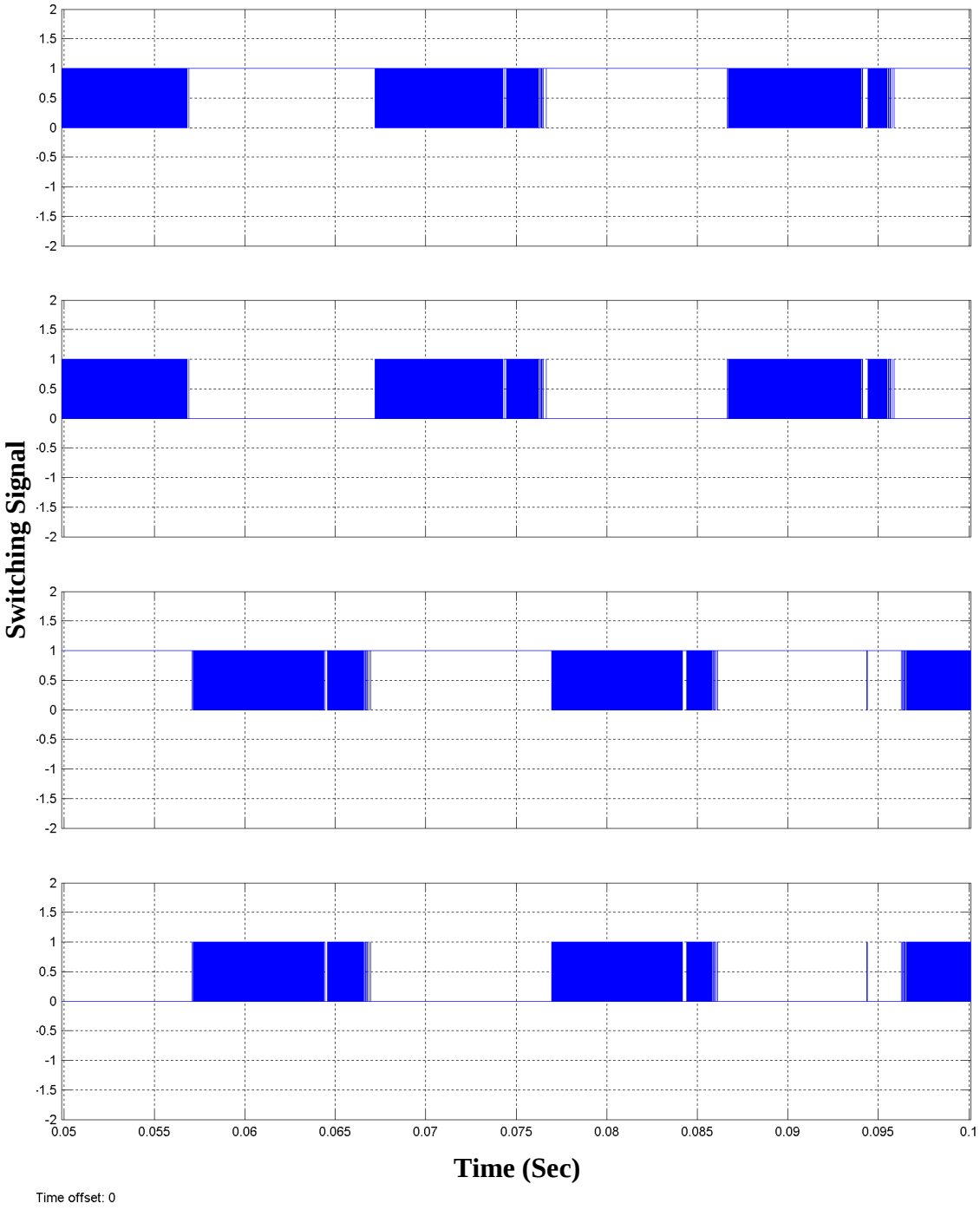

(a) Switching Signals of Four Switches of Phase $\boldsymbol{a}$

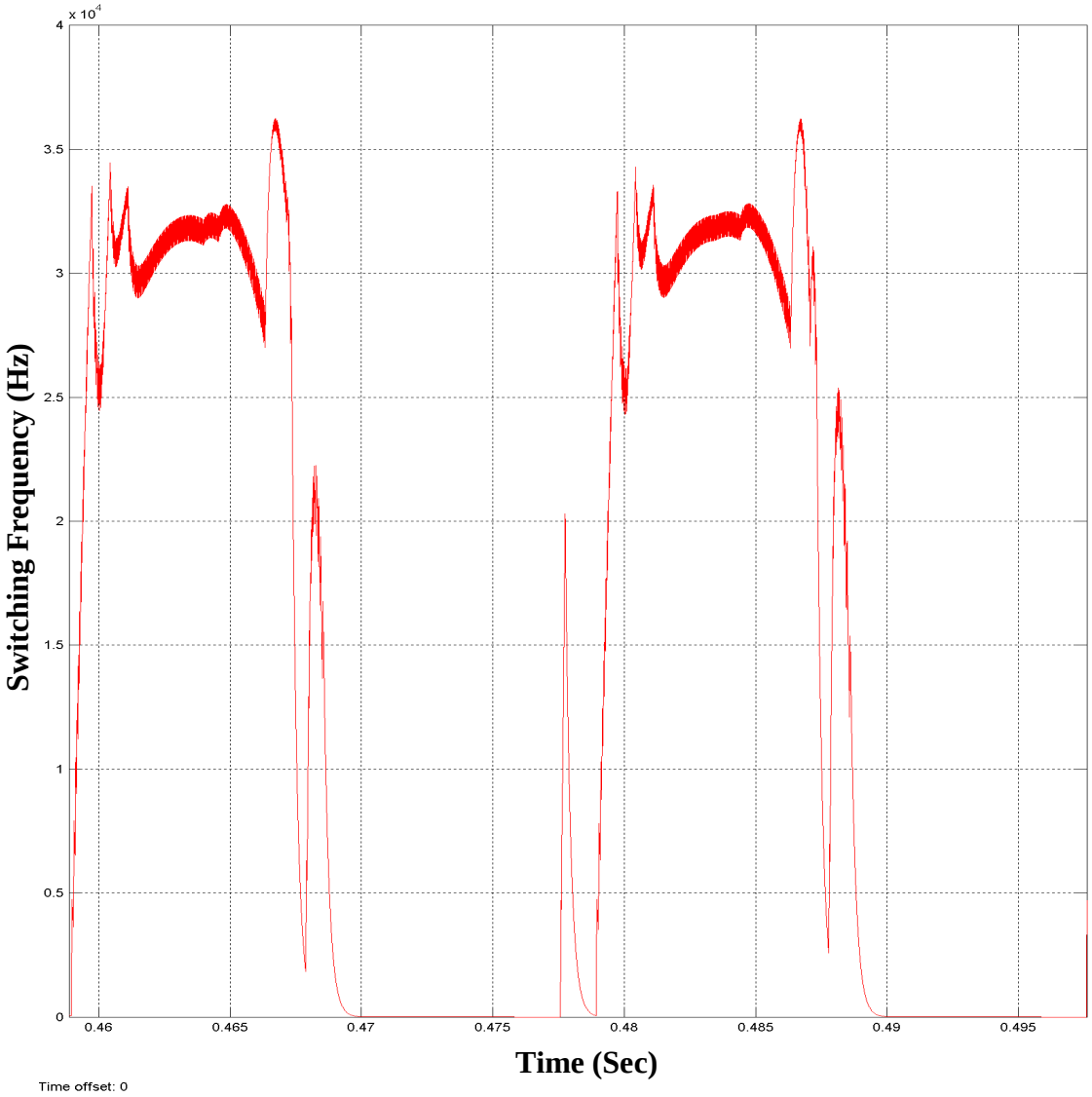

(b) The Variation of Switching Frequency

Figure 4.20: Switching Signals and Variation of Switching Frequency for Double-band Hysteresis of Three-phase Three-level Cascaded H-bridge Inverter Topology

As it can be seen in Figure 4.20 (b), the switching frequency is zero in half of cycle and it confirms that the switching frequency is decreased in comparison with Figure 4.17 (b) which represents single –band hysteresis switching frequency.

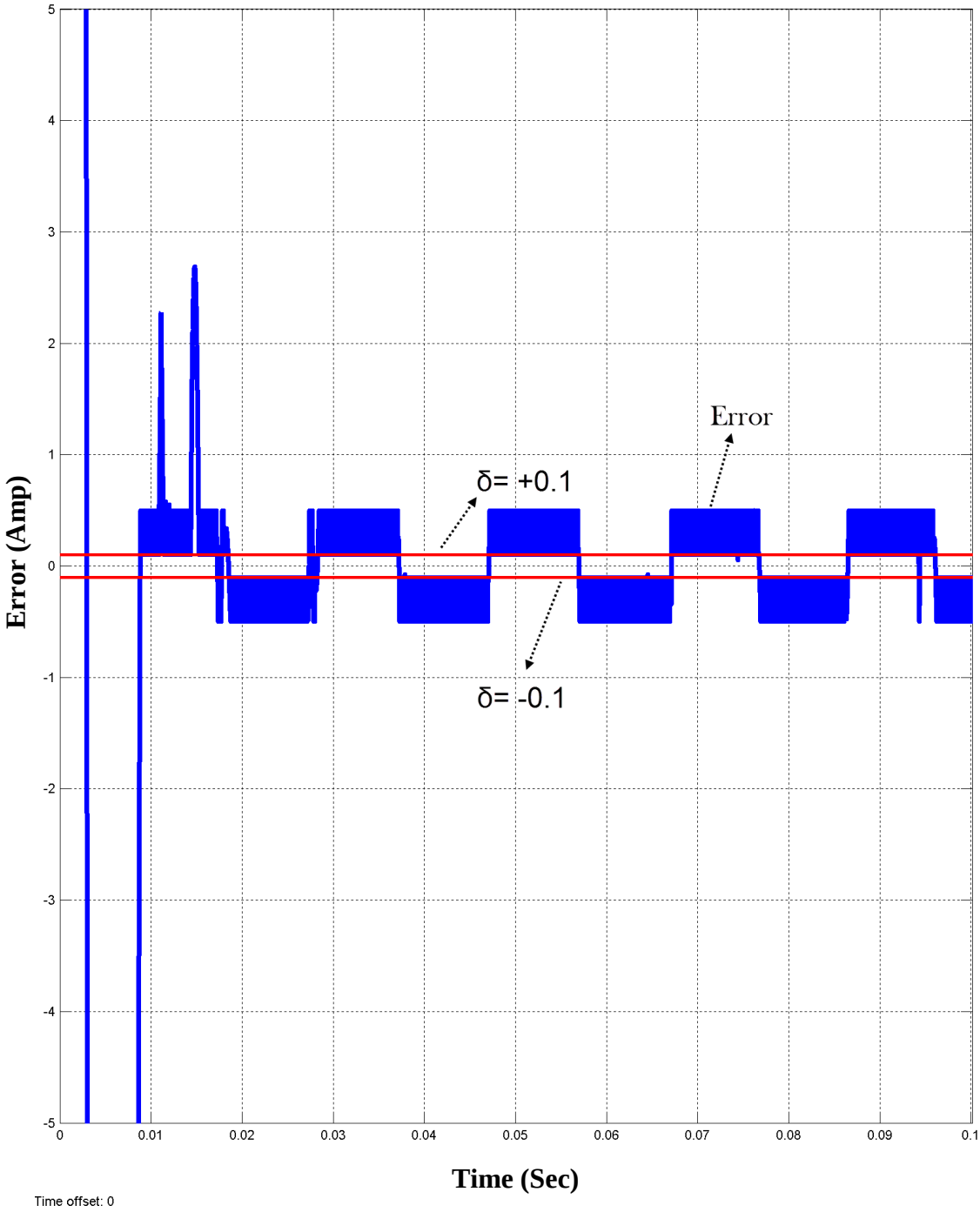

Figure 4.21: Error for Double-band Hysteresis Control

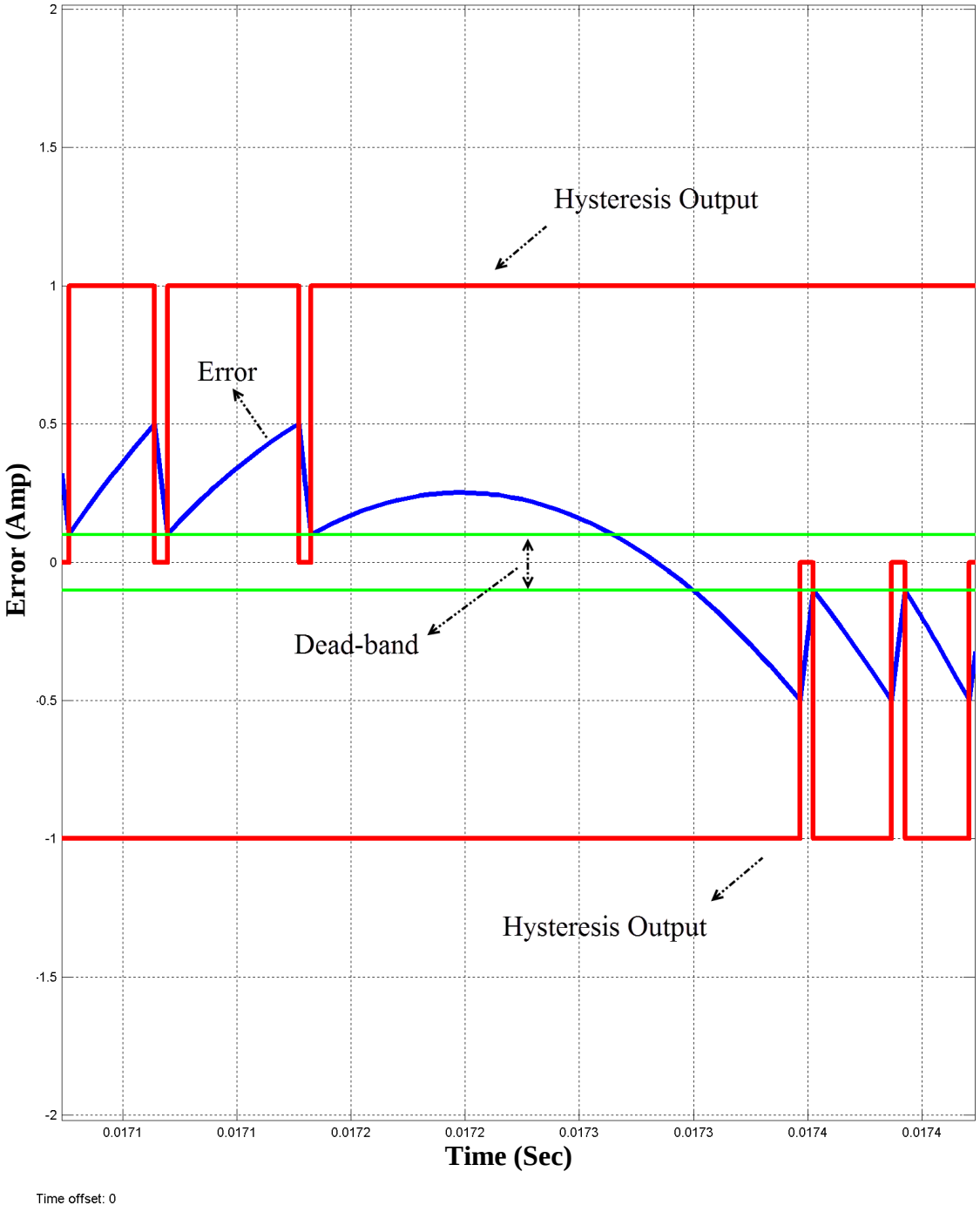

Figure 4.22: Error and Hysteresis Block Output for DBHCC

The DC capacitor voltage v_c and the source current amplitude i_{sm} are shown in Figures 4.23 and 4.24 respectively. Since we selected $v_c^* = 800\text{V}$ as the reference for the

capacitor voltage value, it should converge to this value in the steady state, which is confirmed in Figure 4.23.

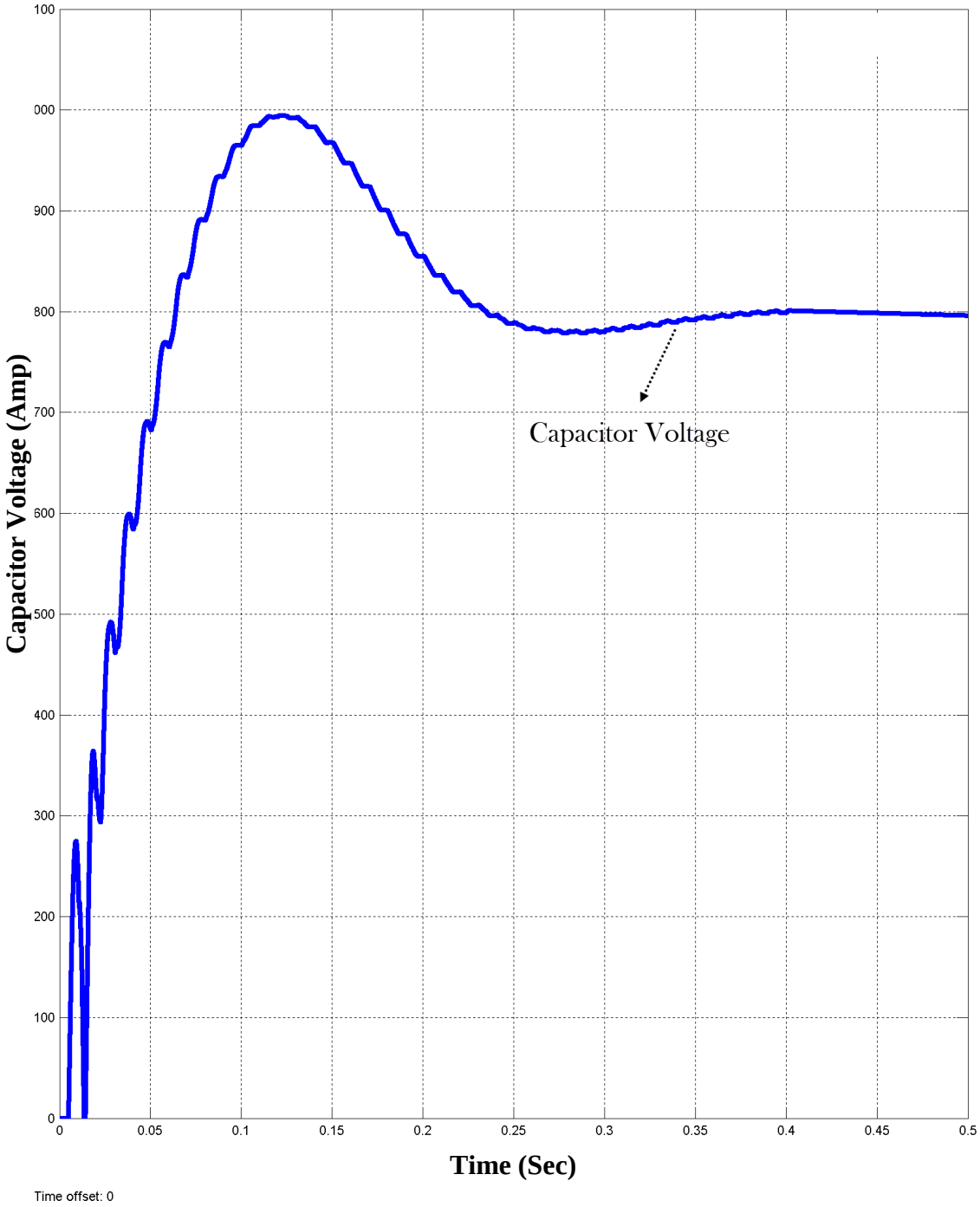

Figure 4.23: Capacitor Voltage

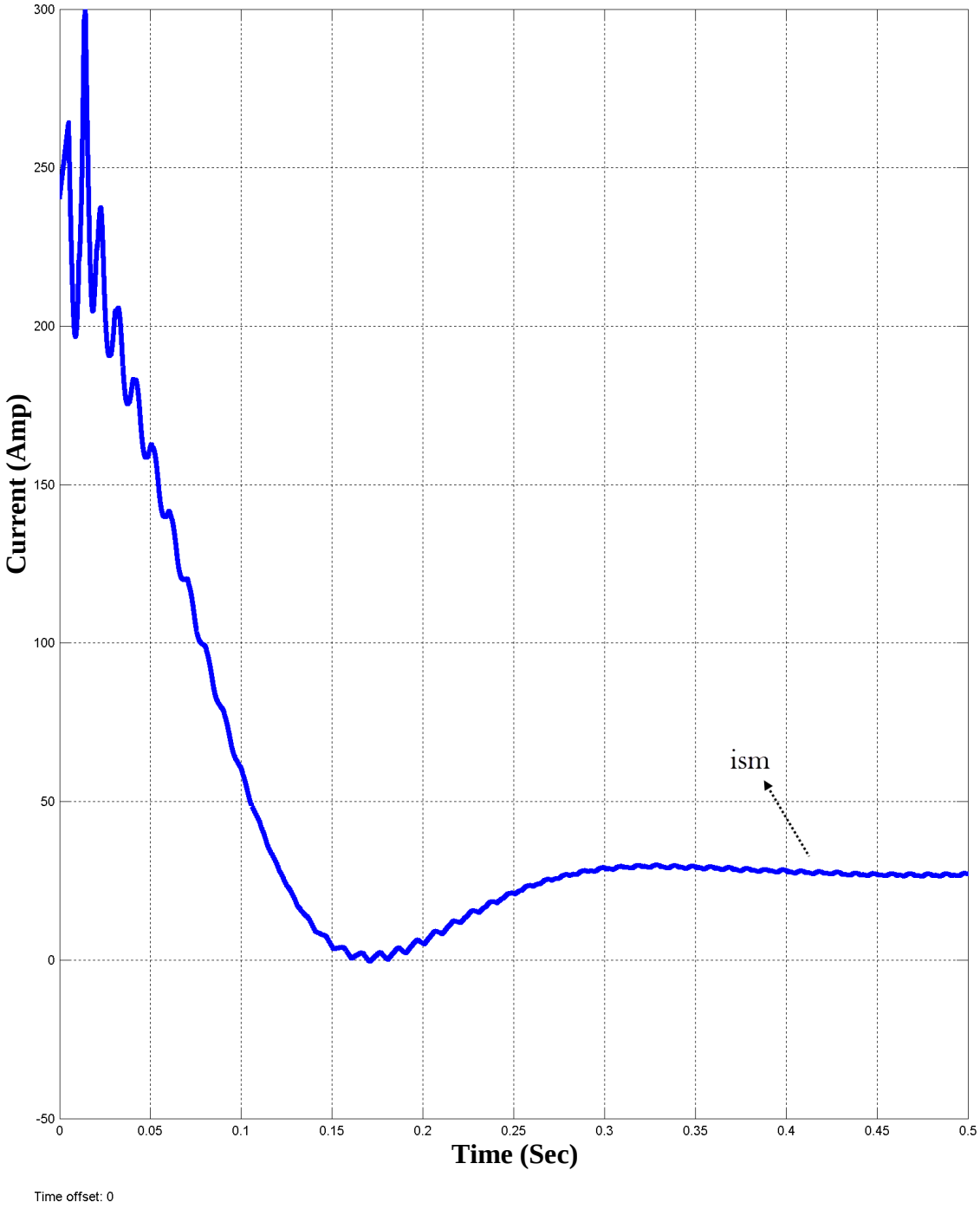

Figure 4.24: Reference of Source Current Amplitude (i_{sm})

Meanwhile, a three-phase breaker and its control block have been devised to connect and disconnect the active filter for testing the operation. In Figure 4.25, at first the active filter is connected for injecting i_c to the system for harmonic compensation. Next, the control block, with the adjusted time ($T = 0.4\ Sec$), disconnects the active

filter from the system. It is obvious, when i_c is injected into the system by the active filter, i_{s_a} is purely sinusoidal, but when the active filter is disconnected ($i_c = 0$) then, $i_{s_a} = i_{l_a}$. Figure 4.25 clearly shows this process only for phase a.

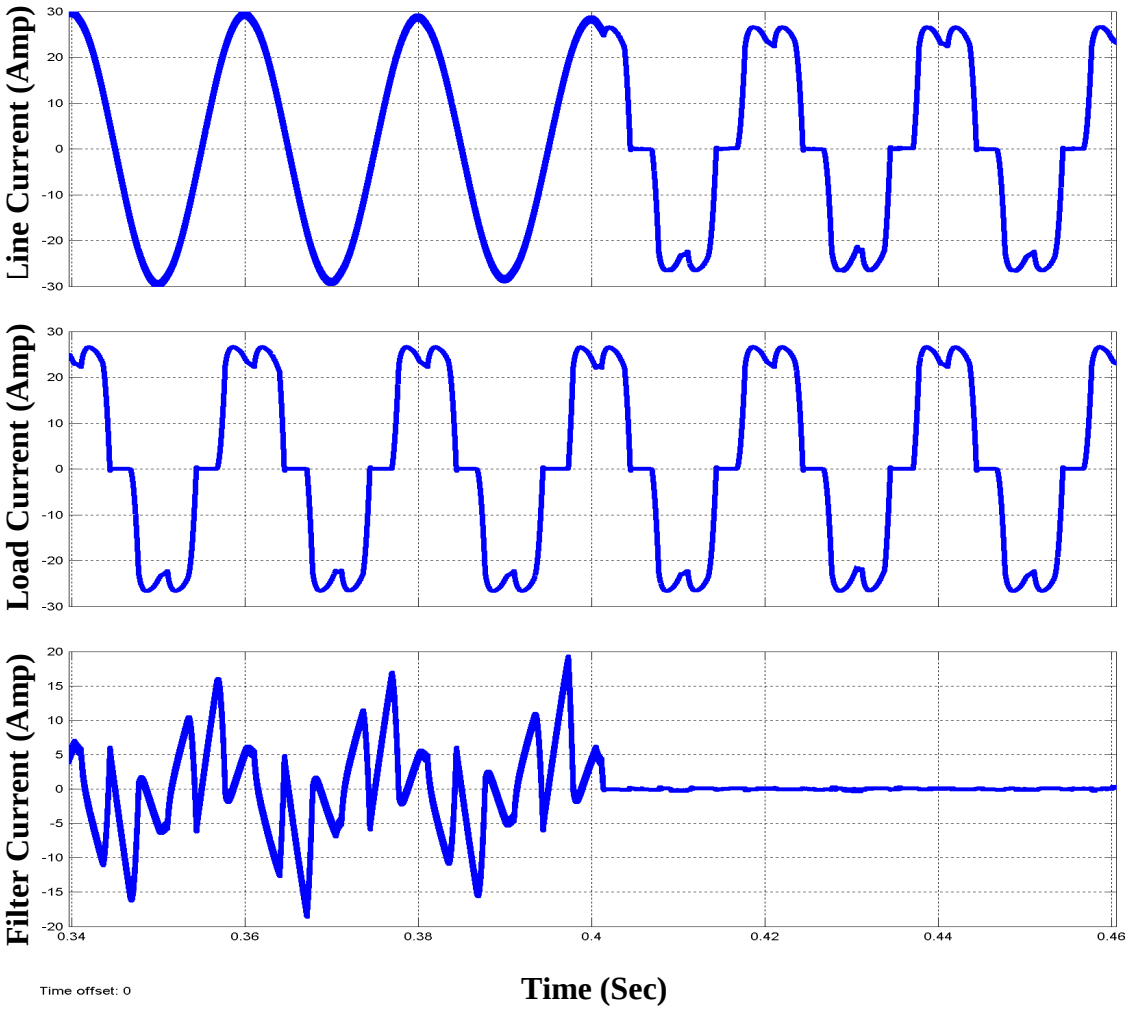

Figure 4.25: Waveforms for Connected and Disconnected Filter

In continuing, harmonic Fourier analysis has been shown in three different conditions. Y-axis in Figure 4.26 represents the harmonics amplitude with respect to the harmonics order (x-axis) when the active filter is disconnected. Figure 4.27 and Figure 4.28 show the obtained harmonic analysis of the system for SBHCC and DBHCC methods respectively.

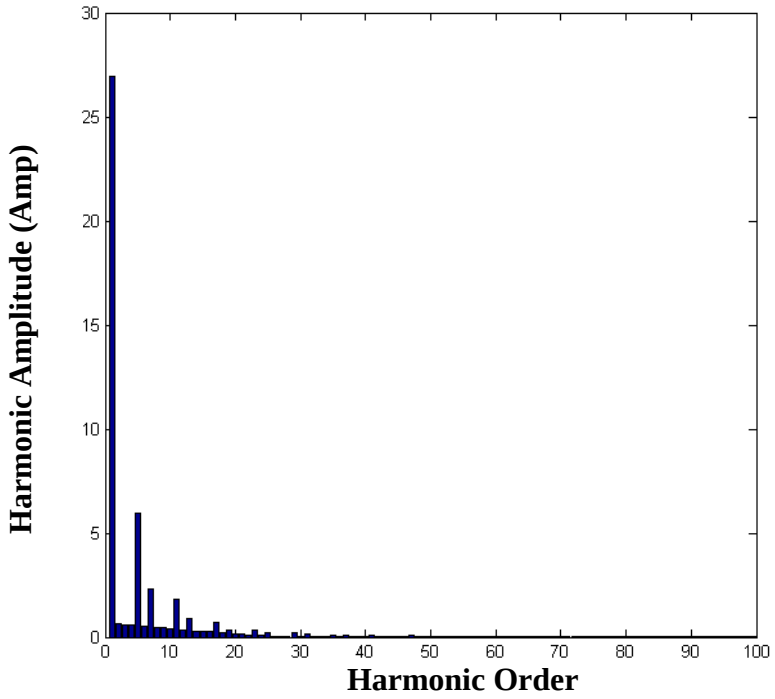

Figure 4.26: Harmonic Analysis of Phase a Source Current with Nonlinear Load and Disconnected Filter

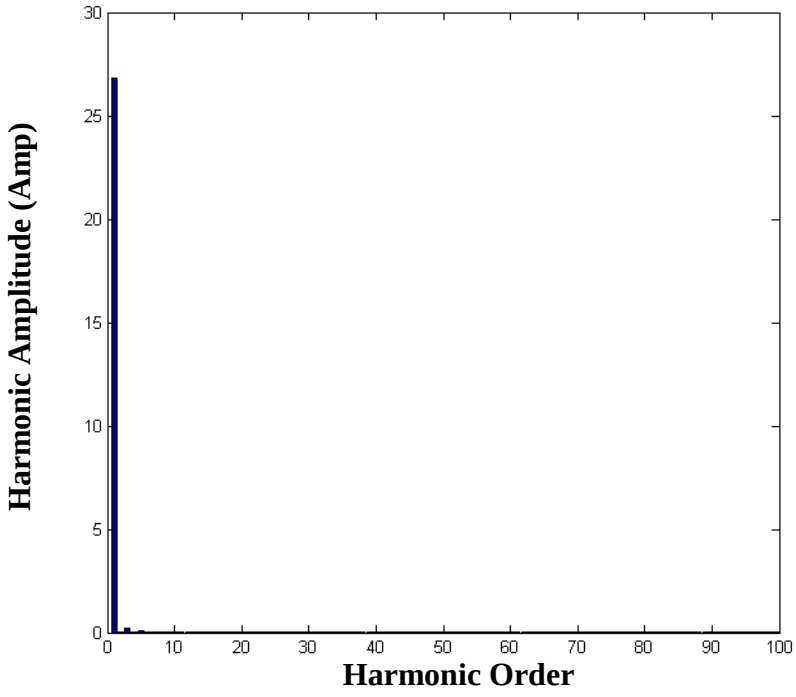

Figure 4.27: Harmonic Analysis of Phase a Source Current with Nonlinear Load by SBHCC Method

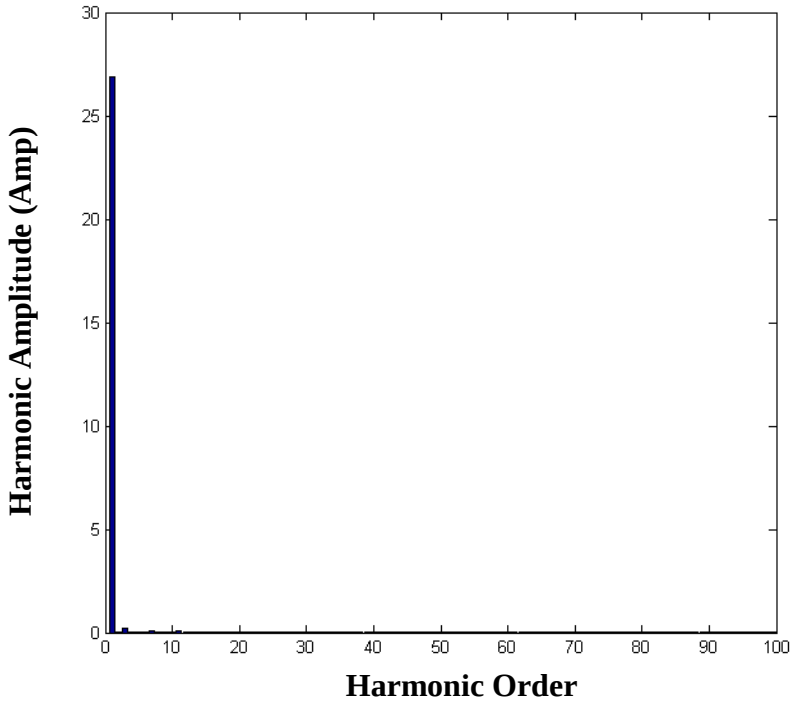

Figure 4.28: Harmonic Analysis of Phase a Source Current with Nonlinear Load by DBHCC Method

It is observed that, THD value is gradually decreased after applying SBHCC method and it also keeps decreasing by DBHCC method. All implementations have been simulated in MATLAB/SIMULINK R2012a. As they are shown in this chapter, i_c has been injected to the system to compensate the negative effect of the non-linear load and makes i_s sinusoidal. Additionally, three-level hysteresis current control permits the system to have a lower THD and lower switching frequency as possible. Table 4.1 indicates all results as below:

Table 4.1: Results of Comparison among Four Different Topologies

Inverter Models	**Three-phase two-level capacitor-midpoint**		**Three-phase three-level cascaded H-bridge**		**Three-phase three-level neutral point clamped**		**Three-phase five-level cascaded H-bridge inverter**	
Hysteresis Applied Methods	Single-band	Double-band	Single-band	Double-band	Single-band	Double-band	Single-band	Double-band
Supply Voltages	310 V, 50 Hz	310 V, 50 Hz	310 V, 50 Hz	310 V, 50 Hz	310 V, 50 Hz	310 V, 50 Hz	310 V, 50 Hz	310 V, 50 Hz
IGBT Switches	6-IGBTs	6-IGBTs	12-IGBTs	12-IGBTs	12-IGBTs	12-IGBTs	24-IGBTs	24-IGBTs
PI-Controller Gains K_p, K_i	-0.3, -6	-0.3, -6	-0.3, -6	-0.3, -6	-0.3, -6	-0.3, -6	-0.3, -6	-0.3, -6
Hysteresis Band (±HB)	±0.5	+0.5,0.1 -0.1,-0.5	±0.5	+0.5,0.1 -0.1,-0.5	±0.5	+0.5,0.1 -0.1,-0.5	±0.5	+0.5,0.1 -0.1,-0.5
DC Capacitor	2×2000 µF	2×2000 µF	3×2000 µF	3×2000 µF	2×2000 µF	2×2000 µF	6×1000 µF	6×1000 µF
THD % for i_{s_a}	1.898%	1.637%	1.730%	1.280%	1.931%	1.638%	1.724%	1.277%

With respect to Figure 4.20 and by considering the computed THD in Table 4.1, in addition to decreasing the switching frequency we can easily deduce that, the proposed current control method has improved performance compared with the single-band hysteresis control, regarding THD and switching frequency in all four topologies considered.

Chapter 5

CONCLUSIONS

In conclusion, shunt active power filter is implemented with respect to the importance of power quality and harmonic elimination. Among various control strategies, three-level hysteresis current control has been proposed by using shunt active power filter for optimizing harmonic elimination and decreasing switching frequency by adding a zero sequence and also it was expected to generate much lower distortion in the output compared with two-level hysteresis. According to the results obtained and by comparing all topologies, there is an optimization in THD values for all topologies separately. Accordingly, three–level hysteresis current controller, not only decreases switching frequency but also, generates lower total harmonic distortion (THD) in output. As a result, two-level can be replaced by three-level hysteresis current control method where having low switching frequency is required.

As a future work, this proposed control method is expected to be improved in near future or it might be optimized by changing the switching algorithms and by applying the stronger controller method for making currents able to follow their references as fast as possible. Also, there is a huge possibility to decrease the settling time and making DC voltage constant in shortest time by optimizing PI-controller.

REFERENCES

[1] B. Singh, K. Al-Haddad and A. Chandra, "A Review of Active Filters for Power Quality Improvement," *IEEE Transactions on Industrial Electronics,* vol. 46, pp. 101-112, 1999.

[2] K. Bimal. Bose, in *Modern Power Electronics and AC Drives*, Knoxville, Tennessee, ELSEVIER, 2006, pp. 105-111.

[3] K. Akagi and R. Hirofumi, in *Instantaneous Power Theory and Applications to Power Conditioning*, Aredes Mauricio, Wiley-IEEE Press, 2007, pp. 12-45.

[4] C. Sankaran , in *Power Quality*, Washington, D.C., CRC Press LLC, 2002, pp. 201-209.

[5] M. El-Habrouk, M.K. Darwish and K. PMehta, "Active Power Filters: A Review," *IEE-proceedings – Electric Power Applications,* vol. 147, pp. 403-413, 2000.

[6] R. Costa-Castelló, R. Griñó, R. P. Parpal and F. Fossas , "High-Performance Control of a Single-Phase Shunt Active Filter," *IEEE Transactions on Control Systems Technology*, vol. 17, pp. 411-421, 2009.

[7] V. Vodovozov, in *Introduction to Power Electronics*, Ventus Publishing ApS, 2010, pp. 56-90.

[8] M. H. Rashid, in *Power Electronics Handbook,* Pensacola, Florida, 2002, pp. 78-81.

[9] H. Kömürcügil and O. Kükrer , "A New Control Strategy for Single-Phase Shunt Active Power Filters Using a Lyapunov Function," *IEEE Transactions on Industrial Electronics,* vol. 53, pp. 117-123, 2006.

[10] P. Kirawanich and R. M. O'Connell, "Fuzzy Logic Control of an Active Power Line Conditioner," *IEEE Transactions on Power Electronics,* vol. 19, pp. 227-235, 2004.

[11] M. Kale and E. Ozdemir, "An Adaptive Hysteresisband Current Controller for Shunt Active Power Filter," *Electric Power Systems Research,* vol. 73, pp. 113-119, 2004.

[12] O. Kükrer and H. Kömürcügil, "A New Current Control Strategy for Three-Phase Three Wire Shunt Active Power Filters," *IEEE ISI,* pp. 113-200, 2008.

[13] B.C kuo and F. Golnaraghi, Automatic Control Systems, 8th ed., United States of America: State Space Engg, 2010, pp. 416-618.

[14] P. M. Kazmierkowski, R. Krishnan and F. Blaabjerg, Control in Power Electronics, Elsevier Science (USA)., 2002, pp. 45-62.

[15] O. Kükrer, H. Kömürcügil and A. Doganalp, "A Three-Level Hysteresis Function Approach to the Sliding-Mode Control of Single-Phase UPS Inverters," *IEEE Transactions on Industrial Electronics,* vol. 56, pp. 3477-3577, 2009.

[16] R. M. Amer, A. M. Osama and A.Z. Sherif, "New Hysteresis Control Method for Three Phase Shunt Active Power Filter," in *Proceedings of the International*

MultiConference Electrical Engineers and Computer Scientists, Hong Kong, 2011.

[17] P. Linash, A. Kunjumuhammed and K. Mishra, "A Control Algorithm for Single-Phase Active Power Filter Under Non-Stiff Voltage Source," *IEEE Transactions on Power Electronics,* vol. 21, pp. 201-209, 2006.

[18] Y. Ping, A. Chen and C. Zhang, "A Novel Adaptive Hysteresis Band Current Control Method for Three-level Based Active Power Filter," in *IEEE 7th International Power Electronics and Motion Control Conference - ECCE Asia*, Harbin, China, 2012.

[19] R. M. Potdar and C. Chowhan, "Comparison of Topologies of Shunt Active Power Filter Implemented on Three Phase Four-wire System," *International Journal of Soft Computing and Engineering (IJSCE),* vol. 1, no. 5, pp. 01-06, 2007.

[20] J. Matas, L. García de Vicuña, J. Miret, J. M. Guerrero and M. Castilla, "Feedback Linearization of a Single-Phase Active Power Filter via Sliding Mode Control," *IEEE Transactions on Power Electronics,* vol. 23, pp. 307-310, 2008.

[21] S. Rao, M. K. Srikanthan and R. K. V. Mishra , "Improved Hysteresis Current Control of Three-level Inverter for Distribution Static Compensator Application," *IET Power Electronics,* vol. 2, no. 5, pp. 402-408, 2008.

[22] N. Mohan, W. P. Robbin, and T. Undeland, in *Power Electronics: Converters, Applications, and Design*, New York: Wiley, 1995, pp. 217-219.

[23] O. Vodyakho and T. Kim, "Shunt Active Filter Based on Three-level Inverter for Three-phase Four-wire Systems," *IET Power Electronics,* vol. 2, no. 3, pp. 09-11, 2008.

[24] H. Québec, "SimPowerSystems User's Guide," Apple Hill Drive Natick, MA, The MathWorks, Inc., 2007, pp. 1-116.

[25] P. Karuppanan, R. Saswat Kumar and K. Mahapatra, "Three Level Hysteresis Current Controller based Active Power Filter for Harmonic Compensation," *IEEE Proceedings of ICETECT,* pp. 552-556, 2011.

[26] F. Ucar, R. Coteli and B. Danial, "Three Level Inverter Based Shunt Active Power Filter Using Multi-Level Hysteresis Band Current Controller," *Przeglad Elektrotechniczny (Electrical Review),,* no. ISSN 0033-2097, pp. 390-399, 2012.

[27] L. Hai, A. L. Thomas , K. Byung-il and S. R. Cheon, "Three-level Hysteresis Current Control for a Three- Phase Permanent Magnet Synchronous Motor Drive," in *IEEE 7th International Power Electronics and Motion Control Conference ECCE*, Harbin, China, 2012.

[28] R. Davoodnezhad, D. G. Holmes, and B. P. McGrath, "Three-Level Hysteresis Current Regulation for a Three Phase Neutral Point Clamped Inverter," in *15th International Power Electronics and Motion Control Conference*, Novi Sad, Serbia, 2012.

[29] Karuppanan, P.,Kumar, R. and Mahapatra, K., "Three Level Hysteresis Current Controller based Active Power Filter for Harmonic Compensation," in

International Conference On EMERGING Trends In Electrical and Computer Technology, Tamilnadu, 2011.

[30] A. Bellini and S. Bifaretti, "Modulation Techniques for Three-Phase Four-Leg Inverters," in *Proceedings of the 6th WSEAS International Conference on Power Systems*, Lisbon, Portugal, 2006.

[31] H. Kömürcügil and O. Kükrer, "A Novel Current-Control Method for Three-Phase PWM AC/DC Voltage-Source Converters," *IEEE Transactions on Industrial Electronics,* vol. 46, pp. 544-554, 1999.

[32] H. Kömürcügil and O. Kükrer, "Globally Stable Control of Three-phase Three-wire Shunt Active Power Filters," *Electr Eng*, vol. 89, pp. 411-418, 2007.

[33] G. Zhou, B. Wub and D. Xu, "Direct Power Control of A Multilevel Inverter Based Active Power Filter," *Electric Power Systems Research*, vol. 77, pp. 284-294, 2007.

APPENDIX

Appendix A: Fourier-series

$$f(t) = \frac{a_0}{2} + \sum_{n=1}^{\infty} a_n \cos\frac{2\pi nt}{T} + \sum_{n=1}^{\infty} b_n \sin\frac{2\pi nt}{T}$$

Let $\omega_0 = 2\pi f_0 = \frac{2\pi}{T}$, called the fundamental angular frequency

$$f(t) = \frac{a_0}{2} + \sum_{n=1}^{\infty} a_n \cos(n\omega_0 t) + \sum_{n=1}^{\infty} b_n \sin(n\omega_0 t)$$

DC component: $\frac{a_0}{2}$

Even part: $\sum_{n=1}^{\infty} a_n \cos(n\omega_0 t)$

Odd part: $\sum_{n=1}^{\infty} b_n \sin(n\omega_0 t)$

And also:

$$a_0 = \frac{2}{T}\int_{t_0}^{t_0+T} f(t)dt$$

$$a_n = \frac{2}{T}\int_{t_0}^{t_0+T} f(t)\cos(n\omega_0 t)\,dt \qquad n = 1,2,\ldots$$

$$b_n = \frac{2}{T}\int_{t_0}^{t_0+T} f(t)\sin(n\omega_0 t)\,dt \qquad n = 1,2,\ldots$$

Let $\omega_n = n\omega_0$, called the nth harmonic of the periodic function

$$f(t) = \frac{a_0}{2} + \sum_{n=1}^{\infty} a_n \cos\omega_n t + \sum_{n=1}^{\infty} b_n \sin\omega_n t$$

$$f(t) = \frac{a_0}{2} + \sum_{n=1}^{\infty} (a_n \cos \omega_n t + b_n \sin \omega_n t)$$

$$\xrightarrow{\times \frac{\sqrt{a_n{}^2 + b_n{}^2}}{\sqrt{a_n{}^2 + b_n{}^2}}} f(t) = \frac{a_0}{2} + \sum_{n=1}^{\infty} \sqrt{a_n{}^2 + b_n{}^2} \left(\frac{a_n}{\sqrt{a_n{}^2 + b_n{}^2}} \cos \omega_n t + \frac{b_n}{\sqrt{a_n{}^2 + b_n{}^2}} \sin \omega_n t \right)$$

$$f(t) = \frac{a_0}{2} + \sum_{n=1}^{\infty} \sqrt{a_n{}^2 + b_n{}^2} (\cos \theta_n \cos \omega_n t + \sin \theta_n \sin \omega_n t)$$

Let $C_0 = \frac{a_0}{2}$

$$f(t) = C_0 + \sum_{n=1}^{\infty} C_n \cos(\omega_n t - \theta_n)$$

Harmonic amplitude: $C_n = \sqrt{a_n{}^2 + b_n{}^2}$

Phase angles: $\theta_n = \tan^{-1}\left(\frac{b_n}{a_n}\right)$